Vol 4, №1, 2025 eISSN 2949-1835
PEER-REVIEWED SCIENTIFIC AND PRACTICAL JOURNAL

Modern Trends in Construction, Urban and Territorial Planning

Building Constructions, Buildings and Engineering Structures
Footings and Foundations, Subsurface Structures
Construction Materials and Products
Technology and Organization of Construction
Structural Mechanics
Urban Planning, Rural Settlements Planning
Facilities Life Cycle Management

www.stsg-donstu.ru
DOI 10.23947/2949-1835

Modern Trends in Construction, Urban and Territorial Planning

Peer-reviewed scientific and practical journal

eISSN 2949–1835

Published since 2022

Periodicity 4 issues per year

DOI: 10.23947/2949–1835

A peer-reviewed scientific and practical journal designed to inform the readers about the latest advancements, trends and prospects in the field of construction, architecture, urban planning and adjacent scientific fields. The journal serves a platform for scientific and educational cooperation of researchers and scholars engaged in field of construction.

The journal is included in the List of the leading peer-reviewed scientific publications (Higher Attestation Commission under the Ministry of Science and Higher Education of the Russian Federation), where basic scientific results of dissertations for the degrees of Doctor and Candidate of Science in scientific specialties and their respective branches of science should be published.

The journal publishes articles in the following fields of science:
– Building Constructions, Buildings and Engineering Structures (Engineering Sciences)
– Footings and Foundations, Subsurface Structures (Engineering Sciences)
– Construction Materials and Products (Engineering Sciences)
– Technology and Organization of Construction (Engineering Sciences)
– Structural Mechanics (Engineering Sciences)
– Urban Planning, Rural Settlements Planning (Engineering Sciences)
– Facilities Life Cycle Management (Engineering Sciences)

Indexing and Archiving	RISC, CyberLeninka, CrossRef, Internet Archive
Name of the Body that Registered the Publication	Extract from the Register of Registered Mass Media ЭЛ № ФС 77 – 83923 dated September 16, 2022, issued by the Federal Service for Supervision of Communications, Information Technology and Mass Media
Founder and Publisher	Federal State Budgetary Educational Institution of Higher Education Don State Technical University (DSTU)
Address of the Founder and Publisher	1, Gagarin Sq., Rostov-on-Don, 344003, Russian Federation
E-mail	sovtrendstr@gmail.com
Telephone	+7 (863) 2–738–372
Website	http://www.stsg-donstu.ru/
Date of Publication No.1,2025	31.03.2025

Современные тенденции в строительстве, градостроительстве и планировке территорий

Рецензируемый научно-практический журнал

eISSN 2949–1835

Издается с 2022 года

Периодичность – 4 выпуска в год

DOI: 10.23947/2949–1835

Журнал создан в целях информирования читательской аудитории о новейших достижениях, тенденциях и перспективах в области строительства, архитектуры, градостроительства и смежных научных направлений. Издание является платформой для научно-образовательного сотрудничества российских и иностранных исследователей, вовлеченных в строительную сферу.

Журнал включен в перечень рецензируемых научных изданий, в котором должны быть опубликованы основные научные результаты диссертаций на соискание ученой степени кандидата наук, на соискание ученой степени доктора наук (Перечень ВАК) по следующим научным специальностям:

2.1.1 – Строительные конструкции, здания и сооружения (технические науки)
2.1.2 – Основания и фундаменты, подземные сооружения (технические науки)
2.1.5 – Строительные материалы и изделия (технические науки)
2.1.7 – Технология и организация строительства (технические науки)
2.1.9 – Строительная механика (технические науки)
2.1.13 – Градостроительство, планировка сельских населенных пунктов (технические науки)
2.1.14 – Управление жизненным циклом объектов строительства (технические науки)

Индексация и архивация	РИНЦ, CyberLeninka, CrossRef, Internet Archive
Наименование органа, зарегистрировавшего издание	Свидетельство о регистрации средства массовой информации ЭЛ № ФС 77 – 83923 от 16 сентября 2022 г., выдано Федеральной службой по надзору в сфере связи, информационных технологий и массовых коммуникаций
Учредитель и издатель	Федеральное государственное бюджетное образовательное учреждение высшего образования «Донской государственный технический университет» (ДГТУ)
Адрес учредителя и издателя	344003, Российская Федерация, г. Ростов-на-Дону, пл. Гагарина, 1
E-mail	sovtrendstr@gmail.com
Телефон	+7 (863) 2–738–372
Сайт	http://www.stsg-donstu.ru/
Дата выхода №1,2025 в свет	31.03.2025

CONTENTS

BUILDING CONSTRUCTIONS, BUILDINGS AND ENGINEERING STRUCTURES

Mailyan LR, Ivanova TA, Andreeva NV, Maharramova IA Design Features of Volumetric Blocks Made of Lightweight Fibrotorcrete with Non-removable Formwork 7

Rozantseva NV, Drozdov AD Modern Technological Solution for Covering the Cylindrical Vault of the Nave during the Construction of St. Tikhon's Church in St. Petersburg 15

BUILDING MATERIALS AND PRODUCTS

Khalyushev AK, Kolesnichenko EA. Optimization of the Paintwork Material Modified by Metal Catalyser Additive..... 26

Verzhbovsky GB, Zaliev AV Forecasting the properties of multicomponent mineral polymer composite materials 35

Nesvetaev GV, Koryanova YuI, Shut VV. Contractional shrinkage of concretes from highly mobile and selfsealing mixtures 41

CONSTRUCTION MECHANICS

Gaijurov PP, Iskhakova ER, Savelyeva NA. Examples of Testing a Program for Modeling Long-Term Deformation of Prestressed Reinforced Concrete Beams 54

LIFE CYCLE MANAGEMENT OF CONSTRUCTION FACILITIES

Lysova EP, Paramonova ON. Development of the Structure of the Life Cycle of the Heating System of a Construction Facility..... 68

Samarskaya NS. Life Cycle Analysis of Construction Facilities Using the Example of Wind Power Facilities ... 76

СОДЕРЖАНИЕ

СТРОИТЕЛЬНЫЕ КОНСТРУКЦИИ, ЗДАНИЯ И СООРУЖЕНИЯ

Маилян Л.Р., Иванова Т.А., Андреева Н.В., Магеррамова И.А. Особенности конструктивных решений объемных блоков из легкого фиброторкретбетона с несъемной опалубкой 7

Розанцева Н.В., Дроздов А.Д. Современное технологическое решение перекрытия цилиндрического свода нефа при строительстве храма святителя Тихона в Санкт-Петербурге. 15

СТРОИТЕЛЬНЫЕ МАТЕРИАЛЫ И ИЗДЕЛИЯ

Халюшев А.К., Колесниченко Е.А. Оптимизация лакокрасочного материала для покрытия древесины с добавкой металлического катализатора.. 26

Вержбовский Г.Б., Залиев А.В. Прогнозирование свойств многокомпонентных минеральнополимерных композитных материалов 35

Несветаев Г.В., Корянова Ю.И., Шуть В.В. Контракционная усадка бетонов из высокоподвижных и самоуплотняющихся смесей 41

СТРОИТЕЛЬНАЯ МЕХАНИКА

Гайджуров П.П., Исхакова Э.Р., Савельева Н.А. Примеры тестирования программы моделирования длительного деформирования предварительно напряженных железобетонных балок 54

УПРАВЛЕНИЕ ЖИЗНЕННЫМ ЦИКЛОМ ОБЪЕКТОВ СТРОИТЕЛЬСТВА

Лысова Е.П., Парамонова О.Н. Разработка структуры жизненного цикла системы отопления строительного объекта 68

Самарская Н.С. Анализ жизненного цикла объектов строительства на примере ветроэнергетических сооружений 76

BUILDING CONSTRUCTIONS, BUILDINGS AND ENGINEERING STRUCTURES

СТРОИТЕЛЬНЫЕ КОНСТРУКЦИИ, ЗДАНИЯ И СООРУЖЕНИЯ

Check for updates

UDC 692
https://doi.org/10.23947/2949–1835-2025-4-1-7-14

Original Empirical Research

EDN: BLPQOB

Design Features of Volumetric Blocks Made of Lightweight Fibrotorcrete with Non-removable Formwork

Levon R. Mailyan[1] ✉, **Tatiana A. Ivanova**[2], **Natalia V. Andreeva**[3], **Inna A. Magerramova** [3]
[1]Don State Technical University, Rostov-on-Don, Russian Federation
[2]Cuban State Agrarian University named after Trublina, Krasnodar, Russian Federation
[3]Balakovo Institute of Engineering and Technology, Balakovo, Russian Federation
✉ Lrm@aaanet.ru

Abstract

Introduction. This article analyzes the design features of volumetric blocks made of fibroblast concrete using a formwork made of moisture-resistant drywall. The basic principles that describe the characteristics of the design with the shaping of these volumetric blocks implemented using shotcrete technology are also outlined. This is especially true for low- and medium-rise buildings.

Materials and methods. To form the construction of fiber-reinforced concrete volumetric blocks with formwork based on moisture-resistant drywall (hereinafter referred to as GCLV), it is suggested that a system of basic principles is used that increases energy efficiency, reduces costs, and promotes the disposal of safe industrial waste.

The application of the basic principles underlying the development of a volumetric block made of lightweight fibrotorcrete with non-removable formwork enabled a systematic approach to a constructive solution to be implemented.

Results. The introduction of an effective innovative method made it possible to develop a reinforced concrete volumetric block created using shotcrete technology. This approach has made it possible to reduce labor costs, increase strength characteristics, and enable the production of bulk blocks both in the factory and directly on the construction site.

Discussion and Conclusion. The multilayer structure of new-generation bulk blocks made of fibrotorcrete created by the authors is based on the key principles that emphasize the effectiveness of their use in the construction of buildings with small and medium storeys.

Keywords: fibroblast concrete volumetric blocks; non-removable gypsum-cardboard formwork; wet shotcrete technology; basic principles of shaping

For citation. Mailyan LR, Ivanova TA, Andreeva NV, Maharramova IA Design Features of Volumetric Blocks Made of Lightweight Fibrotorcrete with Non-removable Formwork. *Modern Trends in Construction, Urban and Territorial Planning*. 2025;4(1):7–14. https://doi.org/10.23947/2949-1835-2025-4-1-7-14

Оригинальное эмпирическое исследование

Особенности конструктивных решений объемных блоков из легкого фиброторкретбетона с несъемной опалубкой

Л.Р. Маилян[1] ✉, **Т.А. Иванова**[2], **Н.В. Андреева**[3], **И.А. Магеррамова**[3]
[1]Донской государственный технический университет, г. Ростов-на-Дону, Российская Федерация
[2]Кубанский государственный аграрный университет им. Трубилина, г. Краснодар, Российская Федерация
[3]Балаковский инженерно-технологический институт, г. Балаково, Российская Федерация
✉ Lrm@aaanet.ru

Аннотация

Введение. В данной статье приводятся конструктивные особенности объемных блоков, изготовленных из фиброторкретбетона с использованием опалубки из влагостойкого гипсокартона. Также изложены основные принципы, которые описывают характеристики конструкции с формообразованием данных объемных блоков, реализованных с помощью технологии торкретирования. Это особенно актуально для мало- и среднеэтажного строительства.

Материалы и методы. Для формообразования конструкции фиброторкретбетонных объемных блоков с опалубкой на основе влагостойкого гипсокартона (далее ГКЛВ) предлагается использовать систему базовых принципов, позволяющих повысить энергоэффективность, снизить затраты и способствующих утилизации безопасных отходов промышленности.

Применение базовых принципов, положенных в основу разработки объемного блока из легкого фиброторкретбетона с несъемной опалубкой, позволило осуществить системный подход к конструктивному решению.

Результаты исследования. Внедрение эффективного инновационного метода позволило разработать железобетонный объемный блок с использованием технологии торкретирования. Этот подход позволил уменьшить затраты труда, повысить прочностные характеристики и обеспечить возможность производства объемного блока как в заводских условиях, так и непосредственно на строительной площадке.

Обсуждение и заключение. Созданная авторами многослойная структура объемных блоков нового поколения из фиброторкретбетона основывается на ключевых принципах, которые подчеркивают эффективность их использования при строительстве зданий малой и средней этажности.

Ключевые слова: фиброторкретбетонные объемные блоки, несъемная гипсокартонная опалубка, технология мокрого торкретирования, базовые принципы формообразования

Для цитирования. Маилян Л.Р., Иванова Т.А., Андреева Н.В., Магеррамова И.А. Особенности конструктивных решений объемных блоков из легкого фиброторкретбетона с несъемной опалубкой. *Современные тенденции в строительстве, градостроительстве и планировке территорий*. 2025;4(1):7–14. https://doi.org/10.23947/2949-1835-2025-4-1-7-14

Introduction. There is an enormous demand for modern technologies in the construction industry, as in order to increase the volume of construction of buildings, it is essential to cut down construction costs and the types of work to be performed. The key is increasing the energy efficiency of design solutions while reducing material and energy costs [12].

Innovative modular structures are being represented by three-dimensional modular buildings. In domestic practice, the strategic approach to developing house-building complexes focuses on designing quick-to-assemble modular facilities helping to reduce the final housing costs as well as the construction time [4–11].

The objective of the study is to create a system for designing and manufacturing volumetric blocks accounting for the features and specifics of the industry. While developing such systems, it is essential to rely on principles accounting for the advantages and effectiveness of using bulk blocks in the construction sector. It is important to bear in mind that architectural and engineering solutions must comply with the unique requirements and conditions associated with the use of these materials. Effective design calls for an integrated approach accounting for not only technological aspects, but also economic and environmental factors. Proper implementation of methods and technologies would help improve quality and reduce construction costs ultimately resulting in improved overall design and production performance. The key is thus to harmonize all design stages, starting from the idea and ending with the actual construction ensuring maximum efficiency and durability of the final product in construction practice.

Materials and Methods. Building design using three-dimensional block housing construction can be optimized by introducing a system of key basic principles (Fig. 1) which are at its core. These principles help to structure the design and account for all the major aspects, which in turn boosts the overall construction efficiency. The implementation of such standards allows one not only to minimize time and financial costs, but also to improve the quality of the final product. The suggested system includes a variety of elements for making design work and integration of modern technologies more comprehensive. As a result, by means of implementing these principles, it is possible to harmonize functionality and aesthetics, which is in compliance with the modern requirements for building construction. This is imperative to ensure the durability and stability of structures in the future, as well as to cater for of users' and customers' needs making design more efficient and adaptable to current conditions.

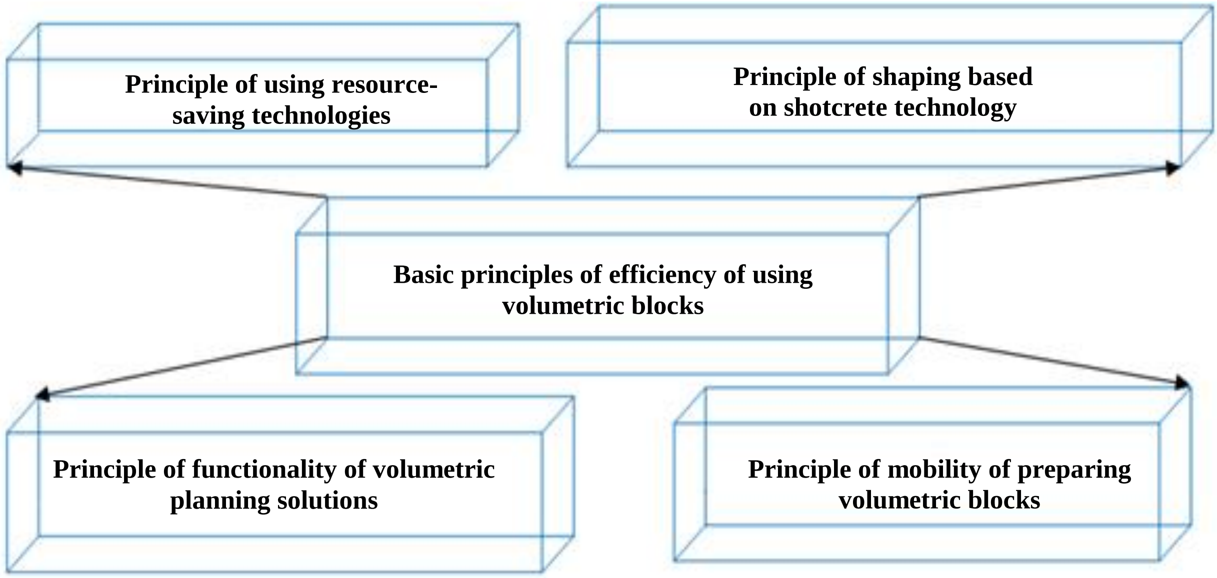

Fig. 1. Basic principles of three-dimensional block housing construction

Principle of introducing *resource-saving technologies* entails the use of regional resources and materials obtained using safely recycled industrial waste. This approach allows not only to optimize the costs of manufacturing building structures, but also to promote recycling of waste from various industries.

Principle of resource-saving is aimed at implementing the state "Strategy for Developing the Industrial Sector in Recycling, Decontamination and Elimination of Production and Consumption Waste until 2030" [1].

Design of a monolithic spatial structure of a volumetric block by means of wet shotcrete technology relies on the *principle of shaping*. A typical feature of the method is the use of non-removable one-sided plasterboard formwork to optimize manufacturing of bulk blocks by reducing labor costs.

The formation of a functional part with the further arrangement of volumetric blocks into various *spatial planning solutions* complies with the *principle of functionality*.

The principle of mobility involves design of production of volumetric blocks not only in a factory, but also directly on a construction site. Based on shotcrete technology, this approach will reduce the cost of transporting heavy structures to a construction site and expand the geographical scope of volumetric-block housing construction. This method will also facilitate the construction process in remote or hard-to-reach areas where traditional delivery methods can be challenging and costly. As a result, the use of mobile production will become a major factor for improving efficiency and cost-effectiveness in the construction sector, opening up new avenues for implementing large-scale block projects. This would not only speed up the construction process, but also make it more accessible to different regions, contributing to the nationwide infrastructure development.

The expansion of the field of use of volumetric blocks designed by means of wet shotcrete technology is due to the fact that they can be manufactured both in an organized production facility and directly on a construction site. This is indicative of the special features of the principle of mobility.

The existing structural solutions of volumetric blocks are entirely ineffective, since they fail to comply with the basic principles of modern volumetric block housing construction, which is in agreement with the state's development strategy in the field of resource conservation. At the same time, the existing forms of three-dimensional blocks do not enable the expansion of the compositional and spatial planning solutions of such buildings. Traditional approaches to design and technology of their construction fail to ensure routine use of three-dimensional block housing in the construction industry. An innovative approach for implementing the basic principles is thus the use of wet shotcrete technology for bulk blocks made of lightweight fibrotorcrete concrete.

The suggested block cap made of lightweight fibrotorcrete is a multilayer structure. Such a block can be used for constructing small and medium-rise buildings. Unlike the classic factory manufacturing technology, the wet shotcrete method is used here suggesting taking the construction of bulk blocks to a new level, as they will be produced directly on a construction site. This will not only expand the geography of construction, but also develop a new range of products of the type, as well as reduce the cost of transporting finished factory products.

The suggested design method relies on the principle of shaping involving the simultaneous formation of a structure in terms of design and production. This approach enables a complete monolithic spatial element to be designed.

Research Results. The basic principle of designing spatial blocks made of fibrotorcrete is the concept of shaping focusing on creating a new space with functional zones.

The patented design of the volumetric block includes transverse walls, window and door openings, and a Π-shaped longitudinal load-bearing structure. The general view of a three-dimensional block of the "hood" type is shown in Fig. 2 [2].

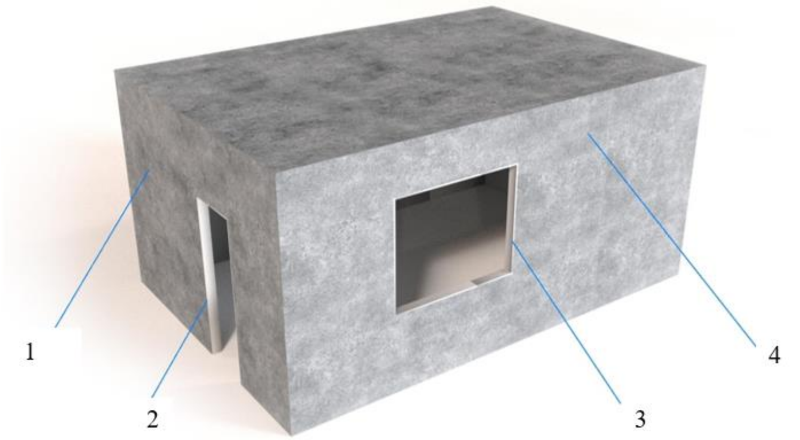

Fig. 2. Structural solution of fibroshotcrete concrete volumetric block:
1 — transverse wall; 2 — doorway; 3 — window opening; 4 — Π-shaped longitudinal load-bearing structure [2]

The fibrotorcrete volumetric block modeled according to the basic principles (Fig. 1) is characterized some distinctive features:

– a one-sided plasterboard formwork acting as an interior cladding;

– use of resource-saving concrete compositions with industrial waste ;

– minimization of technological steps within an organized production by means of wet shotcrete on a construction site.

The high efficiency of the constructive solution using lightweight fiber-reinforced concrete based on industrial waste for producing load-bearing elements has been proven by means of the authors' experimental work [3]. The high effectiveness of their use (including fibrotorcrete volumetric blocks) has been confirmed. This enables the principle of resource conservation to be implemented in practice within the framework of the state's development strategy.

A distinctive feature of the design solution is the use of volumetric blocks of multilayer construction as load-bearing walls (Fig. 3). The size of the load-bearing layer varies depending on the construction region and the energy efficiency of the design solution.

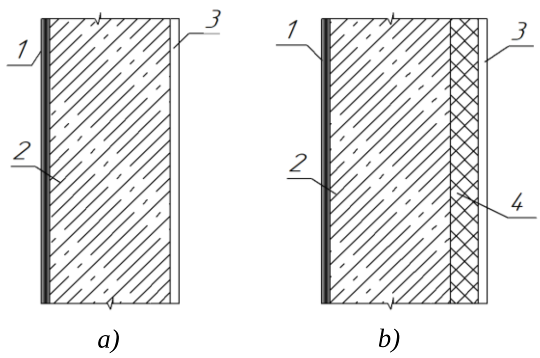

Fig. 3. Supporting structure of the developed volumetric block:
a — a one-layered one, *b* — a two-layered one
(1 — non-removable plasterboard formwork; 2 — fibro shotcrete bearing concrete layer; 3 — shotcrete-plaster; 4 — a layer of plate insulation)

The suggested design solution for a three-dimensional block of a "hood" type configuration expands the possibilities of planning solutions for such buildings. In particular, a volumetric bay window type block cap made of fibrotorcrete concrete is set forth. (Fig. 4, *a*).

The design solution of the "hood" type configuration of a new-generation volumetric block expands the possibilities of planning solutions for such buildings. The article looks at the use of fibrotorcrete concrete to design a three-dimensional bay window-type block hood making it possible to improve the architectural and functional characteristics of buildings. The effectiveness of the use of this material in construction and its impact on the stability and durability of structures is also accounted for.

A new type of volumetric reinforced concrete block of a new generation (Fig. 4, *b*) is a П-shaped load-bearing structure with transverse walls capable of receiving loads with no additional support. Openings for windows and doors are provided in these walls. The block is made of lightweight reinforced fibrotorcrete and is a monolithic spatial element with five faces. In order to increase the bearing capacity, the coupling zones of the supporting frames of the block are reinforced with additional grids along the perimeter. The rigidity of the wall elements with openings is regulated by their width dimensions accounting for the angular sections of the walls.

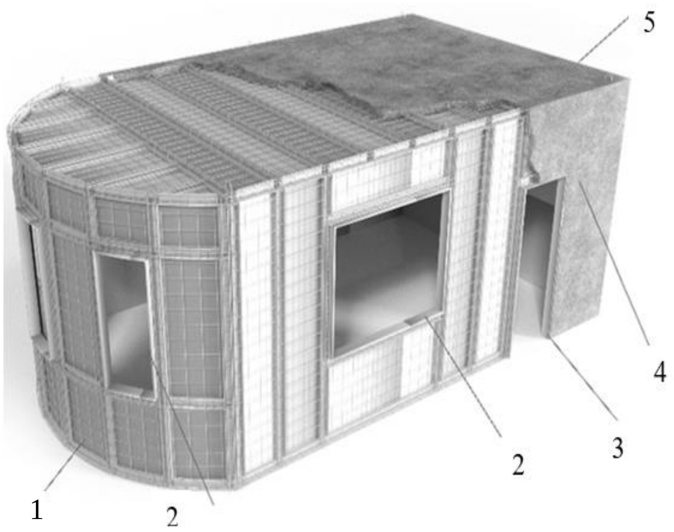

a)

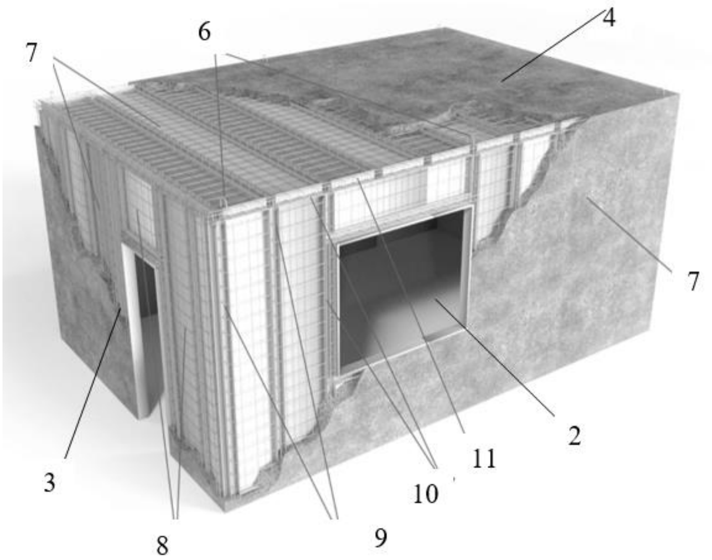

b)

Fig. 4. Constructive solution:
a — volumetric block with a bay window; *b* — rectangular volumetric block (1 — bay window; 2 — window opening; 3 — doorway; 4 — П-shaped longitudinal load-bearing structure; 5 — transverse wall; 6 — mounting loops; 7 — fiber reinforced concrete layer; 8 — reinforcing grid; 9 — frame reinforcing carcass; 10 — metal profile; 11 — strapping reinforcing carcass [2]

One of the major advantages of the suggested design is the possibility of using non-removable formwork made of high-strength moisture-resistant drywall that is one-sided. This allows smooth surfaces suitable for various finishing works to be obtained.

According to regulatory documentation, moisture-resistant formwork is capable of withstanding a humidity of up to 85%, which in turn is acceptable for use in civil buildings with a relative humidity of up to 60%. When the wet mixture is shotcrete onto the drywall formwork, there is instant adhesion and a contact layer is formed ensuring the integrity of the formwork.

The use of drywall formwork helps to cut down labor costs, because it provides a complete interior decoration of the space.

Discussion and Conclusion. As part of the basic principles for constructing new-generation volumetric blocks shotcrete technology enables non-standard spatial planning solutions to be employed and a technological scheme for producing such structures on a construction site to be changed. The inclusion of acceptable types of industrial waste into blocks, increasing the strength of the starting materials and obtaining an economic effect from substituting conventional materials, accounting for geographical features of construction not only contributes to reducing the cost of structures, but also to speeding up waste recycling. This complies with the principles of rational use of natural resources and minimization of a negative environmental impact [1]. The possibility of producing volumetric blocks on a construction site would enhance the scale of volumetric-block housing construction.

References

1. *Industrial Development Strategy for Processing, Disposal and Neutralization of Industrial and Consumer Waste for the Period up to 2030*. Decree of the Government of the Russian Federation No. 84-r dated January 25, 2018. (In Russ.).

2. Golova TA, Mailyan NV, Andreeva NV *Reinforced Concrete Volumetric Block and the Method of its Production.* Patent of the Russian Federation, No. 2781969 C1. 2022. (In Russ.).

3. Golova TA, Andreeva NV, Magerramova IA Production Technology of Non-autoclaved Foam Concrete Dispersed and Reinforced with Modified Fibers. *Bulletin of the Volgograd State University of Architecture and Civil Engineering*. 2020;1(78):126–135. (In Russ.).

4. Abramyan SG, Ulanovsky IA Modular Construction and the Possibility of Using Modular Structures in Building Superstructure. *Don Engineering Bulletin.* 2018;4(51). (In Russ.) URL: https://cyberleninka.ru/article/n/modulnoe-stroitelstvo-i-vozmozhnost-primeneniya-modulnyh-konstruktsiy-pri-nadstroyke-zdaniy/ (accessed: 19.02.2025).

5. Abrahamyan SG, Chestnova AV, Oganesyan OV, Petrosyan RO, Chereshnev LI, Harutyunyan LA Manufacturability of Transforming and Non-transforming Volumetric Block Modules in the Construction of Building Systems. *Don Engineering Bulletin*. 2023;10. (In Russ.) URL: https://cyberleninka.ru/article/n/tehnologichnost-transformiruyuschihsya-i-netransformiruyuschihsya-obemnyh-blok-moduley-pri-vozvedenii-stroitelnyh-sistem (accessed: 19.02.2025).

6. Makarychev KV, Voronin IS, Tarasova KG Prospects of the Technology of Volumetric Block Construction. *International Journal of Humanities and Natural Sciences.* 2023;12-3(87):118-121, (In Russ.) https://doi.org/10.24412/2500-1000-2023-12-3-118-121

7. Ferdous W, Yu B, Ngo T, Manalo A, Mendis P New Advancements, Challenges and Opportunities of Multi-storey Modular Buildings — A State-of-the-art Review. *Engineering Structures.* 2019;183:883–893. https://doi.org/10.1016/j.engstruct.2019.01.061

8. Thai H, Ngo T, Uy B A Review on Modular Construction for High-rise Buildings. *Structures.* 2020;28:1265–1290. https://doi.org/10.1016/j.istruc.2020.09.070

9. Alizadeh SA Volumetric and Block Housing Construction: Experience and Development Prospects. *Architecture and Design.* 2017;1:38-52, (In Russ.) https://doi.org/10.7256/2585-7789.2017.1.23079

10. Belozersky AM Mass Construction from Bulk Blocks in Russia. *Introduction of Modern Structures and Advanced Technologies in the Railway Industry.* 2016;9:280–287. (In Russ.).

11. Kuzmina TK, Avetisyan RT, Mirzakhanova AT Features of Building Construction from Large Modules (Part 1). *Proceedings of Tula State University. Technical Sciences.* 2022;5:95–101, (In Russ.) https://doi.org/10.24412/2071-6168-2022-5-95-102

12. Pakhomova MA, Khramtsov AB Low-rise Construction in Russia and Abroad: a Review of Practices. *Architecture, Construction, Transport.* 2022;3:20-31, (In Russ.) https://doi.org/10.31660/2782-232X-2022-3-20-31

About the Authors:

Levon R. Mailyan, Dr.Sci. (Eng.), Professor of the Department of Construction of University Buildings and Structures, Don State Technical University, (344003, Russian Federation, Rostov-on-Don, 1 Gagarin Sq.), Honored Builder of the Russian Federation, Academician of the Russian Academy of Natural Sciences, ORCID, Lrm@aaanet.ru

Tatiana A. Ivanova, Cand.Sci. (Eng.), Associate Professor of the Department of Architecture at the Kuban State Agrarian University (13 Kalinina St., Krasnodar, 350044, Russian Federation), ORCID, emelyanova-tanya@mail.ru

Natalia V. Andreeva, Cand.Sci. (Eng.), Senior Lecturer, Department of Industrial and Civil Engineering, Balakovo Institute of Engineering and Technology, (140 Chapaeva St., Balakovo, Saratov Region, 413800, Russian Federation), ORCID, anreevane@list.ru

Inna A. Magerramova, Cand.Sci. (Eng.), Associate Professor of the Department of Industrial and Civil Engineering at the Balakovo Institute of Engineering and Technology, (140 Chapaeva St., Balakovo, Saratov Region, 413800, Russian Federation), ORCID, in-namag82@mail.ru

Claimed Contributorship:

LR Mailyan: formation of the basic concept, goals and objectives of the study, scientific supervision, correction of the conclusions.

TA Golova: scientific supervision analysis of the research results, performing the calculations, formation of the conclusions and conclusions.

NV Andreeva: formulation of the conclusions, preparation of the manuscript and graphic materials.

IA Magerramova: search, analysis and systematization of the data, formation of athe reference list.

Conflict of Interest Statement: the authors declare no conflict of interest.

All authors have read and approved the final manuscript.

Об авторах:

Левон Рафаэлович Маилян, доктор технических наук, профессор кафедры строительства уникальных зданий и сооружений Донского государственного технического университета, (344003, Российская Федерация, г. Ростов-на-Дону, пл. Гагарина, 1), заслуженный строитель РФ, академик РААСН, ORCID, Lrm@aaanet.ru

Татьяна Александровна Иванова, кандидат технических наук, доцент кафедры архитектуры Кубанского государственного аграрного университета им. Трубилина (350044, Российская Федерация, г. Краснодар, ул. Калинина, 13), ORCID, emelyanova-tanya@mail.ru

Наталья Викторовна Андреева, старший преподаватель кафедры промышленного и гражданского строительства Балаковского инженерно-технологического института, (413800, Российская Федерация, Саратовская обл., г. Балаково, ул. Чапаева, 140), кандидат технических наук, ORCID, anreevane@list.ru

Инна Александровна Магеррамова, кандидат технических наук, доцент кафедры промышленного и гражданского строительства Балаковского инженерно-технологического института, (413800, РФ, Саратовская обл., г. Балаково, ул. Чапаева, 140), ORCID, in-namag82@mail.ru

Заявленный вклад авторов:

Л.Р. Маилян: формирование основной концепции, цели и задачи исследования, научное руководство, корректировка выводов.

Т.А. Голова: научное руководство, анализ результатов исследований, проведение расчетов, формирование заключения и выводов.

Н.В. Андреева: формулировка выводов, подготовка текста и графических материалов.

И.А. Магеррамова: поиск, анализ и систематизация данных, формирование списка литературы.

Конфликт интересов: **авторы заявляют об отсутствии конфликта интересов.**

Все авторы прочитали и одобрили окончательный вариант рукописи

Received / Поступила в редакцию 24.02.2025

Reviewed / Поступила после рецензирования 03.03.2025

Accepted / Принята к публикации 10.03.2025

BUILDING CONSTRUCTIONS, BUILDINGS AND ENGINEERING STRUCTURES

СТРОИТЕЛЬНЫЕ КОНСТРУКЦИИ, ЗДАНИЯ И СООРУЖЕНИЯ

UDC 624.072.22
https://doi.org/10.23947/2949-1835-2025-4-1-15-25

Original Empirical Research

Modern Technological Solution for Covering the Cylindrical Vault of the Nave during the Construction of the Church of St. Tikhon in St. Petersburg

Nadezhda V. Rozantseva ✉, **Alexander D. Drozdov**
Saint Petersburg State University of Architecture and Civil Engineering, Saint Petersburg, Russian Federation
✉ nrozanceva@lan.spbgasu.ru

EDN: KJZRYO

Abstract

Introduction. The article is dedicated to the history of the development and implementation of the project for the construction of the ceiling of the nave of the church of St. Tikhon, Patriarch of Moscow and All Russia, at 17 Commune Street, St. Petersburg. The church was built and is under construction on an order of a local religious organization with donations from whoever cares to do this and church visitors. The original project envisaged the construction of an arched cylindrical vault above a masonry nave, which called for complex engineering solutions and considerable labor and financial costs. By October 2024, it became clear that construction in the traditional way would not enable the church to be consecrated, having completed this project in a short time and with limited funds. The aim of the study was to develop an alternative solution to the construction of arched brickwork with puffs on the short side of the nave of the temple.

Materials and methods. Having considered the options available, we decided to make use of arched beams as stiffeners, which were supposed to take on some of the load, including from the strut. It was assumed that it was possible to replace the prestressed reinforcement of the upper row with a combined one making it possible to optimize the arch design. In order to identify the required parameters, loads were collected and the stress strain of the arch was calculated, including in the SCAD program provided it was at the operational stage. The reduction of stress zones is achieved by additional reinforcement with rods and clamps.

Results. The research enabled us to reduce costs while maintaining the structural rigidity of the arch. In accordance with the calculations, the formwork drawings have been developed. The process of transferring parameters from drawings to actual dimensions and concreting was meticulously organized by means of modern quality control tools at each stage. The installation of ready-made reinforced concrete structures turned out to be more technologically advanced and faster than a monolithic system.

Discussion and Conclusion. The brick vault project was successfully completed with minimal deviations involved. The support area of the structures and the height of the arch rise fully corresponded to the calculated values. The solution was found to have made it possible to considerably cut down the load on the base, increase the overall structural rigidity, while freeing the space under the dome from tightening, reduce construction times making it possible to meet the deadlines as well as to reduce the costs. The scientific novelty of using arches with a mixed reinforcement system is the simplicity of the design, the absence of the need to increase the cross-section of the truss elements and the possibility of using combined reinforcement.

Keywords: nave, cylindrical vault, intermediate supports, arched beam, combined reinforcement

Acknowledgements. The authors would like to thank the General Director of ZHBI-8 for providing their facilities and manufacturing arches for the church of St. Tikhonas well as the editors and reviewers for their attentive attitude to the article and the above comments making it possible to improve its quality.

For citation. Rozantseva NV, Drozdov AD Modern Technological Solution for Covering the Cylindrical Vault of the Nave during the Construction of St. Tikhon's Church in St. Petersburg. *Modern Trends in Construction, Urban and Territorial Planning.* 2025;4(1):15–25. https://doi.org/10.23947/2949-1835-2025-4-1-15-25

Оригинальное эмпирическое исследование

Современное технологическое решение перекрытия цилиндрического свода нефа при строительстве храма святителя Тихона в Санкт-Петербурге

Н.В. Розанцева ✉, **А.Д. Дроздов**
Санкт-Петербургский государственный архитектурно-строительный университет, г. Санкт-Петербург, Российская Федерация
✉ nrozanceva@lan.spbgasu.ru

Аннотация
Введение. Статья посвящена истории разработки и воплощения проекта строительства перекрытия нефа храма святителя Тихона, патриарха Московского и всея России, на улице Коммуны, дом № 17а, в г. Санкт-Петербурге. Храм строился и строится по заказу местной религиозной организации на пожертвования неравнодушных и прихожан. В первоначальном проекте предполагалось возведение арочного цилиндрического свода над нефом из каменной кладки, что требует сложных инженерных решений и значительных затрат труда и средств. К октябрю 2024 года стало понятно, что строительство традиционным способом не позволит освятить храм, выполнив этот проект в сжатые сроки и при ограничении средств. Целью исследования была, разработка альтернативного решения устройству арочной кирпичной кладки с затяжками по короткой стороне нефа храма.
Материалы и методы. После рассмотрения вариантов принято решение использовать арочные балки в качестве ребер жесткости, которые должны были взять на себя часть нагрузки, в том числе и от распора. Выдвинуто предположение о возможности замены преднапряженной арматуры верхнего ряда на комбинированную, позволяющее оптимизировать конструкцию арки. Для определения требуемых параметров произведен сбор нагрузок, и расчет напряженного состояния арки в том числе и в программе SCAD с учетом ее работы на стадии эксплуатации. Снижение зон напряжений достигнуто дополнительным армированием стержнями и хомутами.
Результаты исследования. Проведённые исследования позволили уменьшить расходы сохраняя конструктивную жесткость арки. В соответствии с расчетами разработаны опалубочные чертежи. Процесс переноса параметров с чертежей в реальные размеры и бетонирование был тщательно организован, использовались современные инструменты для контроля качества на каждом этапе. Монтаж готовых железобетонных конструкций оказался более технологичным и быстрым по сравнению с монолитной системой.
Обсуждение и заключение. Проект кирпичного свода был успешно выполнен с минимальными отклонениями. Площадь опирания конструкций и высота подъема арки полностью соответствовали расчетным значениям. Было установлено, что принятое решение позволило значительно сократить нагрузку на основание, повысить общую конструктивную жесткость, при этом освободив пространство под куполом от затяжек, снизить продолжительность строительства, что позволило уложиться в заданные сроки, и уменьшить стоимость работ.
Научная новизна применения арок со смешанной системой армирования заключается в простоте конструкции, отсутствии необходимости увеличения сечения элементов ферм и возможности использования комбинированной арматуры.

Ключевые слова: неф, цилиндрический свод, промежуточные опоры, арочная балка, комбинированная арматура

Благодарности: Авторы благодарят генерального директора ЖБИ-8 за предоставление своих мощностей и изготовление арок для храма святителя Тихона, а также авторы выражают благодарность редакции и рецензентам за внимательное отношение к статье и указанные замечания, которые позволили повысить ее качество.

Для цитирования. Розанцева Н.В., Дроздов А.Д. Современное технологическое решение перекрытия цилиндрического свода нефа при строительстве храма святителя Тихона в Санкт-Петербурге. *Современные тенденции в строительстве, градостроительстве и планировке территорий*. 2025;4(1):15–25. https://doi.org/10.23947/2949-1835-2025-4-1-15-25

Introduction. Since time immemorial, in the most trying times, humanity have been aspiring to come together into a single cohesive unity under the protectorate of a strong state. During this period, faith serves as the greatest uplifting and unifying force. As a social institution and regulator of economic as well as other relations, the Church has the capacity to unite human society. It shapes people's worldviews, establishes moral and ethical regulations, and also lends one a sense of comfort and security that has been lost as a result of some external factors. All of this contributes to unite individuals based on a shared worldview and religion, to increase social engagement, spiritual revival, and preserve cultural heritage as well as customs, which builds an overall positive image of the country as well as its attractiveness as a tourist destination. It is also of interest to note the economic component when the revival of faith and the construction of temples contribute to creation of jobs and regional economic development. The Church of St. Tikhon, Patriarch of Moscow and

All Russia, at 17a Commune Street, is one of the first churches in the Northwestern District to have been dedicated to a real person directly related to St. Petersburg, a new martyr from the early years of Soviet power, who ran the Patriarchate in the most trying times for the church. A man who actually accomplished his own small feat and devoted his entire life to the Russian Orthodox Church and experienced the "Levashov Golgotha" [1, 2] following the Petrograd trial of 1922. 2025 marks the death of St. Tikhon, Patriarch of Moscow and All Russia.

The church was built and is being built by an order of a local religious organization and funded with the donations from parishioners of the Kursk Root Icon of the Mother of God "Of the Sign" located nearby. Construction got underway in the late 2021. In fact, the church had already been completed, and in early January 2025, Archpriest Alexander Pashkov conducted the first service. An iconostasis will be set up in the nearest future [3]. The stone church was constructed under the challenging conditions: the confined space as most of it was built outside the site designated for religious use, the rather daunting layout of the foundation as well as some funding issues with rigidly set construction deadlines to be met. The original design of the five-domed church was developed by LLC AMC-Project: made of red brick, in the neoclassical style shaped like a ship, with a tent-topped bell tower and main volume. However, it had to experience some modifications for a number of reasons. The latter were due to the need to reduce the construction time (while maintaining structural rigidity and architectural integrity) as well as the cost of the project. The objective of the study is to develop the organization and construction of arched beams on the short side of the nave as an alternative to a cylindrical brick vault with puffs given the preservation of the required height of the cylindrical brick vault and the overall structural rigidity of the church as a whole. The scientific novelty is a new reinforced concrete structure in the previously developed classical temple project with walls already built. This solution enabled the maintainenance of the structural rigidity without having to make use of the required tightening forces, thereby freeing up internal space and reducing the labour costs and indices.

Materials and Methods. Domed and cylindrical arches made of masonry have been known since the Roman Empire. These arches are among the most durable and resistant to maximum loads. The considerable disadvantages of such structures are high load on the base; the complete impossibility of mechanizing work during their construction and thereby cutting down the labour costs and construction time; the need for masons to perform work with very high qualifications; the high cost of such work. The masonry of arches and vaults must be carried out from the heel to the castle simultaneously on both sides, using two teams of masons [4]. The masonry is completed by jamming the vault with castle bricks. Masonry should be carried out in small sections to avoid collapse. All seams of the masonry must be completely filled with mortar. The central axis of each brick must be strictly perpendicular to the surface of the vault. While laying arches made of bricks or stones, it is essential to fill the seams with a liquid solution without rubbing the upper surface of the arches. The laying of arches of double curvature should begin no earlier than a week after the end of the installation of their heel. The outside temperature should be above +10 °C. If the air temperature is from +10 to +5 °C, then the period increases by one and a half times, and at temperatures from +5 to +1 ° C — by two times. The section of the vault can be demoulded no earlier than after 10-20 days at an outdoor temperature of at least +10 °C.

a) *b)* *c)*

Fig. 1. Church of St. Tikhon, Patriarch of Moscow: a — exterior of the temple; b — section of the church considering account the built-in arched beam structure; c - view of the church towards the altar from the inside

At lower positive temperatures, the duration of exposure of the arches on the formwork increases. While laying arches with a lifting boom, the strut must be fixed by tightening and additionally along the arc of the circle, as in our case. Precast reinforced concrete elements made of concrete of a grade not lower than M200, reinforced with structural reinforcement with a diameter of 6-8 mm, are installed in the heels where the faces are adjacent. It is also possible to use steel elements made of corners, sheet and strip steel. The ends of the puffs are passed through these elements. To increase the stability of the support units under the action of the arch strut, outrigger heels are installed in the support units, which form a cornice from the inside of the room. Outrigger heels also increase the stability of the support units. The supporting nodes of the vault must have inclined surfaces formed by stepwise laying of brickswhich must be perpendicular to the axis of the vault. The technology has barely changed since the onset of the construction of stone temples. From all of the above, the conclusion was that it was rather challenging to perform high-quality masonry, to meet a tight deadline while on a tight budget. Fig. 1 shows photographs of the Church of St. Tikhon and a drawing of the section of the temple taking into account the built-in structure. The problem of installing an entirely monolithic dome cover was not looked at. One of the flaws of solid monolithic structures for religious domes is that their construction calls for special skills and technologies, which is more costly than a system of using beam arches.

The First Assumption. In order to avoid tightening, while maintaining structural rigidity, it was critical to reinforce sections of the arch structure with a certain step, i.e., to reinforce the regular frame hidden in the filling masonry, and to make use beam arches protruding from the arch masonry, which would serve as a sort of stiffeners.

The Second Assumption. In arches made completely of clinker bricks, there is frequently extra spacer force occurring, and special devices are needed in order to perceive this spacer [5]. It was decided to reinforce the walls under the heels of these arches with pilasters which will be capable of withstanding the pressure from the weight of the vault and of accepting the strut. It is due to this solution that the arch in an overloaded area is sufficiently reinforced, although there are unnecessary protrusions in the room. The major task facing the designers working on the reinforcement of concrete arches was to design arches of a certain height with a small mass, i.e., those consuming the lowest amount of the material. They can be installed using cranes with a low lifting capacity while maintaining the required rigidity and height of the dome. The height of the arch of the arch depends on its bearing capacity: a large one increases it, because the area of the compressed zone and the moment of inertia of the section rise, i.e., the cross—section of the arch becomes bigger; an arc which is excessively large might cause a drop in the bearing capacity due to reduced rigidity and increased deflections. The optimal height should thus ensure maximum load-bearing capacity with the lowest amount of material consumed and compliance with the requirements for rigidity and crack resistance [6]. One of the key indicators of quality and mechanical safety of operation is the residual load-bearing capacity. It is identified by means of a few criteria: the strength of reinforcement and concrete, stiffness, crack formation and their opening width.

The optimal height is taken based on the bending moment and wall thickness to ensure the minimum cost of the arch in terms of how much material is consumed. The width of the nave of the temple — the length of the arch span — was taken based on the previously projected dimensions — 8.05 m, the required arch elevation — 1150 mm, considering the height of the latter to enter into the previous high-rise design of the nave vault. The height of the arch masonry is 640 mm. For the initial calculation, the height of the reinforced concrete arch, pinched at two ends, was assumed to be at least 1/15 of the span, i.e., approximately 400 mm between the outer edges of the belts. The formula for a parabolic arch was employed to calculate the radius of curvature of the arch which is part of the structure. Substituting these values, we get:

$$R = \frac{h^2 + \frac{\omega^2}{4}}{2h} \approx 6{,}85\text{m},$$

where R — desired radius of curvature; ω — the width of the span (in this case, the width of the nave) — 8,05 m; h — the height of the arch rise from the center of the span to the top of the arch 1,15 + 0,4 = 1,55 m.

0.6 m will thus fall on the support node on each side. The width for the calculation was taken based on the height-width ratio — 468 mm, which is due to the size of the upper platform of the support element. The estimated rebar pitch is 200 mm. The arches are designed using class B40 concrete.

The Third Assumption. In most projects, while using reinforced concrete arches of a similar design, prestressed reinforcement has always been used, which does not cause tensile stresses from operational loads. While designing such beam arches, there have been no studies of the effect on the distribution capacity of the reinforcement spatial system in operation. The features of reinforcement for curved span arches include the use of special indirectly spiral-reinforced reinforcement, such as individual wires, strands and rods of a periodic profile. Bundles with internal anchors and continuous reinforcement on cassettes are also used. Reinforcement tension can take place prior to concreting (on the stops) or following it (on concrete).

The downsides of this design approach are the following:

– it leads to unjustified consumption of reinforcing steel.;

– reinforcement in accordance with the material plots becomes more complicated, i.e., it becomes impossible to discontinue the reinforcement where it is not required along the entire structure.;

– it is necessary to apply great efforts to the force forms while pulling the reinforcement and crimping the concrete during transfer of forces from the stops to the concrete.

Previously used structures for relatively small spans were not cost-saving in terms of how much material was consumed. In this case, the arched beams function as a single spatial system due to the combined arrangement of the upper brick vault. It was thus decided to make use of mixed reinforcement by replacing the permissible number of high-strength beams with conventional bar reinforcement. A stressed Grade A-IV (A600) reinforcement of a periodic profile was designed in the lower belt, Grade A400 longitudinal reinforcement was used in the remaining elements, and elements of transverse and mounting A240 reinforcement were provided to maintain the transversely rigid superstructure. The bearing capacity of a beam arch depends on its geometric dimensions, materials of manufacture and operating conditions. The key factor influencing this indicator is the maximum load that the structure can withstand without deformation or destruction [7].

The loads were collected. Given the brick density $\rho \approx 1800$ kg/m^3 and the the volume of the arch masonry[1]:

$$V = L \cdot \omega \cdot H = 24\text{m} \cdot 8{,}05 \cdot 0{,}64 = 122{,}88\text{m}^3,$$

where ω — width of the arch (equalling that of the niche).

The weight of the vault is thus:

$$P = \rho \cdot V = 221{,}184\text{т}.$$

While calculating the vault, the likelihood of an increase in the constant load distributed over the horizontal projection of the vault, in the direction from the center to the supports along the curve, was considered:

$$g_x = g \cdot \left(\frac{1}{cos\varphi} - 1\right),$$

where g_x — additional constant load caused by the slope of the coating in sections located at a distance from the *x* support, kgf/m; g — constant load in the center of the vault a kg/m; φ — angle of inclination to the horizon of the tangent to the axis of the arch in the investigated section.

There was a task of calculating the permissibility of replacing the upper row of bundles of prestressed reinforcement with rod reinforcement[2] [8] given its further bending into the supporting compressed zone of concrete. In order to confirm the assumption, theoretical calculations of the upper belt were conducted based on the cross section of the reinforcement:

$$A_{\text{тр}} = \frac{N_2}{R_b + 0{,}01 R_{sc}},$$

where R_{sc} = 355 MPa — расчетное сопротивление продольного профиля design resistance of the longitudinal profile of an operating Grade A400 reinforcement. $A_{\text{тр}}$ — required longitudinal cross-sectional area of one reinforcement rod of the upper belt; N_2 — force in the longitudinal reinforcement; R_b — calculated concrete resistance of class B40 concrete — 51,37 MPa.

With the previously assigned width of the arch elements (468 mm), the required cross-sectional height of the upper belt is $h_{\text{тр}} = A_{\text{тр}}/b$; h — 12 mm. The area of the longitudinal operating reinforcement with an average coefficient of longitudinal bending is φ = 0,9. 8 rods with a diameter of 16mm are accepted.

Research Results. In order to validate the studies and obtain a more nuanced answer, the stress state of the beam arch was calculated in the SCAD software package considering the operation of the arch at the operational stage, respectively, the loads from external forces were assigned for the stage. The accepted concrete class is B40.

[1] SP (СП) 20.13330.2011. Loads and Impacts.

[2] Krylov S.B, Chistyakov E.A, Zenin S.A., Sokolov B.S., Sharipov R.Sh., Kudinov O.V. *Monolithic Reinforced Concrete Structures with Stressed Reinforcement without Adhesion to Concrete, Design Guidelines: a Methodological Guide*. Moscow; 2017. 206 p.

The original task was to reduce the amount of prestressed reinforcement and replace the upper row of prestressed reinforcement with rod one accompanied by its bending according to the materials plot into the compressed concrete zone supposed to reduce losses in material consumption and maintain the operability of the structure. It can be seen from the isofields that the analytical calculation was performed correctly. Unlike the supporting section where the stresses in the support area are visible from the isofields on the plan, the replacement with class A400 reinforcement does not impact the bearing capacity of the arch in terms of bending moment. The obtained results of the isofields are shown in Fig. 2. It was decided to reduce such stress zones by applying additional reinforcement with conventional rod fittings and clamps, i.e., to apply mixed reinforcement.

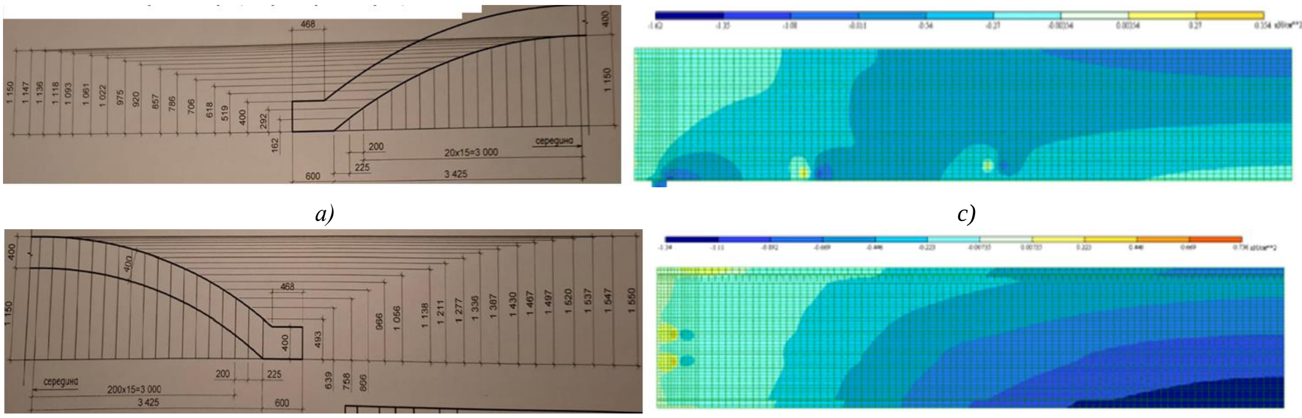

Fig. 2. Sketch for calculating the beam arch in the SCAD program: *a* — formwork diagram, center drawing (left side); *b* — shuttering drawing (right side); *c* — isofields of normal arch stresses (longitudinal section along the axis); *d* — isofields of normal arch stresses in the plan

The bordering rods are made integral with their joining in the upper zone of the support nodes and in the lower zone of the truss. The area of the longitudinal upper rods is at least 0.05% of the cross—sectional area of the support units, the diameter is 16 mm, while spatial frames and additional transverse fittings in the form of A240 steel clamps are installed at the bends of the support units to ensure reliable anchoring of the stretched reinforcement of the lower belt. In the span area, 15 rods of transverse reinforcement with a pitch of 200 mm are accepted, while additional elements are installed in 100 mm increments on the lower belt and at least 200 mm from the end of the support unit. The most challenging issue in the production of such reinforced concrete structures by means of a bench method is the accuracy of transferring parameters from drawings to actual dimensions, which is a complex and demanding task calling for a high level of professionalism. Even the slightest deviations from the set parameters might cause grave consequences with the geometry of the finished product distorted as well as the arched beam not quite matching the actual required parameters. For instance, a lack of reinforcement reduces the load-bearing capacity of the structure, while an excess of reinforcement causes an increase in the weight and cost of the product.

In order to prevent such problems from occurring, the process of transferring dimensions from the drawing to the actual structure was meticulously organized. It was also decided to form an arch on the edge as the most optimal position for concreting and transportation[3]. The alignment was performed on the geodetic substructure. In order to minimize the risks associated with possible errors in the production, the ADA 3D Liner 4V laser plane builder and the GeoMax Zoom50 1 A5 Polar total station were used. A number of actions were continuously performed[4] as part of continuous control[5] [9].

The formwork must have strength, stability, and tightness, the concrete must not leak, closely reproduce the shape of the future product, and be easy to install and remove to minimize time and labor costs. Errors during the formwork assembly might generate cracks, crevices and other defects. As the formwork was for a single order, and only eight such arches were required, the plane was made of bent plywood. In order to withstand the pressure of freshly poured concrete and prevent deformation and displacement, it was loosened with bars. The reinforcement frame was bent in place with

[3] SP (СП) 70.13330.2012. Bearing and Hedging Structures.
[4] SP (СП) 126.13330.2012 Geodetic Works in Construction.
[5] Letchford A.N., Shinkevich V.A. *Construction Control Guidelines*. SPb.; 2016. 592 p. (ISBN 978-5-904362-07-2)

little heating given the requirements for strength and rigidity of the structure. All the components are made according to the developed project considering the building codes and regulations. After the reinforcement frame had been checked for compliance with the deck shape, it was moved inside the formwork and secured based on the dimensions of the protective layer. B40 grade concrete mix was used, the work was carried out to ensure uniform pouring of concrete and prevent voids. The process is shown in Fig. 3. It was after it had been delivered to the construction site that the final product was tilted to its design position.

a) *b)* *c)*

Fig. 3. Visualization of the process of creating a reinforced concrete structure:
a — reinforcement carcass; *b* — single formwork; c — final arched beam on the edge

The work was assessed at each stage. An additional bonus is that the decision enabled the load on the base to be significantly reduced, including by reducing the height of the masonry from 1 m to 0.64 m, increase the overall structural rigidity, while freeing the space under the dome from tightening.

Discussion and Conclusion. The project was designed with minimal deviations and did not call for any adjustments during the installation, the support area of the structures and the height of the arch rise were in full agreement with the calculated values. By the onset of the arch installation, the walls had been constructed, supporting pilasters, adjustable supporting scaffolding adopted, a formwork template ("circles") and a template for angles for brickwork made. All of these were performed with an automobile crane (Fig. 4). The formwork templates under the brickwork of the vault was moved with a winch. In order to create a flow-through method of work and reduce the construction time, the dome of the nave started being laid with a one-day delay by installing the arches. All the movements were performed using scaffolding.

a) *b)*

Fig. 4. Arched beam installation: *a* — a beam mounted on a support pilaster; *b* — crane mounting with a tip

The masonry of the dome vault was performed with the installation of bricks "on the edge" simultaneously by two teams of masonry workers on both sides of the nave from the heels to the top with the seams thoroughly litigated to considerably reduce labor costs as well as to improve the stability of the vault. The work was being closely monitored during the laying. In order to prove the method had been correctly chosen, the cost of bricklaying the nave vault was calculated according to "The Uniform Standards and Prices for Construction, Installation and Repairs"[6] considering the installation of the embedded parts and the tightening of the arch as well as the installation arches as stiffeners. The calculation results are shown in Table 1 and 2.

Table 1

Calculation of labor and machine time costs for the brickwork of the vault

№	Justification (CNTD) (ЕНиР)	Technological processes	Measurement unit	Amount of work	Time standard		Labour costs	
					workers, person-h	vehicles, vehicle-h	workers, person-h	vehicles, vehicle-h
1	E3-20A	Supply and installation of scaffolding with a vehicle crane	10 m^3	4.33	1.44	0.48	0.78	0.26
2	E15-35	Installing the formwork template in the operating position	m^2	1135.68	0.37	0	52.53	0
3	E1-6	Supplying the solution to the site	m^3	174.44	0.84	0.42	18.32	9.16
4	E1-6	Supplying the bricks to the site	1000 items	37.472	0.36	0.18	1.69	0.84
5	E3-10	Laying a brick vault on cement mortar	m^3	726.84	3.8	0	345.25	0
6	E3-9	Installing supporting parapets	m^3	10.56	3.5	0	4.62	0
7	E3-18	Installing steel elements and parts into the walls	100 kg	6.8	1.1	0.33	0.94	0.28
8	E25-7	Unwinding and moving the steel rope	100 m of the rope	0.736	2.6	0	0.24	0
9	E3-18	Installing steel element puffs	100 items	0.16	24.5	1.24	0.5	0.03
10	E25-7	Winding and moving	100 m of the rope	0.736	2.9	0	0.27	0
11	E25-7	Adding an extra incision for each additional one	100 m of the rope	0.736	0.69	0	0.07	0
12	E4-1-28	Caulking and stitching	10 m	4.8	1.4	0.56	0.84	0.34
13	E3-10	Lowering the formwork on the wedges	m^2	1135.68	0.55	0	78.08	0
14	E1-6	Rearranging the scaffolding with a crane	100 t	0.33	23	11.5	0.95	0.47
15	E25-20	Moving the formwork template with a manual winch	items	20	0.76	0	1.90	0
							506.93	**11.39**

*Note: the calculated costs do not consider the production and disassembly of the formwork template for the vault.

[6] CNTD (ЕНиР). The Uniform Standards and Prices for construction, Installation, and Repairs. VolumeE 1. Internal Construction Transport Works: https://docs.cntd.ru/document/1200000897
CNTD (ЕНиР). Volume E 3. Stonework: https://docs.cntd.ru/document/1200001038
CNTD (ЕНиР). Volume 4. Installation of Prefabricated and Monolithic Structures: https://www.ects.ru/images/1685/Image/enir_7_vypusk_1_betonnye_i.pdf
CNTD (ЕНиР). Volume 25. Rigging: https://docs.cntd.ru/document/1200001092

Table 2

Calculating labor and machine time costs for installing brick masonry on reinforced concrete beams

№	Justification (CNTD) (ЕНиР)	Name of technological works	Measurement unit	Amount of work	Time standard		Labour costs	
					workers, person-h	vehicles, vehicle-h	workers, person-h	vehicles, vehicle-h
1	E3-20A	Supplying and installing the scaffolding with a car crane	10 m^3	4.33	1.44	0.48	0.78	0.26
2	E4-1-29	Constructing a concrete bed	m^2	4.656	0,22	0	0.13	0.00
3	E4-1-6	Installing the arches	1 item	8	1.7	0.16	1.7	0.16
4	E15-35	Installing the formwork template in the operating position	m^2	1135.68	0.37	0	52,53	0
5	E1-6	Supplying the solution to the site	m^3	174.44	0.84	0.42	18.32	9.16
6	E1-6	Supplying the bricks to the site	1000 items	37.472	0.36	0.18	1.69	0.84
7	E3-10	Laying a brick vault on cement mortar	m^3	726.84	3.8	0	345.25	0
8	E1-6	Rearranging the scaffolding with a crane	100 t	0.33	23	11,5	0.95	0.47
9	E25-20	Moving the formwork template with a manual winch	items	20	0.76	0	1.90	0
							423.23	**10.90**

*Note: the calculated costs do not consider the production and disassembly of the formwork template for the vault.

According to the calculations, technical and economic indicators have been listed (Table 3).

Table 3

Technical and economic indicators

Indicator	For the brick vault	For the vault fitted with ferroconcrete arches
Labour costs, person-cm	506.93	423.23
Costs of machine time of the vehicle crane, vehicle-cm	11.39	10.9
Number of operations	15	9
Total duration of the work given the formation of the teams, person-cm	156.6	111.9
Duration in months	7.2	5.08

Based on the obtained data and the construction outcomes, the fact that the correct decision had been made was confirmed. The beam arches were the stiffeners. They offer the following advantages:

– cost-efficiency — construction costs are reduced by using fewer materials;

– arches are characterized by a lower weight and volume compared to traditional solutions leading to a reduction in transportation costs.

It was also suggested that a combined reinforcement frame could be made use of. Beam arches are highly resistant to various types of loads. In order to minimize risks, the calculations were double-checked in the SCAD program. Such verification calculations enable the quality of work to be improved through the course of construction of critical structural elements and a three-dimensional model of the future product to be designed. A test of the structure even prior to the start of the installation cycle at the calculation stage enabled stresses in the reference zone to be identified by means of isofields, which made it possible to correct the shortcomings at the design stage. The installation of ready-made reinforced concrete structures is highly technologically advanced. On top of that, unlike a monolithic system, it barely depends on weather conditions; it does not call for a long exposure in the formwork, as factory-manufactured products are employed with a multi-series when the formwork can be used on a few serial elements cuttinf down production costs. A well-developed and standardized process simplified construction, reduced the duration of work and met deadlines cutting down the costs of work.

Modern construction is being faced with the need to keep on searching for ways to optimize processes designed to reduce the construction time of various facilities, including religious buildings. Traditional approaches based on the use of brick vaults with complex systems of tabs and strands are rather time-consuming.

The use of arched beams enabled the principle of reasonable saving of materials and labor costs to be showcased.

The efficient organization of the dimensional transfer process and control at all the construction stages enabled minimization of errors and discrepancies between the design documentation and the actual construction. Modern technologies and geodetic equipment have improved the quality, reliability and efficiency of the construction considering the use of available resources.

The use of arched beams instead of the traditional approach using embedded parts and puffs is a promising direction in modern technology for the construction of religious buildings. This method would considerably reduce the construction time: in our case, the difference in the duration of construction was about two months, which also saved funds without compromising the level of quality and safety. Given all of these advantages, a further increase in the demand for the suggested method in the construction of religious buildings is highly likely.

The scientific novelty of using arches (instead of trusses as well) with a mixed reinforcement system is the following:

– simple assembly design and manufacturing technology compared to segment trusses or a tightening device;

– there is no need to increase the cross-section of the truss elements and their reinforcement compared to diagonal trusses due to rigid assemblies;

– in the manufacture of solid molds, it is possible to make use of combined reinforcement only with a prestressed lower belt: it has been confirmed that the use of nonstressed reinforcement complete with prestressed reinforcement in these reinforced concrete structures does not disrupt its bearing capacity;

– the possibility of manufacturing beam arches in simple formwork with no use of inserts. Beam arches can also be employed in restoration of historical buildings where it is critical to preserve the original architectural style while improving the technical characteristics of the structure.

References

1. Damaskin (Orlovsky). *Martyrs, Confessors and Ascetics of Piety of the Russian Orthodox Church of the 20th century. Biographies and Materials for them.* Book 4. Tver: Bulat, 2000; Book 6. Tver: Bulat, 2002. (In Russ.).

2. Tsypin V. *History of the Russian Church.* 1917-1997. Moscow: Publishing House of the Spaso-Preobrazhensky Valaam Monastery, 1997: 831 p. (In Russ.).

3. *Church of St. Tikhon, Patriarch of Moscow and All Russia* (In Russ.) URL: https://globus.aquaviva.ru/khram-svyatitelya-tikhona-patriarkha-moskovskogo-i-vseya-rossii-na-ulitse-kommuny (accessed: 11.02.2025).

4. Yudina A.F., Verstov V.V., Badin G.M. *Technological Processes in Construction.* M.: Publishing Center "Academy", 2013: 304 p. (In Russ.).

5. Orlovich R.B., Chakalidi V.X. Ways of Strengthening Cylindrical Stone Vaults. *Construction and Reconstruction.* 2017. №1(69):50-55, (in Russ.) URL: https://construction.elpub.ru/jour/article/view/8 (accessed: 11.02.2025)

6. Shannat I. *Stress-strain of Reinforced Concrete Monolithic Multi-wave Shells with Contoured Elements in the Form of Prefabricated Bevel-free Trusses.* Abstract of the dissertation for the degree of Candidate of Technical Sciences. Moscow, 1992:19p. URL: https://tekhnosfera.com/napryazhenno-deformirovannoe-sostoyanie-zhelezobetonnyh-monolitnyh-mnogovolnovyh-obolochek-s-konturnymi-elementami-v-vide (accessed: 11.02.2025).

7. Koyankin A.A., Mitasov V.M. Stress-strain of a Prefabricated Monolithic Element Considering Loading of the Assembled Part. *Bulletin of the Tomsk State University of Architecture and Civil Engineering*. 2021;23(3):129–142. (In Russ.) https://doi.org/10.31675/1607-1859-2021-23-3-129-142

8. Osipenko Yu.G., Kuznetsov V.S., Shaposhnikova Yu.A. Effect of Using High-strength Reinforcement without Adhesion to Concrete on the Strength of Monolithic Girderless Floors. *Bulletin of MGSU*, 2017, vol. 12No.8(107): 885-891 https://doi.org/10.22227/1997-0935.2017.8.885-891

About the Authors:

Nadezhda V. Rozantseva, Cand.Sci. (Eng.), Associate Professor of the Department of Construction Organization at St. Petersburg State University of Architecture and Civil Engineering (4 2nd Krasnoarmeyskaya St., 190005, St. Petersburg), ScopusID, ORCID, nrozanceva@lan.spbgasu.ru

Alexander D. Drozdov, Cand.Sci. (Eng.), Associate Professor of the Department of Construction Organization at St. Petersburg State University of Architecture and Civil Engineering (4 2nd Krasnoarmeyskaya St., 190005, St. Petersburg), ScopusID, ORCID, drosdov@list.ru

Claimed Contributorship:

NV Rozantseva: development of the idea, aims and objectives of the study, calculations, analysis and drawing conclusions, manuscript preparation, revision of the manuscript.

AD Drozdov: scientific guidance, formation of the basic concept.

Conflict of interest statement: **the authors do not have any conflict of interest.**

All authors have read and approved the final version of manuscript.

Об авторах:

Розанцева Надежда Владимировна, кандидат технических наук, доцент кафедры организации строительства Санкт-Петербургского государственного архитектурно-строительного университета (190005, Российская Федерация, г. Санкт-Петербург, ул. 2-я Красноармейская, 4), ScopusID, ORCID, nrozanceva@lan.spbgasu.ru

Дроздов Александр Данилович, кандидат технических наук, доцент кафедры организации строительства Санкт-Петербургского государственного архитектурно-строительного университета (190005, Российская Федерация, г. Санкт-Петербург, ул. 2-я Красноармейская, 4), ScopusID, ORCID, drosdov@list.ru

Заявленный вклад авторов:

Н.В. Розанцева: разработка идеи, цели и задачи исследования, проведение расчетов, анализ и формирование выводов подготовка текста, доработка текста.

А.Д. Дроздов: научное руководство, формирование основной концепции.

Конфликт интересов: **авторы заявляют об отсутствии конфликта интересов.**

Все авторы прочитали и одобрили окончательный вариант рукописи

Received / Поступила в редакцию 14.02.2025
Reviewed / Поступила после рецензирования 28.02.2025
Accepted / Принята к публикации 10.03.2025

BUILDING MATERIALS AND PRODUCTS

СТРОИТЕЛЬНЫЕ МАТЕРИАЛЫ И ИЗДЕЛИЯ

Check for updates

UDC 667.6
https://doi.org/10.23947/2949-1835-2025-4-1-26-34

Original Empirical Research

Optimization of the Paintwork Material Modified by Metal Catalyser Additive

EDN: GTWFIR

Alexander K. Khalyushev ✉, **Elena A. Kolesnichenko**
Don State Technical University, Rostov-on-Don, Russian Federation
✉ khaljushev@mail.ru

Abstract
Introduction. Current trends in the paint and varnish materials industry are embracing environmental friendliness and versatility lending wooden products good aesthetic and protective properties. The structure of wood, as a natural material, is constantly undergoing intensive and progressive processes of oxidative degradation under environmental conditions affecting the strength of wood and causes significant structural changes. Therefore the interest in improving the durability of paint coatings under the influence of environmental factors on their performance justifies the intensification of research in the development of new effective solutions. One of the effective ways to prevent the destruction of the wood structure is to apply a protective layer of paint and varnish material by chemically modifying the surface and, above all, by introducing siccatives. The introduction of siccatives makes it possible to ensure a uniform drying rate throughout the entire volume and additionally disperse the pigment, which improves the physical and mechanical properties of the paintwork and increases its durability.
The purpose of the research work is to establish the effect of the addition of a metallic catalyst in the form of highly dispersed precipitation waste from an electric arc furnace on the physical and mechanical properties of paint and varnish materials.
Materials and Methods. The initial components for obtaining oil paint compositions (paintwork material) were used in the experiments as: binder-natural olifa, pigment-ochre, fine aggregate-chalk. To the intensification of the drying process, the addition of metal catalyser, which is a highly dispersed waste of deposition from electric arc furnace, was introduced. The granulometric composition of chalk was evaluated using scanning electron microscopy, and dust using a microsizer 201c laser analyzer.
Results. According to the results of the optimisation, regression equations represented as a polynomial of the second degree and the optimal material composition of the paint material were obtained. In order to solve the problem of drying, a metal catalyser was added to the optimal composition in the amount of 0.05 % of the binder weight. A comparison of the obtained results of regulatory tests of the physical and mechanical properties of the two formulations, the control (without additives) and the modified with the addition of a metal catalyst in the form of dust, indicate the prospects of its use as a siccative.
Discussion and Conclusion. The introduction of a siccative into the oil-based paint and varnish material in the form of a by-product of highly dispersed precipitation waste from an electric furnace accelerated the polymerization process and improved the physical and mechanical properties of the modified composition in comparison with the control one. Improving the physical and mechanical characteristics of oil paint will increase the resistance of coatings to environmental factors and thus increase its durability.

Keywords: paintwork material, adhesion, nominal viscosity, metal catalyser, fine aggregate, binder

For citation. Khalyushev AK, Kolesnichenko EA. Optimization of the Paintwork Material Modified by Metal Catalyser Additive. *Modern Trends in Construction, Urban and Territorial Planning.* 2025;4(1):26–34. https://doi.org/10.23947/2949-1835-2025-4-1-26-34

Оригинальное эмпирическое исследование

Оптимизация лакокрасочного материала для покрытия древесины с добавкой металлического катализатора

А.К. Халюшев ✉, **Е.А. Колесниченко**
Донской государственный технический университет, г. Ростов-на-Дону, Российская Федерация
✉ khaljushev@mail.ru

Аннотация
Введение. Современные тенденции в отрасли производства лакокрасочных материалов идут в направлении экологичности и многофункциональности придавая деревянным изделиям хорошие эстетические и защитные свойства. Структура древесины, как натурального материала постоянно подвергается интенсивным и прогрессирующим процессам окислительного разрушения в условиях воздействия окружающей среды, что влияет на прочность древесины и вызывает значительные структурные изменения. В этой связи интерес к улучшению стойкости лакокрасочных покрытий при воздействии факторов окружающей среды на их эксплуатационные характеристики, оправдывает активизацию исследований в разработке новых эффективных решений. Одним из эффективных способов предотвращения разрушения структуры древесины является нанесение защитного слоя лакокрасочного материала путем его химической модификации поверхности и прежде всего за счет введения сиккативов. Введение сиккативов позволяет обеспечить равномерную скорость высыхания по всему объему и дополнительно диспергировать пигмент, что улучшает физико-механические свойства лакокрасочного покрытия и повышает его долговечность.

Цель научно-исследовательской работы — установить влияние добавки металлического катализатора в виде высокодисперсного отхода осаждения от электродуговой печи на физико-механические свойств лакокрасочного материала.

Материалы и методы. В качестве исходных компонентов для получения масляных составов красок при проведении экспериментов применяли: связующее вещество — натуральная олифа, пигмент — охра, наполнитель — мел. Для ускорения процесса высыхания добавляли металлический катализатор, являющийся высокодисперсным отходом осаждения от электродуговой печи (далее — пыль). Гранулометрический состав мела оценивали с помощью сканирующей электронной микроскопии, а пыли — с помощью лазерного анализатора Microsizer 201c.

Результаты исследования. По результатам оптимизации были получены уравнения регрессии, представленные в виде полинома второй степени и оптимальный вещественный состав лакокрасочного материала. Для решения проблемы высыхания в оптимальный разработанный состав масляной краски вводили добавку металлического катализатора в количестве 0,05 % от массы связующего.

Сравнение полученных результатов нормативных испытаний физико-механических свойств двух составов контрольного (без добавки) и модифицированного с добавкой металлического катализатора в виде пыли говорят о перспективности её применения в качестве сиккатива.

Обсуждение и заключение. Введение в лакокрасочный материал на масляной основе сиккатива в виде побочного продукта высокодисперсного отхода осаждения от электродуговой печи ускорило процесс полимеризации и улучшило физико-механические свойства модифицированного состава в сравнении с контрольным. Улучшение физико-механических характеристик масляной краски позволит повысить стойкость покрытий к воздействию факторов окружающей среды и таким образом повысить его долговечность.

Ключевые слова: адгезия, условная вязкость, лакокрасочный материал, металлический катализатор, наполнитель, связующее

Для цитирования. Халюшев А.К., Колесниченко Е.А. Оптимизация лакокрасочного материала для покрытия древесины с добавкой металлического катализатора. *Современные тенденции в строительстве, градостроительстве и планировке территорий*. 2025;4(1):26–34. https://doi.org/10.23947/2949-1835-2025-4-1-26-34

Introduction. The growing consumption in the global market of paint and varnish materials can be put down to the trend of "green" buildings in civil engineering generating a soaring demand for effective "green" paint and varnish materials. Oil and paint industry is moving in two relevant areas of great practical interest, i.e., bioresources and renewables. In fact, as the industry is putting more emphasis on ecological and multifunctional synthetic fillers [1, 2] whose production does not normally take into account the characteristics of environmental sustainability [3], scientific research emphasizes the use of natural additives in coatings [4, 5]. Scientists have thus recently investigated the results of the use of linseed oil [6], pigments obtained from wood waste [7], microbial staining [8], pigments extracted from fungi [9] and cellulose fibers [10] in wood coatings. The paint and varnish material lending wood products specific aesthetic effects with new pigments [11] and distinctive gloss indicators [12] is indicative of the trend gaining momentum in the market of protective coatings for wood. On the one hand, while using innovative pigments, unique aesthetic effects should be provided making them weather-resistant without compromising the protective qualities of the organic coating [13]. On the other hand, the combination of wood paints with diverse types of pigments might lead to grave problems potentially reducing the protective effectiveness of the organic coating, introducing a gap in the polymer matrix and showing a low level of inherent durability of the pigment [14, 15].

The use of oily formulations shields wooden products and structures from occasional moisture exposures causing rotting accompanied by a loss of integrity and load-bearing capacity. The film-forming substance in oil formulations are drying oils, which, according to their content of polymers and processed vegetable oils, are classed into:

1) natural drying oils;
2) semi-natural drying oils;
3) artificial drying oils.

Natural drying oils are obtained by heating linseed, hemp or other vegetable oils to an average of 150 °C. At the same time, the addition of solidification accelerators (siccatives) is introduced in an amount of 2–4%. Due to this treatment, drying oil takes on the property of quickly "drying out" in the air forming an elastic film. Oil-based colorful formulations are obtained by meticulously grinding drying oil with pigments insoluble in oils in machines. While grinding colourful formulations, homogeneous suspensions should be obtained where each particle of pigment or filler has a shell of binder adsorbed on the surface of the particles. The wettability of the pigments by the binder, the strength of the resulting shells and thereby the properties of the paint compositions depend on those of both the pigment and the wetted liquid. Pigments can be hydrophilic (iron meerkat, ochre) and hydrophobic (graphite, soot, lead whitewash). When hydrophilic pigments are mixed with oil binders that do not contain surfactants, there is only a mechanical mix with reduced painting properties. The presence of surfactants in the composition enhances the wettability of the pigment with oils. One of the drawbacks of drying oils is the relatively long drying time. Despite certain disadvantages [16] the use of metal catalysts can reduce the drying time considerably.

The wettability scheme of the surfactant pigment in the presence of a metal catalyst in Fig. 1 is the following. Surfactants are attached by a polar group to the surface of the pigment and form a hydrophobic shell that is well wetted with an oil binder, and the inner surface of the shell binds firmly to the pigment and the metal catalyst.

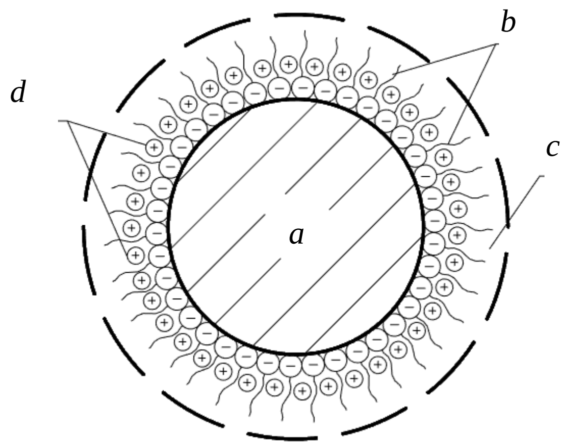

Fig. 1. Scheme of wettability of surfactant pigment in the presence of a metal catalyst:
a — pigment; *b* — oriented molecules of the surfactant pigment; *c* — oil binder; *d* — metal catalyzer

The objective of the research is to identify the effect of adding a metal catalyst in the form of highly dispersed precipitation waste from an electric arc furnace on the physical and mechanical properties of oil paint.

Materials and Methods. The initial components for obtaining oil compositions of paints during the experiments were as follows: the binder is natural drying oil, the pigment is ochre, the filler is chalk (CaO — 50.90%; PP — 41.50%) with a specific surface area of 420-436.5 m^2/kg. Experimental studies carried out by means of scanning electron microscopy (Fig. 2) show that chalk particles are mostly characterized by a rounded shape ranging from 2 to 20 microns in size.

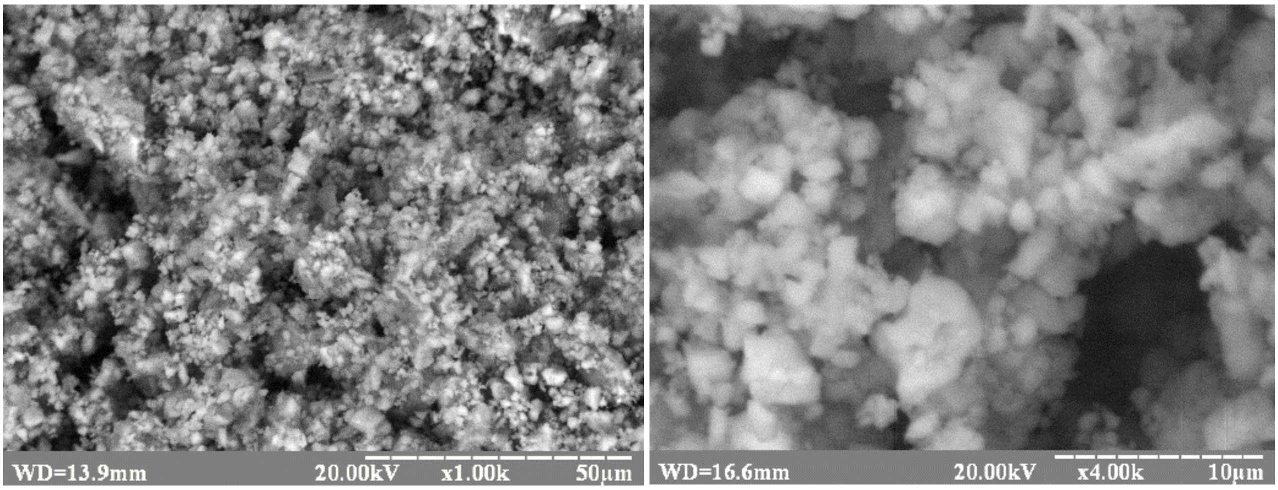

Fig. 2. Scanning electron microscopy (SEM)

In order to accelerate drying, an additive of a metal catalyst was introduced, which is a highly dispersed precipitation waste from an electric arc furnace. The chemical composition of the metal catalyst are mainly metal oxides (ZnO — 46.7%; Fe_2O_3 — 32.4%, etc.). The granulometric composition of the dust performed with a Microsizer 201c laser analyzer is shown in Fig. 3.

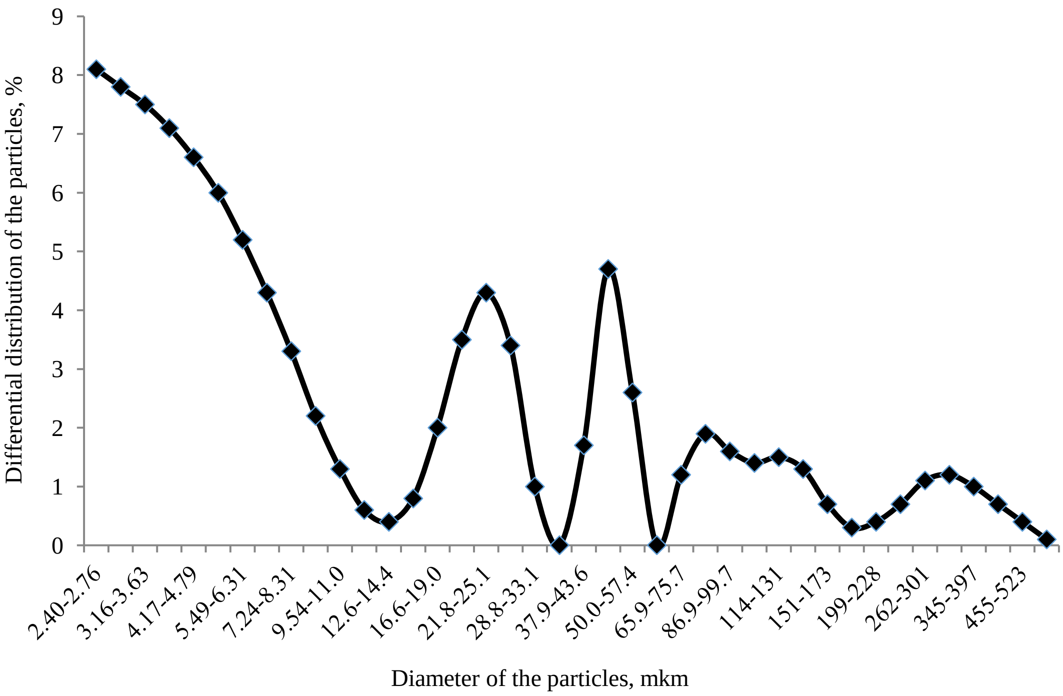

Fig. 3. Granulometric composition of the metal catalyst

The fundamental properties of oil paints depend on the amount and type of pigment, and the amount of binder varies a lot. According to the results of the literature review, it is assumed that the amount of the binder lies in the range of 20–40%, the filler — 15–40% and the pigment — 15–35%.

Optimization. The development of the composition of an effective paint and varnish material for wood coating was determined with the optimal ratio between the components. The experimental data was processed by means of the least squares method in matrix form. The variable factors were: x_1 — pigment content, %; x_2 — filler content, %. The function of the output parameters were the following: y_1 — adhesion to the paintwork, MPa; and y_2 — conditional viscosity, C. The values of the variation factors and their physical value are in Table 1.

Table 1

Significance of variation factors in a complete factor experiment (CFE) 2^k

№	Factor code	Physical value of the factor	Measurement unit	Variation range	Factor levels		
					–1	0	+1
1	x_1	pigment content	%	± 5	15	25	35
2	x_2	filler content	%	± 10	17.5	27.5	37.5

Identifying the drying time. A thin layer of paint and varnish material was applied to the prepared 70 ×150 mm steel plates without leaving any gaps. With a light touch of the fingers, the stickiness was gone, and only after that were 0.5 g of Ballotini glass beads (with a fraction from 100 to 355 microns) poured onto the surface of the plates in one layer from a height of 50 mm to an area with a diameter of 22 mm. After 60 seconds, the plate was tilted at an angle of about 20 ° in relation to the horizontal and swept away with a soft brush. The degree of drying is achieved if all the Ballotini balls are removed with no damage to the surface layer. The time corresponding to the degree of drying is recorded.

Identifying the conditional viscosity based on the B3-246 viscometer. The paint and varnish material with a volume of 150 cm^3 was filtered through a sieve to eliminate foreign inclusions. Prior to testing on the B3-246 viscometer, the nozzle was thoroughly cleaned with a solvent. The nozzle of the tank was closed with a rod and the resulting composition was poured to a horizontal mark on its inner surface. A glass measuring cup was placed under the nozzle of the viscometer. After the paintwork had been poured, the rod was lifted. As the test paint and varnish material were coming out of the nozzle, a stopwatch was turned on and the conditional viscosity was identified according to the time.

Identifying the mass fraction of non-volatile substances. For the test, a metal cup with an inner diameter of the bottom (75 ± 5) mm and a side height of at least 5 mm was used. By weighing, the mass of an empty dry cup m_0 was identified using an analytical balance with an accuracy of 1 mg. A sample of the paint and varnish material was then added and the mass in the cup (m_1) was identified, while evenly distributing it over the diameter of the cup. After the mass had been identified, the samples with the cup were placed in a drying cabinet with a temperature of 105-110°C and dried to a constant mass. Having been dried and cooled at room temperature, the mass of the cup with the dried residue (m^2) was identified yet again. The mass fraction of non-volatile substances *HB*, %, was calculated using the formula:

$$\text{HB} = \frac{(m_2 - m_0)}{(m_1 - m_0)} 100\%, \quad (1)$$

where m_2 is the mass of the cup with the remainder, g; m_0 is the mass of the empty cup, g; m_1 is the mass of the cup with the sample prior to the tests, g.

Identifying the adhesion of the paintwork by the strength of the tear. A paint and varnish material was applied to the selected metal prepared surface, which was pre-primed in several layers. After the paintwork had been cured, metal discs were glued to the samples, and the remaining glue was removed and held in such a manner until it solidified completely. Next, the samples were fixed in an adhesive device, and the metal discs glued to the samples were pivotally connected to the adhesive gripper as shown in Fig. 4. According to a visual assessment of the adhesive strength R_{ad} = 1.8 MPa, the zone and nature of the disc separation from the metal base were recorded.

Fig. 4. Adhesive meter ONYX-1.AP.020

Identifying the adhesion with the method of lattice incisions. The optimal oil composition was applied in two layers to the prepared plates measuring 60×150×1 mm. The tests were conducted with a razor blade and at least six parallel incisions were made along a ruler with a length of at least 20 mm at a distance of 1-3 mm from each other. After the incisions had been made and the loose pieces of the coating had been removed, a soft brush was applied diagonally across the surface of the grate.

Research Results. According to the results of the experiment, regression equations (2) and (3) were obtained presented as a polynomial of the second degree. Regression equations processed using the least squares method were subjected to statistical analysis based on the estimates of variances. The calculation of the regression coefficients and statistical criteria is shown in Tables 2, 3. A graphical interpretation of the obtained equations is shown in Fig. 5, 6.

$$y_1(x_1,x_2)=2{,}09–0{,}235\cdot x_1+0{,}18\cdot x_2–0{,}55\cdot x_1\cdot x_2–0{,}335\cdot x_1^2+0{,}02\cdot x_2^2 \quad (2)$$

$$y_2(x_1,x_2)=15{,}59–3{,}94\cdot x_1+2{,}94\cdot x_2+0{,}278\cdot x_1\cdot x_2+0{,}278\cdot x_1^2-0{,}667\cdot x_2^2 \quad (3)$$

Table 2

Calculated coefficients of the equations

Name of the output parameter of the equation	Coefficients of the equations					
	b_0	b_1	b_2	b_3	b_4	b_5
y_1	2.09	–0.235	0.18	–0.55	–0.335	0.02*
y_2	15.59	–3.944	2.94	0.278*	0.278*	–0.67*

* — insignificant coefficients

Table 3

Statistical optimization criteria

Name of the output parameter of the equation	Statistical criteria			
	F	D^2_0	S_0	ζ
y_1	6.242	4.107	0.064	0.111
y_2	3.035	0.87	0.933	1.618

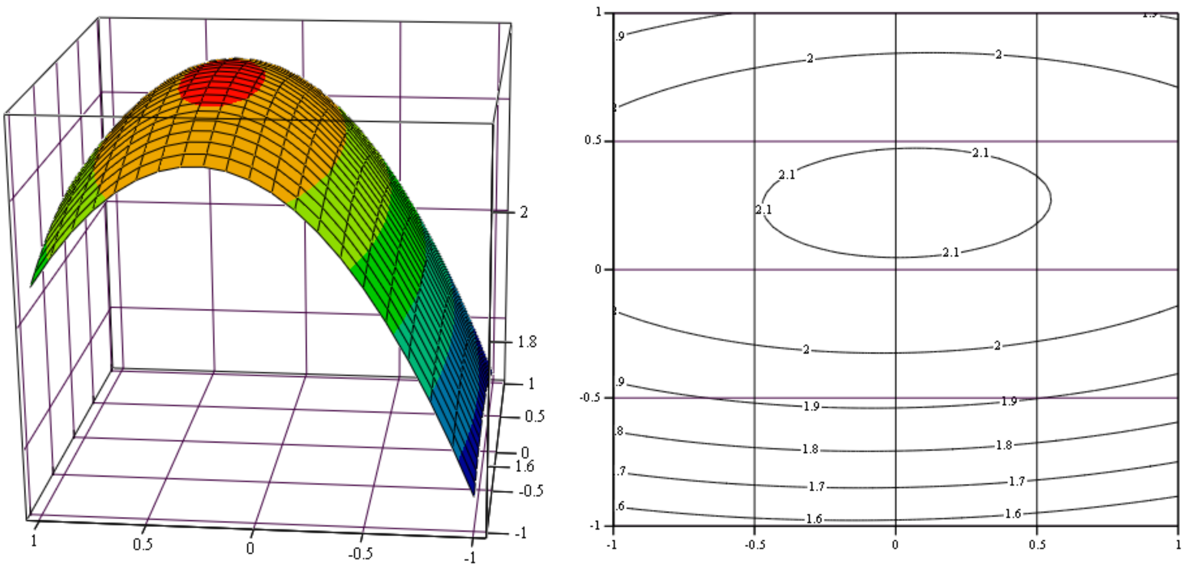

a) *b)*

Fig. 5. Dependence of the adhesion on the amount of the pigment x_1 and the filler x_2: *a* — in space; *b* — on the plane

An analysis of the results of the obtained model in the form of regression equations shows that the coefficient b_1 with the factor x_1 (the amount of the pigment) has a negative impact on both of the output parameters (y_1; y_2). Furthermore, the amount of the pigment has a greater effect on the conditional viscosity of the paintwork (b_1 = –3.944) than on the adhesion to the paintwork (b_1 = –0.235). At the same time, a positive value of the b_2 coefficient at the factor x_2 (the amount of the filler) indicates that an increase in the filler concentration results in a positive effect on both adhesion to the paintwork (b_2 = 0.18) and the conditional viscosity (b_2 = 2.944). The combined interaction of these factors (x_1; x_2) is insignificant, but negatively impacts adhesion (b_3 = –0.55) in the first case and positively impacts the conditional viscosity (b_3 = 0.278) in the second one. The remaining coefficients can be neglected as they are insignificant in terms of the conditional viscosity (b_4; b_5) and adhesion (b_5), since it is less than the root-mean-square error in identifying the coefficients.

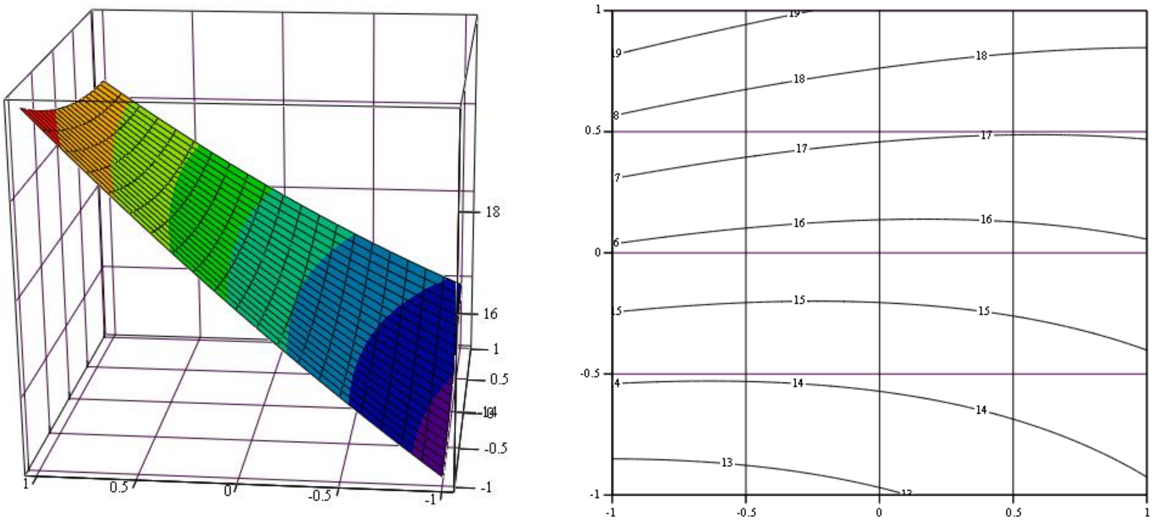

a) *b)*

Fig. 6. Dependence of the conditional viscosity on the amount of the pigment x_1 and the filler x_2: *a* — in space; *b* — on the plane

In general, based on the inequality $F < q_F$, with a probability of 0.95, the suggested models are adequate and be employed to describe the optimization process within 0.5. As a result, the optimal composition of the paint and varnish material based on drying oil and pigment in the form of ochre was identified. The material composition of the paint and varnish material is shown in Table 4.

Table 4

Optimal material composition of oil paint

Name of the composition	Content of the components, %			Index	
	Binder	Pigment (ochre)	Filler (chalk)	adhesion to the coating, MPa	conditional viscosity, sec
C№ 3	45	17.5	37.5	1.8	120

In order to address the problem of drying in the optimal composition of the paint and varnish material (Table 4) a metal catalyst additive was added in an amount of 0.05% by the weight of the binder. The use of this additive as a siccative was due to its necessary influence in the two directions. The first one was as a dispersing agent of pigments, and the other one was to improve oxygen penetration into the film volume and thereby to accelerate the drying of the coating. This should cause a reduction in the formation of a matte effect and allow one to maintain a high gloss surface. The results of comparing the physical and mechanical properties of the compositions with the addition of a metal catalyst (№4) and without additives are in Table 5.

Table 5

Results of comparison of the physical and mechanical properties of the oil paint compositions

№	Name of the index	Name of the composition	
		Control (C№ 3)	Operating (C№ 4)
1	Conditional viscosity according to the VZ-246 type viscometer with a nozzle diameter of 4 mm at a temperature of (20,0± ± 0,5) ºC, sec	120	110
2	Drying time to degree 1, no more, at a temperature of (20 ± 2) ºC, min	20	15.5
3	Mass fraction of non-volatile substances, %	88,5	90,4
4	Adhesion of the coating, points	2	1
5	Adhesion of the coating, MPa	1.8	2.15

Discussion and Conclusion. Based on the optimization results, regression equations were obtained as a polynomial of the second degree and the optimal material composition of the paint and varnish material. In order to address the drying problem, a highly dispersed by-product of deposition from an electric arc furnace was introduced into the optimal composition as a metal catalyst in an amount of 0.05% by the weight of the binder. It was found that the drying time to degree 1 of the operating composition (from № 4) is 22.5% lower compared to the control composition (from № 3), the mass fraction of non-volatile substances is 19.8% lower, and the adhesion of the paint coating is 19.4% higher respectively. The composition of an effective oil paint based on drying oil, ochre, chalk and a siccative additive in the form of a metal catalyst was developed and introduced in order to accelerate the drying and additional dispersion of the pigment, thereby improving the coating's resistance to atmospheric influences. The obtained comparative data from the regulatory tests of the physical and mechanical properties of oil paint using a by-product of deposition from an electric arc furnace are indicative of the prospects of its use as a siccative for paint and varnish materials.

References

1. Binoj J, Raj RE, Daniel B. Comprehensive Characterization of Industrially Discarded Fruit Fiber, Tamarindus Indica L. as a Potential Eco-Friendly Bioreinforcement for Polymer Composite. *Journal of Cleaner Production.* 2017;142:1321–1331. https://doi.org/10.1016/j.jclepro.2016.09.179

2. Kumar P, Duhan S, Duhan JS. Agro-Industrial Wastes and their Utilization Using Solid State Fermentation: a review. *Bioresources and Bioprocessing.* 2018;5:1–15. https://doi.org/10.1186/s40643-017-0187-z

3. Sanjay M, Madhu P, Jawaid M, Senthamaraikannan P, Senthil S, Pradeep S. Characterization and Properties of Natural Fiber Polymer Composites: a Comprehensive Review. *Journal of Cleaner Production*. 2018;172:566–581. https://doi.org/10.1016/j.jclepro.2017.10.101.

4. Richard S, Rajadurai JS, Manikandan V. Influence of Particle Size and Particle Loading on Mechanical and Dielectric Properties of Biochar Particulate-Reinforced Polymer Nanocomposites. *International Journal of Polymer Analysis and Characterization.* 2016;21:462–477. http://dx.doi.org/10.1080/1023666X.2016.1168602

5. Mustapha R, Rahmat AR, Majid RA, Mustapha SNH. Vegetable Oil-Based Epoxy Resins and their Composites with Bio-Based Hardener: a Short Review. *Polymer-Plastics Technology and Materials*. 2019;58:1311–1326. https://doi.org/10.1080/25740881.2018.1563119 .

6. Sansonetti E, Cirule D, Kuka E, Andersone I, Andersons B. Investigation of Linseed Oil-Based Wood Coatings: Effect of Artificial Weathering. *Key Engineering Materials*. 2019;800:223–227. http://dx.doi.org/10.4028/www.scientific.net/KEM.800.223

7. Calovi M, Rossi S. From Wood wWaste to Wood Protection: New Application of Black Biorenewable Water-Based Dispersions as Pigment for Bio-Based Wood Paint. *Progress in Organic Coatings*. 2023;180:10757. https://doi.org/10.1016/j.porgcoat.2023.107577

8. Liu Y, Yu Z, Zhang Y, Wang H. Microbial Dyeing for Inoculation and Pigment Used in Wood Processing: Opportunities and Challenges. *Dyes Pigments.* 2021;186:109021. https://doi.org/10.1016/j.dyepig.2020.109021

9. Vega Gutierrez SM, Stone DW, He R, Vega Gutierrez PT, Walsh ZM, Robinson SC. Potential Use of the Pigments from Scytalidium Cuboideum and Chlorociboria Aeruginosa to Prevent 'Greying' Decking and Other Outdoor Wood Products. *Coatings*. 2021;11:511. http://dx.doi.org/10.3390/coatings11050511

10. Calovi M, Rossi S. Impact of High Concentrations of Cellulose Fibres on the Morphology, Durability and Protective Properties of Wood Paint. *Coatings*. 2023;13:721. https://doi.org/10.3390/coatings13040721

11. Yan X, Chang Y, Qian X. Effect of the Concentration of Pigment Slurry on the Film Performances of Waterborne Wood Coatings. *Coatings*. 2019;9:635. http://dx.doi.org/10.3390/coatings9100635

12. Yan X, Wang L, Qian X. Influence of Thermochromic Pigment Powder on Properties of Waterborne Primer Film for Chinese Fir. *Coatings*. 2019;9:742. http://dx.doi.org/10.3390/coatings9110742

13. Kaestner D, Petutschnigg A, Schnabel T, Illy A, Taylor A. Influence of Wood Surface Color on the Performance of Luminescent Pigments. *Forest Products Journal.* 2016;66:211–213. http://dx.doi.org/10.13073/FPJ-D-15-00036

14. Reinprecht L, P´anek M. Effects of Wood Roughness, Light Pigments, and Water Repellent on the Color Stability of Painted Spruce Subjected to Natural and Accelerated Weathering. *BioResources*. 2015;10(4):7203–7219. http://dx.doi.org/10.15376/biores.10.4.7203-7219.

15. Zhang Z-M, Du H, Wang W-H, Wang Q-W. Property Changes of Wood-Fiber/HDPE Composites Colored by Iron Oxide Pigments after Accelerated UV Weathering. *Journal of Forestry Research*. 2010;21:59–62. https://doi.org/10.1007/s11676-010-0009-z

16.Hubmann M, Curtis JM. A Biobased Reactive Accelerant and Diluent for Solvent-Free Drying Oils. *Progress in Organic Coatings*. 2021;157:106024. http://dx.doi.org/10.1016/j.porgcoat.2020.106024

About the Authors:

Alexander K. Khalyushev, Cand. Sci.(Eng.), Associate Professor of the Department of Technological Engineering and Expertise in the Construction Industry, Don State Technical University (1 Gagarin Square, Rostov-on-Don, 344003, RF), ORCID, khaljushev@mail.ru

Elena A. Kolesnichenko, student of the Faculty of Road Transport, Department of Environmental Economics and Cadastre, Don State Technical University (1 Gagarin Square, Rostov-on-Don, 344003, RF), ORCID, vaisalena57@gmail.com

Claimed Contributorship:

AK Khalyushev: scientific supervision, basic concept and research objective formulation, working with the text of the manuscript, analysis and generalization of the research results, revisiting the conclusions.

EA Kolesnichenko: performing the calculations, editing the figures, proofreading the manuscript, analysis and generalization of the research results.

Conflict of interest statement: **the authors do not have any conflict of interest.**

All authors have read and approved the final version of manuscript.

Об авторах:

Халюшев Александр Каюмович, кандидат технических наук, доцент кафедры технологического инжиниринга и экспертизы строительной индустрии Донского государственного технического университета (344003, Российская Федерация, г. Ростов-на-Дону, пл. Гагарина, 1), ORCID, khaljushev@mail.ru

Колесниченко Елена Андреевна, студентка дорожно-транспортного факультета, кафедры экономики природопользования и кадастра Донского государственного технического университета (344003, Российская Федерация, г. Ростов-на-Дону, пл. Гагарина, 1), ORCID, vaisalena57@gmail.com

Заявленный вклад авторов:

А.К. Халюшев: научное руководство, формирование основной концепции, цели и задачи исследования, подготовка текста, анализ результатов исследований, корректировка выводов.

Е.А. Колесниченко: проведение расчетов, оформление рисунков, доработка текста, формирование выводов.

Конфликт интересов: **авторы заявляют об отсутствии конфликта интересов**

Все авторы прочитали и одобрили окончательный вариант рукописи

Received / Поступила в редакцию 14.01.2025
Reviewed / Поступила после рецензирования 28.01.2025
Accepted / Принята к публикации 12.02.2025

BUILDING MATERIALS AND PRODUCTS
СТРОИТЕЛЬНЫЕ МАТЕРИАЛЫ И ИЗДЕЛИЯ

UDC 624
https://doi.org/10.23947/2949-1835-2025-4-1-35-40

Original Empirical Research

Forecasting the Properties of Multicomponent Mineral Polymer Composite Materials

Gennady B. Verzhbovskiy, **Alan V. Zaliev** ✉
Don State Technical University, Rostov-on-Don, Russian Federation
✉ alan-zaliev@mail.ru

EDN: XFIOHK

Abstract
Introduction. Advances in the construction industry are causing new composite materials to emerge. This is preceded by experimental studies, particularly analytical techniques for predicting the properties of new materials. Polymer composite materials (PCMs) which have proved to be efficient in other industries are commonly utilized in construction as well. PCMs have a number of features that should be taken into consideration while developing analytical techniques. PCM is considered under the condition of isotropy of the final material and compliance with the mixture rule during its manufacture. The objective of the study is to analytically determine the predicted strength limits of multicomponent composite materials with mineral fillers.
Materials and methods. There are diverse methods for identifying the characteristics of polymer composites. An integral method for determining the modulus of elasticity and the Poisson's ratio of a binary polymer composite material is set forth, based on the assumption that there is a relationship between the elastic potentials of the composite components. The transition of analytical forecasting of characteristics from binary to multicomponent polymer composite material is also shown.
Results. The major characteristic of building polymer composites is their strength. A formula has been obtained for the analytical determination of the predicted tensile strength of a binary polymer composite material, and the predicted tensile strength for some multicomponent polymer composite materials has been obtained based on these formulas as well.
Discussion and Conclusion. The results enable us to conclude that while forming the composition of a multicomponent polymer composite material, it is recommended that fillers with similar characteristics, in particular, elasticity modules are combined.

Keywords: multicomponent polymer composite, binary polymer composite, polymer matrix, powder filler, mixture rule, modulus of elasticity, Poisson's ratio, modulus of deformation, shear modulus, volume fraction, tensile strength

Acknowledgements. The authors appreciate the reviewers, whose critical assessment of the submitted materials and suggestions helped to significantly improve the quality of this article.

For citation. Verzhbovsky GB, Zaliev AV Forecasting the properties of multicomponent mineral polymer composite materials. *Modern Trends in Construction, Urban and Territorial Planning*. 2025;4(1):35–40. https://doi.org/10.23947/2949-1835-2025-4-1-35-40

Оригинальное эмпирическое исследование

Прогнозирование свойств многокомпонентных минерально-полимерных композитных материалов

Г.Б. Вержбовский, **А.В. Залиев** ✉
Донской государственный технический университет, Ростов-на-Дону, Российская Федерация
✉ alan-zaliev@mail.ru

Аннотация
Введение. Прогресс строительной индустрии приводит к возникновению новых композитных материалов. Этому предшествуют экспериментальные исследования, в частности, аналитические приемы прогнозирования свойств

новых материалов. В строительстве широкое распространение получили полимерные композитные материалы (ПКМ), которые хорошо зарекомендовали себя и в других отраслях промышленности. ПКМ имеют ряд особенностей, которые следует принимать во внимание в процессе разработки аналитических методик. Рассмотрение ПКМ происходит при условии изотропии конечного материала и подчинения правилу смеси при его изготовлении. Целью настоящего исследования является аналитическое определение прогнозируемых пределов прочности многокомпонентных композитных материалов с минеральными наполнителями.

Материалы и методы. Существуют различные методики определения характеристик полимерных композитов. Предложена интегральная методика определения модуля упругости и коэффициента Пуассона бинарного полимерного композитного материала, основанная на предположении, что между упругими потенциалами составных частей композита существует связь. Также показан переход аналитического прогнозирования характеристик от бинарного к многокомпонентному полимерному композитному материалу.

Результаты исследования. Важнейшей характеристикой строительных полимерных композитов является их прочность. Получена формула для аналитического определения прогнозируемого предела прочности бинарного полимерного композитного материала, также на основе данных формул получен прогнозируемый предел прочности для некоторых многокомпонентных полимерных композитных материалов.

Обсуждение и заключение. Полученные результаты позволяют сделать вывод о том, что при формировании состава многокомпонентного полимерного композитного материала целесообразно сочетать наполнители с близкими по величине характеристиками, в частности, модулями упругости.

Ключевые слова: многокомпонентный полимерный композит, бинарный полимерный композит, полимерная матрица, порошковый наполнитель, правило смеси, модуль упругости, коэффициент Пуассона, модуль деформации, модуль сдвига, объемная доля, предел прочности

Благодарности. Авторы выражают благодарность рецензентам, чья критическая оценка представленных материалов и высказанные предложения по их совершенствованию способствовали значительному повышению качества настоящей статьи.

Для цитирования. Вержбовский Г.Б., Залиев А.В. Прогнозирование свойств многокомпонентных минерально-полимерных композитных материалов. *Современные тенденции в строительстве, градостроительстве и планировке территорий*. 2025;4(1):35–40. https://doi.org/10.23947/2949-1835-2025-4-1-35-40

Introduction. The development of the construction industry is causing more and more new materials, commonly composites, to emerge. This happens prior to a stage of experimental research where a rational composition is selected, as well as experimental samples are tested. Research can be time-consuming and costly, thus analytical techniques for predicting the properties of new materials are of interest. Polymer matrix composite materials (PCMs) are commonly used in various fields, including construction. Further on materials with a polymer matrix and one or more powder fillers formed by simply mixing these components without any chemical reactions between them will be considered. In this case, the PCMs obey the mixture rule [1]. Let us also assume that the composite as a whole and its individual components are isotropic and obey Hooke's law. For these materials, it is essential to obtain analytical expressions enabling the strength limits of the composite to be identified depending on the strength of its components.

Materials and Methods. There are diverse methods for identifying the characteristics of polymer composites, which assume that all of the material parts are subjected to the same deformations [2] or equal stresses [3], so developers of new materials make use of both approaches yileding an interval property assessment which is subsequently narrowed by means of the Hashin–Strikman [4] or Mori–Tanaka [5] methods. In [6], an integral method for identifying the modulus of elasticity and the Poisson's ratio of a binary material with a polymer matrix and a powder filler was set forth based on the assumption that there is a relationship between the elastic potentials of the composite components (1).

$$s\sigma_1\varepsilon_1 = \sigma_2\varepsilon_2, \quad (1)$$

where the indices “1” and “2” refer to the matrix and filler, respectively, and the parameter s is the ratio of the elastic modulus of the components $s = E_1/E_2$.

In [6], formulas were obtained for identifying the elastic modulus and Poisson's ratio of a binary composite (2) expressed in terms of volumetric deformation and shear modulus:

$$E_\Sigma = \frac{9K_\Sigma G_\Sigma}{3K_\Sigma + G_\Sigma}, \nu_\Sigma = \frac{3K_\Sigma - 2G_\Sigma}{2(3K_\Sigma + G_\Sigma)}. \quad (2)$$

The values included in the right-hand sides of expressions (2) are given by equalities (3) and (4):

$$K_\Sigma = (K_1 K_2)^{\frac{1}{2}} \cdot \frac{m_1 K_1^{\frac{1}{2}} + m_2 K_2^{\frac{1}{2}} s^{\frac{1}{2}}}{m_1 K_2^{\frac{1}{2}} + m_2 K_1^{\frac{1}{2}} s^{\frac{1}{2}}}, \quad (3)$$

$$G_\Sigma = (G_1 G_2)^{\frac{1}{2}} \cdot \frac{m_1 G_1^{\frac{1}{2}} + m_2 G_2^{\frac{1}{2}} s^{\frac{1}{2}}}{m_1 G_2^{\frac{1}{2}} + m_2 G_1^{\frac{1}{2}} s^{\frac{1}{2}}}. \quad (4)$$

In the latter expressions the index "Σ" refers to the composite as a whole, and m_1 and m_2 are the volume fractions of the matrix and filler, respectively, with $m_1 + m_2 = 1$. The examples of binary composites with a polypropylene matrix and various fillers provided in [6] are in good agreement with the theoretical results and the experimental values in [7], i.e., the discrepancy does not exceed 10%. PCM formulations are becoming increasingly complex, and materials with two or more fillers have emerged [8] for which it is also desirable to have similar methods for predicting their characteristics. [9] shows how dependencies (2) can be extended to composites of a more complex composition. For a PCM consisting of n components, expressions (2) must be applied (n – 1) times, sequentially adding new components to the binary composite. At each step, the sum of the volume fractions of the binary material is taken as one.

Research Results. In [9], as an example, the modulus of elasticity and the Poisson's ratio were identified for a three-component PCM with a polypropylene matrix (40%) and fillers made of wood flour (50%) and chalk (10%). At the same time, two variants of the "initial material" — a binary composite - were considered in order to assess the dependence of the final results on the accounting procedure for the fillers (Table 1). All the values in the table, except the dimensionless values, are provided in MPa.

Table 1

Modules of volumetric deformation of composites with a polypropylene matrix

Composite	Matrix			Filler			K_Σ	G_Σ	s	E_Σ	ν_Σ
	m_1	K_1	G_1	m_2	K_2	G_2					
"Initial material" — polypropylene (PP) and wood flour (WF)											
PP + WF	0.44	2917	493	0.56	8333	3846	4091	974	0.14	2707	0.39
Total	0.9	4091	974	0.1	7500	3462	4237	1052	0.3	**2914**	**0.385**
"Initial material" — polypropylene (PP) and chalk (C)											
PP+ C	0.8	2917	493	0.2	7500	3462	3182	599	0.16	1692	0.41
Total	0.5	3182	599	0.5	8333	3846	4226	1053	0.17	**2917**	**0.385**

As can be seen from Table 1, the selected total desired values do not depend on the accounting procedure for fillers. Fillers for building composites with a polymer matrix can be a wide variety of materials. Wood flour, a wood polymer composite (WPC), is typically used. There have been attempts to make use of chalk, talc, marble flour, and other powdery materials such as mineral polymer composites (MPCs) as fillers [7, 10, 11]. The factors restricting the wide use of these composites in construction are the complex technology of manufacturing products using complex extrusion equipment and the high cost of the final products. Nevertheless, it is possible to set up inexpensive mass production, e.g., of composite wall blocks, if extrusion is switched to injection molding technology currently used for producing paving slabs, and employ cement dust and fine gravel as a filler, which have now become readily available due to the consequences of hostilities in the populated areas of the eastern part of Ukraine. Unfortunately, lots of buildings and structures in the liberated territories cannot be restored and are being demolished resulting in a large amount of waste to be potentially reused. It is also possible to utilize dust generated in the factories of the construction industry and mostly easily recycled. Let us look at several materials whose cost and properties from open sources are given in Table 2.

Table 2

Characteristics of possible PCM fillers

Filler	Average price per tonn, roubles	Elasticity modulus, MPa	Poisson's ratio	Density ρ, kg/m^3	$K_э$
wood flour	11000	10000	0.3	450	**0.909**
aerosil	9900	6500	0.15	2450	0.657
barite	11750	6000	0.28	4480	0.511
plaster	20000	1400	0.16	2300	0.070
kaolin	5500	5000	0.25	2600	0.909
quartz	5750	7400	0.11	2600	1.287
chalk	2050	8500	0.29	1800	4.146
marble	2000	30000	0.15	2650	15.000
muscovite (mica)	22500	250	0.3	2700	0.011
talcum powder	3050	3500	0.25	2800	1.148
cement dust	950	19000	0.14	1400	20.000
fine crushed stone	550	20000	0.18	2600	36.364

Note that the value of the Poisson's ratio for wood flour is shown in Table 2 differs from the known one for wood. The difference is accounted for by the fact that small particles of wood flour become isotropic, as with such particle sizes the influence of the structural features of the starting material on the coefficient disappears. The relative high cost of composite products can be cut down by using cheaper fillers, therefore, in the last column of the table is the ratio of the elasticity modulus of the filler to its cost, i.e., the coefficient of efficiency of the filler. Obviously, the higher the K_e value, the cheaper the composite. If wood flour is taken as the base material, fillers with a K_e of at least 0.909 will be of interest. These materials are shown in Table 2. The most essential characteristic of building polymer composites is their strength. In [6], a formula was obtained for determining the predicted tensile strength of a binary PCM analytically:

$$\sigma_{com\Sigma} = \frac{3K_i - 2G_i}{3K_i t_i - 2G_i r_i}\sigma_i. \quad (5)$$

with

$$t_1 = \frac{G_1^{1/2}}{m_1 G_1^{1/2} + s^{1/2} m_2 G_2^{1/2}}, t_2 = \frac{s^{1/2} G_2^{1/2}}{m_1 G_1^{1/2} + s^{1/2} m_2 G_2^{1/2}}, \quad (6)$$

$$r_1 = \frac{K_1^{1/2}}{m_1 K_1^{1/2} + s^{1/2} m_2 K_2^{1/2}}, t_2 = \frac{s^{1/2} K_2^{1/2}}{m_1 K_1^{1/2} + s^{1/2} m_2 K_2^{1/2}}. \quad (7)$$

The ultimate strength of the composite is assumed to be the minimum of the two calculations for *i*, equal to 1 and 2.

(5) can also be used in order to predict the properties of multicomponent materials, which is proved by the results in Table 3 where the combination of fillers chalk and wood flour is also looked at (Table 1).

Table 3

Compressive strength of composite, MPa

Composite	Matrix			Filler			K_Σ	G_Σ	s	σ_{com1}	σ_{com2}
	m_1	K_1	G_1	m_2	K_2	G_2					
"Initial material" — polypropylene (PP) and wood flour (WF)											
PP + WF	0.44	2917	493	0.56	8333	3846	4091	974	0.14	31.1	26.8
Total	0.9	4091	974	0.1	7500	3462	4237	1052	0.3	**27.0**	**17.4**
"Initial material" — polypropylene (PP) and chalk (C)											
PP + C	0.8	2917	493	0.2	7500	3462	3182	599	0.16	29.9	16.8
Total	0.5	3182	599	0.5	8333	3846	4226	1053	0.17	**17.7**	**26.8**

Discussion and Conclusion. Analytical formulas have been thus obtained in order to predict the strength of multicomponent composite materials with a polymer matrix and mineral fillers considerably reducing the time spent on developing new materials by cutting down the number of physical experiments. The numerical results shown in Table 3 enable us to conclude that while forming the composition of a multicomponent PCM, it is advisable that fillers with similar modulus of elasticity are combined. Among the materials in Table 2, marble, cement dust, and fine crushed stone are preferrable. These fillers can be obtained as a result of recycling demolished buildings and structures, including in military zones. The strength of the multicomponent PCMs examined in the paper proves to be sufficient for manufacturing wall blocks which can be produced directly in construction areas and utilized as a construction material for walls and partitions of buildings for various purposes.

References

1. Bartenev GV, Zelenev YuV. *Physics of Polymers.* Moscow: Higher School; 1982. 280 p. (In Russ.).
2. Voigt Voigt V. *Lehrbuch der Kristallphysik.* Berlin: Teubner; 1928. 962 p.
3. Reuss Reuss A. Berechnung der Fliessgrenze von Mischkristallen auf Grund der Plastizitätsbedingung für Einkristalle. *Journal of Applied Mathematics and Mechanics*. 1929;9(1):49–58. http://dx.doi.org/10.1002/zamm.19290090104
4. Hashin Z, Shtrikman S. A variational approach to the elastic behavior of multiphase materials. *Journal of the Mechanics and Physics of Solids*. 1963;11:127–140. https://doi.org/10.1016/0022-5096(63)90060-7
5. Klusemann B. Homogenization methods for multi-phase elastic composites: Comparisons and benchmarks. *Technische Mechanik.* 2010;30(4):374–386. URL: https://www.researchgate.net/publication/256374208_Homogenization_methods_for_multi-phase_elastic_composites_Comparisons_and_benchmarks (дата обращения 15.01.2025).
6. Verzhbovsky GB. *Low-rise Prefabricated Buildings and Structures Made of Composite Materials.* Rostov-on-Don: P-Press; 2015. 280 p. (In Russ.).
7. Klesov AA. *Wood-polymer Composites.* St. Petersburg: NOT; 2010. 735 p. (In Russ.).
8. Savvinova ME, Petukhova ES. Choice of Promising Fillers for Polyethylene PE80B and PE2HT11. *Don Engineering Bulletin*. 2013;1. (In Russ.) URL: http://www.ivdon.ru/ru/magazine/archive/n1y2013/1518 (accessed: 15.01.2025).
9. Verzhbovsky GB. Forecasting the Physical Properties of Multicomponent Composite Materials with a Polymer Matrix. *Don Engineering Bulletin.* 2022;7. (In Russ.) URL: http://wwvv.ivdon.ru/ru/magazine/archive/n7y2022/7829 (accessed: 15.01.2025).
10. Mikhailin YuA. *Structural Polymer Composite Materials.* St. Petersburg: NOT; 2013. 822 p. (In Russ.).
11. Ochsner A, Silva LFM, Altenbach H. *Mechanics and Properties of Composed Materials and Structures.* Berlin Heidelberg: SpringerVerlag; 2012. 195 p. https://doi.org/10/1007/978-3-642-31497

About the Authors:

Gennady B. Verzhbovskiy: Dr.Sci. (Eng.), Professor, Head of the Department of Metal, Wood and Plastic Structures at the Don State Technical University (344003, Russian Federation, Rostov-on-Don, Gagarin Square, 1), ResearcherID, ORCID, vergen2005@yandex.ru

Alan V. Zaliev: Postgraduate student of the Department of Metal, Wood and Plastic Structures at the Don State Technical University (344003, Russian Federation, Rostov-on-Don, Gagarin Square, 1), ORCID, alan-zaliev@mail.ru

Claimed Contributorship:

GB Verzhbovskiy: scientific supervision, concept formation, analysis of research results, revision of the manuscript, correction of the conclusions.

AV Zaliev: performing the calculations, preparing the manuscript, forming the conclusions.

Conflict of interest statement: **the authors do not have any conflict of interest.**

All authors have read and approved the final version of manuscript.

Об авторах:

Вержбовский Геннадий Бернардович, доктор технических наук, профессор, заведующий кафедрой металлических, деревянных и пластмассовых конструкций Донского государственного технического университета (344003, Российская Федерация, г. Ростов-на-Дону, пл. Гагарина, 1), ResearcherID, ORCID, vergen2005@yandex.ru

Залиев Алан Витальевич, аспирант кафедры металлических, деревянных и пластмассовых конструкций Донского государственного технического университета (344003, Российская Федерция, г. Ростов-на-Дону, пл. Гагарина, 1), ORCID, alan-zaliev@mail.ru

Заявленный вклад авторов:

Г.Б. Вержбовский: научное руководство, формирование концепции, анализ результатов исследований, доработка текста, корректировка выводов.

А.В. Залиев: проведение расчетов, подготовка текста, формирование выводов.

Конфликт интересов: **авторы заявляют об отсутствии конфликта интересов.**

Все авторы прочитали и одобрили окончательный вариант рукописи.

Received / Поступила в редакцию24.01.2025
Reviewed / Поступила после рецензирования 05.02.2025
Accepted / Принята к публикации 20.02.2025

BUILDING MATERIALS AND PRODUCTS
СТРОИТЕЛЬНЫЕ МАТЕРИАЛЫ И ИЗДЕЛИЯ

Check for updates

UDC 693.557 *Original Empirical Research*
https://doi.org/10.23947/2949-1835-2025-4-1-41-53

Autogenous Shrinkage of Concretes from Highly Mobile and Self-Compacting Mixtures

Grigory V. Nesvetaev ✉, **Yulia I. Koryanova**, **Vladimir V. Shut**
Don State Technical University, Rostov-on-Don, Russian Federation
✉ nesgrin@yandex.ru

EDN: TWGDIA

Abstract

Introduction. The influence of the chemical and mineralogical composition of Portland cements and the chemical base of superplasticizers on the magnitude and kinetics of autogenic (contractional) shrinkage of concretes from highly mobile and self-compacting concrete mixtures has been revealed. The relevance of the issue is due to the commonly overlooked role of autogenic shrinkage in the formation of the field of temperature-shrinkage stresses in the early hardening period of massive monolithic structures. In order to calculate intrinsic stresses, data on the magnitude and kinetics of autogenic shrinkage are required, and the insufficiency and some inconsistency of data on the effect of superplasticizing additives on the magnitude and kinetics of autogenic shrinkage, depending on the material composition of cement and the chemical and mineralogical composition of clinker, are critical to the expediency of obtaining new data on the issue. The objective of the work is to develop scientific ideas about the influence of prescription factors and material properties on the quantitative and qualitative parameters of autogenic shrinkage using the example of materials commonly used in the production of monolithic reinforced concrete structures in the Rostov region.

Materials and methods. Experimental studies were conducted using six Portland cements from four manufacturers that are fast-hardening according to GOST 31108-2020 classification. Superplasticizing additives based on polycarboxylate esters and naphthalene formaldehydes in a dosage of 0.5% of the commercial product were employed. The properties of cements are identified according to GOST 30744-2001 and GOST 310.5-88. Deformations of the hardening cement paste (stone) were determined by means of the Le Chatelier method. The amount of autogenic shrinkage of concrete was determined by the calculation method based on the amount of autogenic shrinkage of cement, taking into account the true value of the I/C of concrete and the concentration of aggregate in concrete.

Results. The ratio of "autogenic shrinkage/total contraction" of the investigated cements with additives at the age of 5 days was 0.37–0.74, the quantitative values of the total contraction of the studied cements in combination with additives at the age of 5 days ranged from 2.93 to 3.43 ml/100 g of cement, which does not contradict the available data. Change in the amount of autogenic shrinkage in the presence of additives at the age of 5 days was from 0.64 to 1.65 relative to the non-additive standard. The effect of additives on the kinetics of autogenic shrinkage was manifested both in acceleration or deceleration, and in the absence of any effect. The calculated value of autogenic shrinkage of concretes of classes B25–B35 from highly mobile and self-sealing mixtures at the age of 5 days ranged from 0.36 to 1.18 mm/m.

Discussion and Conclusion. Scientific ideas about the kinetics of autogenic shrinkage have been developed depending on the type of cements and additives. In order to describe the change in autogenic shrinkage over time, a formula similar to the formula EN 1992-1-1 for the change in concrete strength over time is set forth. The classification of concretes according to the kinetics of autogenic shrinkage is suggested. The patterns of changes in the amount of autogenic shrinkage of concretes from highly mobile and self-compacting concrete mixtures have been clarified considering the influence of the composition and properties of cements in combination with several superplasticizing additives. The most probable value of the indicator of the degree d = 1.6 – 1.8 is determined in the well-known formula for calculating the autogenic shrinkage of concrete.

Keywords: general contraction, contractional shrinkage, autogenic shrinkage, superplasticizing additives, highly mobile concrete mixtures

For citation. Nesvetaev GV, Koryanova YuI, Shut VV. Contractional shrinkage of concretes from highly mobile and self-sealing mixtures. *Current Trends in Construction, Urban and Territorial Planning.* 2025;4(1):41–53. https://doi.org/10.23947/2949-1835-2025-4-1-41-53

Оригинальное эмпирическое исследование

Контракционная усадка бетонов из высокоподвижных и самоуплотняющихся смесей

Г.В. Несветаев ✉, **Ю.И. Корянова** , **В.В. Шуть**
Донской государственный технический университет, Ростов-на-Дону, Российская Федерация
✉ nesgrin@yandex.ru

Аннотация
Введение. Выявлено влияние особенностей химико-минералогического состава портландцементов и химической основы суперпластифиуаторов на величину и кинетику аутогенной (контракционной) усадки бетонов из высокоподвижных и самоуплотняющихся бетонных смесей. Актуальность вопроса обусловлена часто игнорируемой ролью аутогенной усадки в формировании поля температурно-усадочных напряжений в ранний период твердения массивных монолитных конструкций. Для расчета собственных напряжений требуются данные о величине и кинетике аутогенной усадки, а недостаточность и некоторая противоречивость данных о влиянии суперпластифицирующих добавок на величину и кинетику аутогенной усадки в зависимости от вещественного состава цемента и химико-минералогического состава клинкера предопределяют целесообразность получения новых данных по данному вопросу. Цель работы состоит в развитии научных представлений о влиянии рецептурных факторов и свойств материалов на количественные и качественные параметры аутогенной усадки на примере широко применяемыми при производстве монолитных железобетонных конструкций в Ростовской области материалов.
Материалы и методы. Экспериментальные исследования выполнены с использованием шести быстротвердеющих по классификации ГОСТ 31108-2020 портландцементов четырех производителей. Использованы суперпластифицирующие добавки на основе эфиров поликарбоксилатов и нафталинформальдегидов в дозировке 0,5 % по товарному продукту. Свойства цементов определены по ГОСТ 30744-2001 и ГОСТ 310.5-88. Деформации твердеющего цементного теста (камня) определялись по методу Ле-Шателье. Величина аутогенной усадки бетона определялась расчетным методом по величине аутогенной усадки цемента с учетом истинного значения В/Ц бетона и концентрации заполнителя в бетоне.
Результаты исследования. Соотношение «аутогенная усадка/общая контракция» исследованных цементов с добавками в возрасте 5 сут. составило 0,37–0,74, количественные значения общей контракции исследованных цементов в сочетании с добавками в возрасте 5 сут. составили от 2,93 до 3,43 мл/100 г цемента, что не противоречат известным данным. Изменение величины аутогенной усадки при наличии добавок в возрасте 5 сут. составило от 0,64 до 1,65 относительно бездобавочного эталона. Влияние добавок на кинетику аутогенной усадки проявилось как в ускорении либо замедлении, так и в отсутствии влияния. Расчетная величина аутогенной усадки бетонов классов В25–В35 из высокоподвижных и самоуплотняющихся смесей в возрасте 5 сут. составила от 0,36 до 1,18 мм/м.
Обсуждение и заключение. Развиты научные представления о кинетике аутогенной усадки в зависимости от вида цементов и добавок. Для описания изменения аутогенной усадки во времени предложена формула, подобная формуле EN 1992-1-1 изменения прочности бетона во времени. Предложена классификация бетонов по кинетике аутогенной усадки. Уточнены закономерности изменения величины аутогенной усадки бетонов из высокоподвижных и самоуплотняющихся бетонных смесей с учетом влияния состава и свойств цементов в сочетании с некоторыми суперпластифицирующими добавками. Определено наиболее вероятное значение показателя показателя степени d = 1,6 – 1,8 в известной формуле для расчета аутогенной усадки бетона.

Ключевые слова: общая контракция, контракционная усадка, аутогенная усадка, суперпластифицирующие добавки, высокоподвижные бетонные смеси

Для цитирования. Несветаев Г.В., Корянова Ю.И., Шуть В.В. Контракционная усадка бетонов из высокоподвижных и самоуплотняющихся смесей. *Современные тенденции в строительстве, градостроительстве и планировке территорий*. 2025;4(1):41–53. https://doi.org/10.23947/2949-1835-2025-4-1-41-53

Introduction. The risk of premature cracking of massive monolithic reinforced concrete structures is caused by tensile stresses resulting from temperature and shrinkage deformations [1, 2]. They are frequently overlooked while assessing the level of tensile stresses [3, 4]. Shrinkage deformations are generally not the dominant factor contributing to premature cracking of massive monolithic reinforced concrete structures, but taking them into consideration enables a more reliable assessment of the level of stresses that take place [5], particularly with a considerable overlap time and in the case of concrete mix supplies from different concrete mixing plants, since with the possible use by manufacturers of different cements and additives, during the early hardening period there might be significant differences in shrinkage deformations of the same concrete grade. In order to reliably assess the role of shrinkage deformations, it is essential to take their nature, magnitude and patterns of development into account . The hydration and hardening of Portland cement is known to be accompanied, among other things, by its own deformations caused by mass exchange processes with the external environment (shrinkage during drying or "drying shrinkage" including carbonation shrinkage, hereinafter referred to as DS) and changes in the volume of the hardening system due to hydration, which occur as a result of a decline in the volume of neoplasms during hydration relative to the total volume of the reacting substances. This is historically known as "contraction" or "general contraction" (from the Latin la contraddizione, hereinafter referred to as OK) and consists of contractional porosity (CP) and contraction shrinkage (CS) [6]. V.V. Nekrasov was the first Russian researcher to have meticulously investigated the OK [7]. For more than 30 years, the terms "chemical shrinkage" have been largely used in foreign literature to denote OK and "autogenous shrinkage" to denote CS [5, 8–10]. One of the earliest mentions of the term "autogenous shrinkage" can be found in [11]. In the Russian literature, the terms "general" and "external" contraction or chemical shrinkage are found to denote OK and CS, respectively [12]. In this paper, the terms OK (general contraction = "chemical shrinkage") and CS ("autogenous shrinkage") will be used further on.

The first mention of CS dates back to 1933. (Nilender Yu.A.), and according to [9] — to 1934 (Lyman), whereas in [9] it is noted that the value of CS depends on the type of cement and can vary up to 3 times. There is some information about the changing ideas about the role of CS in the process of premature cracking of concrete in Table 1.

Table 1

Some ideas about the role of CS in the formation of the concrete structure

Data	CS
Nilender Yu.A. (1933)	5-10 times lower than DS
Spindel M. (1936)	Considerably higher than DS
Aleksandrovskiy S.V. (1962)	Low compared to DS and is not involved in crack formation
Mikhailov V.V. (1974)	Fairly considerable (1 mm/m per day)
Bazhenov Yu.M. (1987)	Does not change the size but rather a porous structure
Kholmyanskiy M.M. (1997)	Low compared to DS and has no significant impact on crack formation
Larrard Roy (1993)	DS 0,42, КУ 0,58 of the total one
Tazawa, Miyazawa (1997)	DS 0,17–0,5, КУ 0,83–0,5 of the total one[1]
Persson (1998)	DS 0,49–0,54, КУ 0,32–0,38 of the total one
Nesvetaev G.V., Timonov S.A. (2001)	DS 0,27–0,87; КУ 0,72–0,13[1, 2] of the total one

Note: 1 — depending on W/C; 2 — 8 supplies of cement from 6 manufacturers.

The value of CS depends on the properties of cement, the strength of concrete, and the presence of additives. According to EN 1992-1-1, CS (according to EN $\varepsilon_{ca}(\infty)$) is identified using the formulas depending on the strength of concrete f_{ck} and time *t*:

$$\varepsilon_{ca}(\infty) = 2{,}5(f_{ck} - 10)10^{-6}, \quad (1)$$

$$\varepsilon_{ca}(t) = \beta_{as}(t)\cdot\varepsilon_{ca}(\infty), \quad (2)$$

$$\beta_{as}(t) = 1 - exp(-0{,}2t^{0{,}5}). \quad (3)$$

As the strength of concrete is known to depend on W/C, CS obviously depends on W/C:

$$\frac{\varepsilon_{\text{КУ},W/C}}{\varepsilon_{\text{КУ},\frac{W}{C}=0{,}27}} = k\cdot exp\left(b\frac{W}{C}\right), \quad (4)$$

where k = 3,6 and 2,9 respectively according to the averaged data EN 1992-1-1 and some experimental data (Malinina L.A, Nesvetaev G.V. and Timonov S.A., Persson B.) with b = –4,7 and –4,0 and and the indicator of the accuracy of the approximation R^2 respectively 0,99 and 0,54, which, according to the experimental data, indicates a strong influence on the dependence (4) of other factors — first of all, the properties of cement and the presence of additives — apart from W/C.

Fly ash has almost no effect on CS, and the effect of microcrosilicon depends on the dosage — both an increase and a decrease in CS are possible. According to [13], at the age of 4 days, slag increases CS up to 1.5 times. According to [14], 10% of silica increases shrinkage by up to 1.33 times, and depending on the dose of the superplasticizer, CS varies from 0.75 to 1.25. The hardening accelerator reduces CS by about 13%, and the setting retarder increases it by up to 1.5 times. The air-entrapping additive greatly reduces CS.

The largest divergence of opinions in the literature is regarding the size of CS. Some data is shown in Table2. It should be remembered that the CS values shown in Table 2 were obtained using a variety of methods.

Table 2

Some literature data on CS

Data	CS, mm/m						
	cement dough (stone)			concrete or a solution			
	72 h	120 h	no data	24/48 h	72 h	120 h	no data
[15]	1.2	1.47			0.12–0.24	0.147–0.295	
[16]	0.6 0.3	0.75 0.39			0.060–0.120 0.030–0.060	0.075–0.15 0.039–0.078	
[17]					0.8–1.0 0.44–0.55 0.238–0.475 0.18–0.225		
[18]	0.25	0.275			0.025–0.050	0.0275–0.055	
[19]							0.1–0.5
[13]			0.75–1.2				
[14]							0.4–1.05
[20]							0.35–1.25
[21]					0.071–0.817		
[22]						0.14–0.53	
[23]				0.203/0.235			
[24]					0.4–0.62		

According to [13], the CS/CP ratio at the age of 10 hours was 0.3. According to [6], while examining 5 supplies of cement from 4 manufacturers, the CS/CP ratio was 0.32–0.5 and as SP was introduced, it ranged from 0.3 to 0.8.

We assume the large variation in the values of CS according to some literature data is largely due to the lack of a unified methodology for measuring it [19, 20, 25]. The key point is certainly the time of the beginning of the CS measurement as the development of contraction occurs immediately after the start of cement hydration. CS starts being measured at considerably different times depending on a method chosen. According to [19], with reference to the recommendations of RILEM and DIN 1045-1, CS starts being measured at the age of 1 day, but studies also indicate the beginning of measurement immediately following setting. On top of that, samples of different shapes and sizes can be used [19, 25].

Fig. 1 schematically shows the development of OK, CS, and CP over time [6]. At the first stage (1 in Fig. 1), prior to the formation of a crystalline aggregate, there are deformations of the cement paste in the plastic stage prior to setting. In some foreign sources [14], it is noted that this is an induction period and that of the start of intense hydration, with OK = CS at the first stage. Further on, due to the start of the formation of a crystalline intergrowth (skeleton), the deformations of the uninsulated (CP) and isolated (CS) mixtures start differing, and CA = CS + CP. It is from this moment on that the countdown should start while measuring CS, i.e. following setting, as noted in, e.g., in [8], and a change in the timing of the start of crystal cluster formation affects the CS/OK ratio [6].

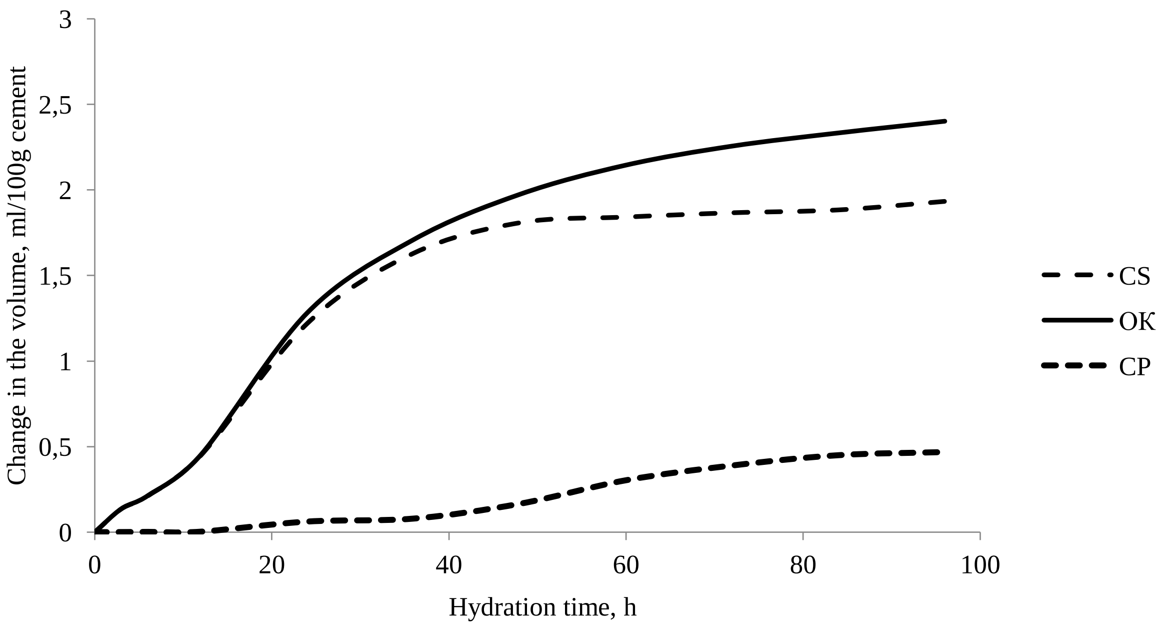

Fig. 1. Scheme of the development of OK, CS and CP over time

Highly mobile and self-sealing concrete mixtures commonly used in the production of massive monolithic reinforced concrete structures are characterized by an increased content of binder dough and the presence of modern effective diluent additives [26, 27]. Significant differences in the estimation of CS and insufficient data on the effect of superplasticizers (SPs) on CS and kinetics given the chemical and mineralogical composition of clinker and the material composition of cement, are central to the essence of research in this area. Therefore the objective of the study is to clarify the patterns of changes in the magnitude and kinetics of CS of concretes from highly mobile and self-sealing mixtures considering the influence of the composition and properties of cements in combination with some compounds commonly used in the production of monolithic reinforced concrete structures in the Rostov region.

Materials and Methods. Experimental studies were conducted using six Portland cements from four manufacturers (Table 3).

Table 3

Some properties of the investigated cements

№	PC	Properties of the cements			
		Strength, MPa, at the age of		НГ, %	НС, min.
		2 days	28 days		
1	CEM I 42,5N[1, 5]	22.4	51.5	22.75	115
2	CEM II/A-Sh 42,5N[1, 5]	23.4	55.3	25,0	150
3	CEM I 42,5N[2, 5]	28.5	50.9	26,5	150
4	CEM 0 52,5N[3, 5]	35.9	62.9	30,0	180
5	CEMI 42,5N[3, 5]	30.1	55.6	26,25	170
6	CEM II/A-P 42,5N SS[4,6]	23.5	54.6	27,25	150

Notes: 1–4 — manufacturers; 5 — GOST 31108-2020; 6 — GOST 22266-2013

All the investigated cements are classified as fast-hardening ones according to GOST 31108-2020. SP was used in a dosage of 0.5 % by weight of cement for a commercial product:

– POLYPLAST SP-4 according to TU 5745-026-58042865-2007 — a a mixture of naphthalenesulfonic acid-based copolymers;

– LINAMIX PC II according to TU 5745-033-58042865-2008 — based on polyoxyethylene derivatives of polycarboxylic acids and polyethylene glycol.

The properties of cements were identified according to GOST 30744-2001 and GOST 310.5-88. Deformations of hardening cement paste (stone) were identified using the Le Chatelier method by means of an uninsulated scheme for identifying OK and an isolated scheme (in an elastic shell) for CS [12]. CS took 120 hours (5 days) to measure, as it is this period posing the greatest threat of premature cracking of lots of massive monolithic structures. In order to switch from volumetric deformations of cement stone ΔV, %, to linear ones ε_{CS}, mm/m, while measured using an isolated scheme due to the small values, the following dependence was used:

$$\varepsilon_{\text{CS}} = 3{,}33\Delta V. \tag{5}$$

The CS of concrete ε_{con} was identified using a calculation method based on the CS of cement ε_{cem} considering the actual W/C of concrete and filler content V_a in concrete using the formula [28]:

$$\varepsilon_{con} = \varepsilon_{cem}(1 - V_a)^d, \tag{6}$$

where d = 1,2–1,7 — according to the data by Sheikin A.Ye. ; d = 1,4–1,8 — according to the data by Scherbakov Ye.N. [29]; d = 1,7 — according to the data [8, 10, 30]; V_a is assumed to be 0,7 in accordance with the recommendations [8, 28].

Research Results. Table 4 shows the data on the CS/OK ratio of the investigated cements with additives.

Table 4

CS/OK ratio in the investigated cements with additives

Composition	CS/OK ratio at 120 h for PC based on Table 3					
	1	2	3	4	5	6
PC	0.37	0.53	0.48	0.59	0.54	0.56
PC + Linamix	0.61	0.49	0.48	0.4	0.6	0.7
PC + SP-4	0.49	0.68	0.34	0.57	0.61	0.74

Almost all of the results agree with the previously specified range of 0.3–0.8. The values OK are shown in Table 5.

Table 5

OK of the investigated cements with additives

Composition	OK, ml/100 g cement , at 120 h for PC based on Table 3					
	1	2	3	4	5	6
PC	2,93	3,43	3,0	3,24	3,32	3,42
PC + Linamix	2,98	2,3	4,3	3,5	3,35	3,06
PC + SP-4	3,35	3,46	3,61	4,17	3,75	3,95

Formulas are known for identifying OK based on the mineralogical composition of clinker and the material composition of cement [20, 29]:

$$\text{OK} = aC_3S + bC_2S + cC_3A + dC_4AF + eSO_3. \quad (7)$$

For PC №1 according to Table 3, for which all the essential calculation data were known, Table 6 shows the calculated values according to a variety of formulas.

Table 6

Calculated and measured values of OK at 120 h

Value	Formula					
	Danyushevskiy V.S.	Volzhenskiy A.V.	Powers T.S.	Nekrasov V.V.	Nesvetaev G.V.[2]	Paulini P.
Calculated	2,73 0,93[1]	4,17 1,42	3,52 1,2	5,1 1,74	2,99 1,02	4,17 1,42
Measured	2,93					

Notes: 1 — in relation to the measured value ; 2 — based on (8).

The best correspondence between the calculated and measured values was obtained using the formula by Nesvetaev G.V. [29]:

$$OK = 0{,}0364C_3S + 0{,}021C_2S + 0{,}1474(C_3A - 2{,}67SO_3) + 0{,}1C_4AF + 0{,}433SO_3 \quad (8)$$

In order to describe the change in CS over time, a dependence similar to the formula for the change in concrete strength over time is employed according to EN 1992-1-1:

$$R_\tau(CS_\tau) = R_{[\tau]}\big(CS_{[\tau]}\big)\cdot exp, \quad (9)$$

where R_τ, CS_τ — the compressive strength and CS at the time τ, days, respectively; $R_{[\tau]}$, $CS_{[\tau]}$ — compressive strength and CS in 28 (*R*) and 5 (CS) days, respectively; *k*, *d* —coefficients shown in Table 7.

Table 7

Coefficients *k* and *d* (9)

Properties of concrete (*Y*)	Coefficients (9)	Cement solidification rate — criterion R_2/R_{28} based on EN 206.1			
		quick > 0.5	normal 0.3–0.5	slow 0.15–0.3	very slow < 0.15
Compressive strength, *R*	*k*	< 0.25	0.25–0.43	0.43-0.7	≥ 0.7
	d	0,5			
	[τ]	28 сут.			
Autogenous shrinkage, ε_{KY}	*k*	≲ 0.33	0.3–0.4	> 0.4	–
	d	≲ 0.65	0.66–0.9	> 0.9	–
	[τ]	5 сут			–

As both the compressive strength of concrete and CS depend on the degree of cement hydration, they naturally change over time according to similar laws allowing one to set forth a classification of concretes according to CS kinetics as shown in Table 7 apart from the well-known classification of concretes according to the rate of hardening based on EN 206.1.

Fig. 2–7 shows the measurement results the values of the CS of the cement stone of the cements according to Table 1 for 120 hours, including with SP.

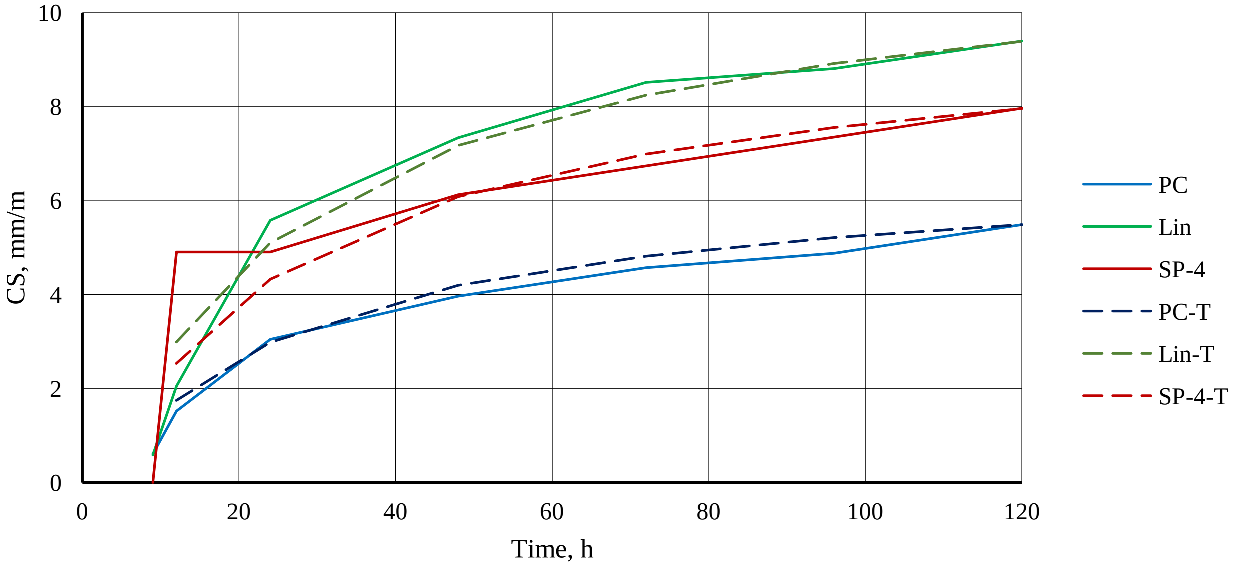

Fig. 2. Change of CS of PC № 1 over time based on Table 3:
PC, Lin, SP-4 — the additive-free standard, with Linamix and SP-4 additives respectively ;
with index T (9) — for a quick hardening rate based on Table 7 (k = 0,33; d = 0,65)

It is obvious from the results in Fig. 2 that

– the kinetics of CS of PC № 1 is almost perfectly described by formula (9) at k = 0,33, d = 0,65 (Table 7);

– if there is SP Linamix, CS grows by 1.71 times at the age of 5 days and SP-4 by 1.45 times ;

– SP has almost no effect on the kinetics of CS, k = 0,33/0,33, d = 0,65/0,65 according to SP Linamix/SP-4.

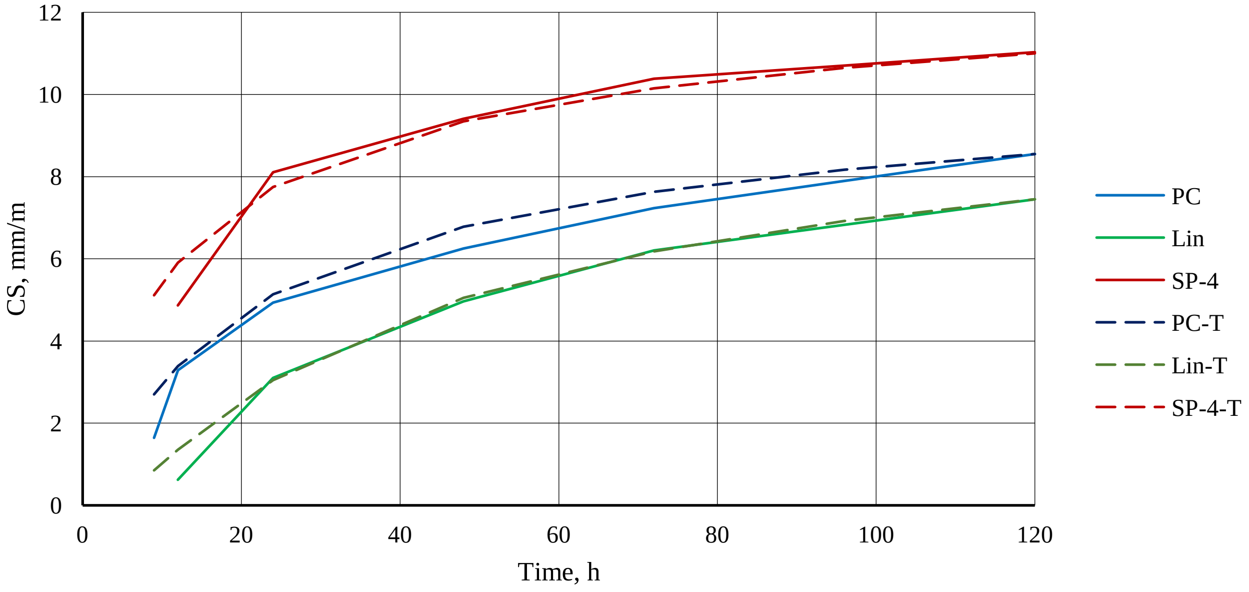

Fig. 3. Change of CS of PC № 2 over time based on Table 3:
the same designations as in Fig. 2

From the results in Fig. 3 it is obvious that

– the kinetics of CS of PC № 2 (contains slag as a mineral additive) is quite well described by formula (9) at k = 0.33, d = 0.65 (Table 7);

– if there is SP Linamix, CS at the age of 5 days is 0.87 of the standard and at SP-4 — 1.29;

– SP-4 slightly increases the kinetics of CS of k = 0.26, d = 0.53, SP Linamix slows down the kinetics of CS, k = 0.45, d = 0.68.

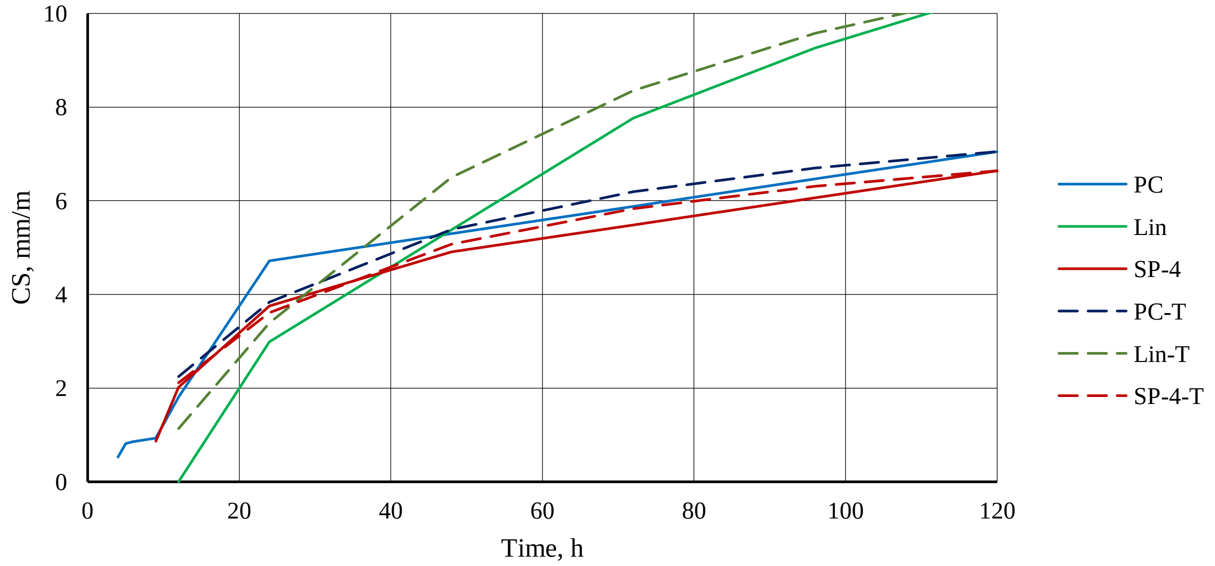

Fig. 4. Change of CS of PC № 3 over time based on Table 3:
the same designations as in Fig. 2

From the results in Fig. 4 it is obvious that

– the kinetics of CS of PC № 3 is quite well described by formula (9) at k = 0.33, d = 0.65 (Table 7);

– if there is SP Linamix, CS at the age of 5 days grows by 1.48 times and at SP-4 drops to 0.94 in relation to the additive-free standard;

– SP Linamix greatly slows down the kinetics of CS of k = 0.48, d = 0.75, SP-4 has almost no effect on the kinetics of CS of k = 0.33, d = 0.65.

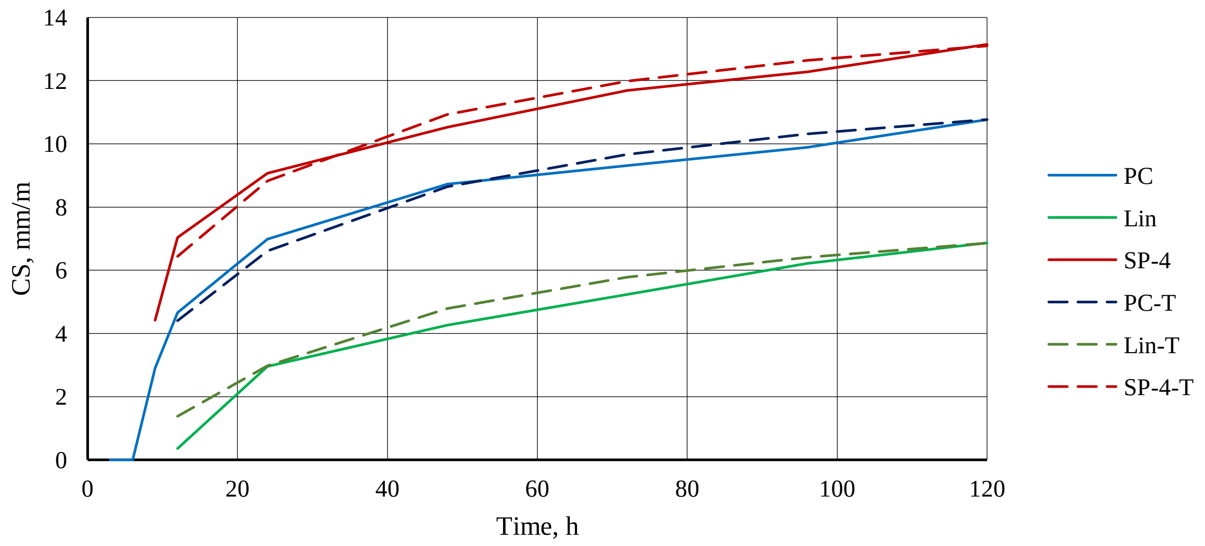

Fig. 5. Change of CS of PC № 4 over time based on Table 3:
the same designations as in Fig. 2

From the results in Fig. 5 it is obvious that

– the kinetics of CS of PC № 4 (cement grade 52.5) is quite well described by formula (9) at k = 0.3, d = 0.6 (Table 7);

– if there is SP Linamix, CS at the age of 5 days drops to 0.64 in relation to the additive-free standard and at SP-4 it grows by 1.22 times;

– SP Linamix slows down the kinetics of CS, k = 0.4, d = 0.77, SP-4 at the age of up to 48 h greatly increases the kinetics of CS of k = 0.27, d = 0.56.

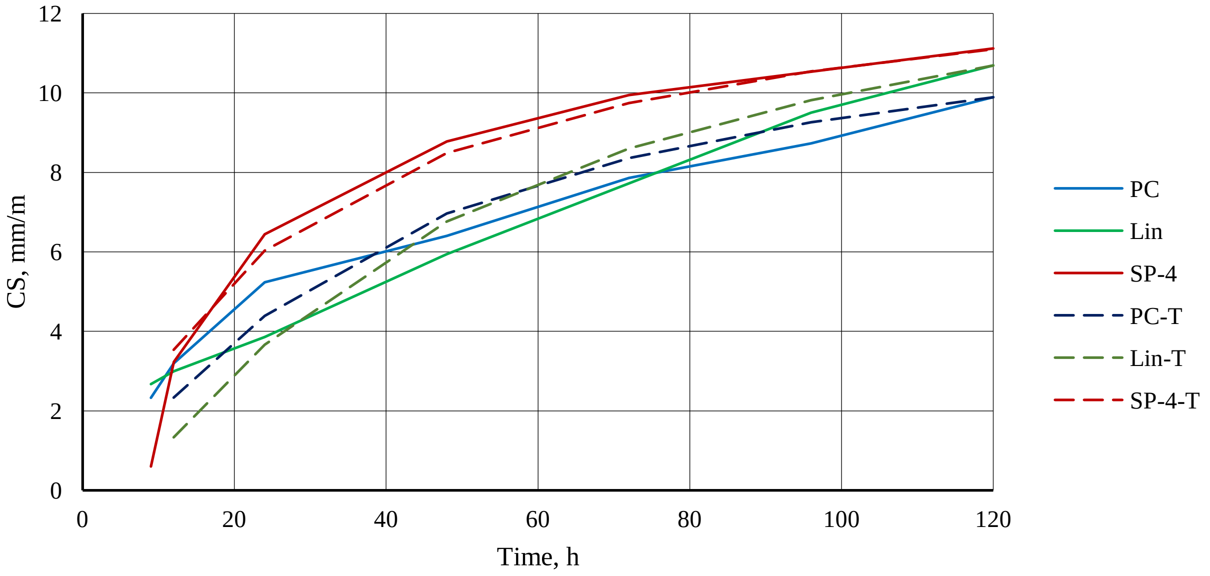

Fig. 6. Change of CS of PC № 5 over time based on Table 3:
the same designations as in Fig. 2

From the results in Fig. 6 it is obvious that

– the kinetics of CS of PC № 5 is fairly well described by formula (9) at k = 0.36; d = 0.70 (Table 7);

– if there is SP Linamix, CS at the age of 5 days grows by 1.08 times and at SP-4 by 1.12 times in relation to the additive-free standard;

– SP Linamix slows down the kinetics of CS, k = 0.49, d = 0.72, SP-4 somewhat increases the kinetics of CS of k = 0.33, d = 0.65.

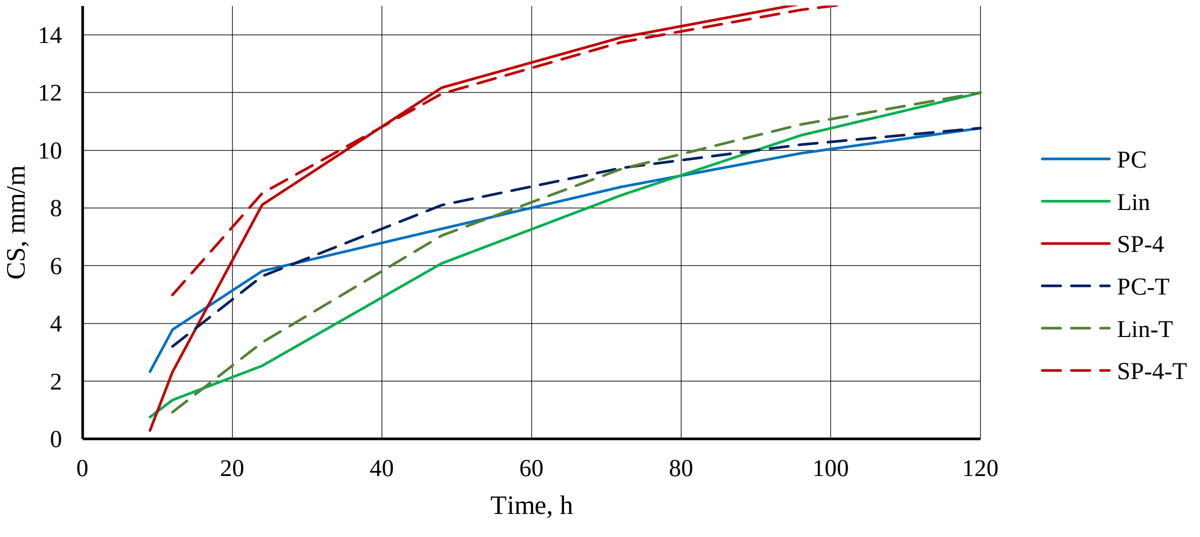

Fig. 7. Change of CS of PC № 6 over time based on Table 3: the same designations as in Fig. 2

From the results in Fig. 7 it is obvious that

– the kinetics of CS of PC № 6 (contains flask as a mineral supplement) is quite well described by formula (9) at k = 0.35; d = 0.65 (Table 7);

– if there is SP Linamix, CS at the age of 5 days grows by 1.11 times and at SP-4 by 1.45 times in relation to the additive-free standard;

– SP Linamix greatly slows down the kinetics of CS, k = 0.51, d = 0.78, SP-4 has almost no effect on the kinetics of CS, k = 0.33, d = 0.65.

The final analysis of the effect of SP on the kinetics of CS is shown in Table 8.

Table 8

Effect of SP on CS of the investigated cements

Cements based on Table 3	Index of cement stone with additives	
	$CS_{SP}/CS_Э$ at 120 h	Kinetics of CS
1	1,71/1,45[1]	no effect/no effect
2	0,87/1,29	slows down/somewhat increases
3	1,48/0,94	greatly slows down/no effect
4	0,64/1,12	slows down/increases
5	1,08/1,12	slows down/increases
6	1,11/1,45	greatly slows down/almost no effect

Note: 1 — in the numerator with Linamix, in the denominator with SP-4.

Fig. 8 shows the calculated CS values of concretes of grades B25–B35 commonly used for the construction of monolithic reinforced concrete structures in accordance with the obtained CS measurement results of the investigated cements, including those with additives, at various values of *d* in (5).

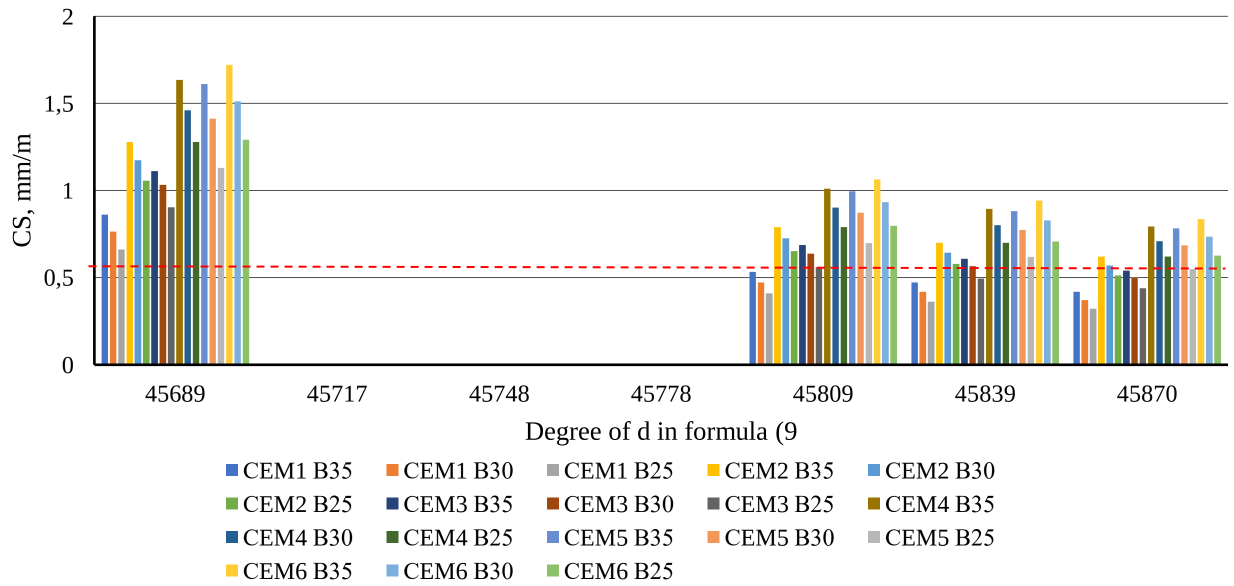

Fig. 8. Calculated values of CS of the concrete grades on the investigated cements at different values of *d* in (5)

In Fig. 8, the red dotted line indicates the maximum (1.25 mm/m) and minimum (0.4 mm/m) CS values of concrete according to some literature data (Table 2). Obviously, the most probable value of *d* in (6) is 1.6–1.8. Research in the field of experimental identification of the CS of concretes requires a follow-up.

Discussion and Conclusion. The patterns of changes in the value and kinetics of CS of concretes from highly mobile and self-sealing mixtures have been clarified considering the effect of the composition and properties of cements in combination with some SPs commonly used for the production of monolithic reinforced concrete structures in the Rostov region. The studies conducted on six different Portland cements from four manufacturers in combination with the commonly used SP of various chemical compositions POLYPLAST SP-4 and LINAMIX PK II have proved the hypothesis of a considerable effect of the chemical and mineralogical composition of cements and the chemical base of superplasticizers on the kinetics and numerical values characterizing contraction, particularly, autogenous shrinkage, which is essential for assessing the stress-strain in the early hardening period of massive monolithic structures.

The CS values of the investigated cements at 120 h have been obtained in the range from 2.93 to 3.43 ml/100 g of cement, which is in good agreement with the available literature data. The obtained values of the CS/OK ratios in the range of 0.37–0.74 at 120 h do not contradict the known data. When the SP was introduced into the concrete, CS at the age of 120 hours ranged from 0.64 to 1.71 in relation to the additive-free standard. The effect of SP on the kinetics of CS depends on both the type of cement and the SP composition.

The calculated values of the CS of concretes of grades B25–B35 from highly mobile and self–compacting concrete mixtures at 120 hours, depending on the type of cement and joint venture, were 0.32-1.06 mm/m, which is in good agreement with some available literature data.

References

1. Bjøntegaard Ø. *Basis for and practical approaches to stress calculations and crack risk estimation in hardening concrete structures — State of the art.* Blindern: Sintef; 2011. 142 p. URL: https://sintef.brage.unit.no/sintef-xmlui/bitstream/handle/11250/2411102/coin31.pdf?sequence=1 (accessed: 07.02.2025).

2. Semenov K, Kukolev M, Zaichenko N, Popkov S, Makeeva A, Amelina A. et al. Unsteady temperature fields in the calculation of crack resistance of massive foundation slab during the building period. In: *International Scientific Conference on Energy, Environmental and Construction Engineering.* Cham: Springer; 2019. Pp. 455–467.

3. Nesvetaev GV, Chepurnenko AS, Koryanova YuI, Sukhin DP. Evaluation of someTechniques for Calculating Temperature Stresses during Concreting of Massive Reinforced Concrete Foundation Slabs. *Don Engineering Bulletin.* 2022;7(91). (In Russ.) URL: http://www.ivdon.ru/uploads/article/pdf/IVD_20__7_Nesvetaev_Chepurnenko.pdf_8331ae3d10.pdf (accessed: 07.02.2025).

4. Chepurnenko AS, Nesvetaev GV, Koryanova YuI, Yazyev BM. Simplified Model for Determining the Stress-Strain State in Massive Monolithic Foundation Slabs During Construction. *International Journal for Computational Civil and Structural Engineering*. 2022;18(3):126–136. https://doi.org/10.22337/2587-9618-2022-18-3-126-136

5. Sellevold E, Bjøntegaard Ø, Justnes H, Dahl PA. High performance concrete: early volume change and cracking tendency. In: *RILEM International Symposium on Thermal Cracking in Concrete at Early Ages*. Munich; 1994. Pp. 229–236. URL: https://www.researchgate.net/publication/283349354_High_Performance_Concrete_Early_Volume_Change_and_Cracking_Tendency (accessed: 07.01.2025).

6. Nesvetaev GV, Korchagin IV, Koryanova YuI. On the Contraction of Portland Cement in the Presence of a Superplasticizer. *Scientific Review*. 2014;7(3):842–846. (In Russ.) URL: https://www.researchgate.net/publication/366120707_O_KONTRAKCII_PORTLANDCEMENTA_V_PRISUTSTVII_SUPERPLASTIFIKATORA (accessed: 07.01.2025).

7. Nekrasov VV. Changing the Volume of the System during Hardening of Hydraulic Binders. *Bulletin of the USSR Academy of Sciences*. 1945;6:592–610. (In Russ.)

8. Rasoolinejad M, Rahimi-Aghdam S, Bazˇant ZP. Prediction of autogenous shrinkage in concrete from material composition or strength calibrated by a large database, as update to model B4. *Materials and Structures.* 2019;52(2):33. https://doi.org/10.1617/s11527-019-1331-3

9. Miyazawa S, Tazawa E. Prediction model for autogenous shrinkage of concrete with different type of cement. In: *Proceedings of the 4th international seminar on self-desiccation and its importance in concrete technology*. Gaithersburg: NIST; 2005.

10. Grasley Z, Lange D, Brinks A, D'Ambrosia M. Modeling autogenous shrinkage of concrete accounting for creep caused by aggregate restraint. In: *Proceedings of the 4th international seminar on self-desiccation and its importance in concrete technology*. Gaithersburg: NIST; 2005. Pp. 78–94. URL: https://www.researchgate.net/publication/269575700_Modeling_Autogenous_Shrinkage_of_Concrete_Accounting_for_Creep_Caused_by_Aggregate_Restraint (accessed: 07.01.2025).

11. Powers TC, Brownyard TL. *Studies of the Physical Properties of Hardened Portland Cement Paste*. Chicago: Portland Cement Association: 1948. 992 p.

12. Panchenko AI, Kharchenko IYa, Vasiliev SV. Durability of concrete with compensated chemical shrinkage. *Construction materials*. 2019;8:48–53. https://doi.org/10.31659/0585-430X-2019-773-8-48-53

13. Khairallah RS. *Analysis of Autogenous and Drying Shrinkage of Concrete.* Hamilton: McMaster University; 2009. 154 p. URL: https://macsphere.mcmaster.ca/bitstream/11375/9421/1/fulltext.pdf (accessed: 08.02.2025).

14. Esping O, Löfgren I. *Cracking due to plastic and autogenous shrinkage-investigation of early age deformation of self-compacting concrete-experimental study. Technical report*. Sweden: Chalmers University of Technology; 2005. https://doi.org/10.13140/RG.2.2.27325.36323

15. Bentz DP, Jensen OM, Hansen KK, Oleson JF, Stang H, Haecker CJ. Influence of cement particle size distribution on early age autogenous strains and stresses in cement-based materials. *Journal of the American Ceramic Society.* 2004;84(1):129–135. https://doi.org/10.1111/j.1151-2916.2001.tb00619.x

16. Koenders EAB, Van Breugel K. Numerical modelling of autogenous shrinkage of hardening cement paste. *Cement and Concrete Research*. 1997;27(10):1489–1499. https://doi.org/10.1016/S0008-8846(97)00170-1

17. Kumarappa DB, Peethamparan S, Ngami M. Autogenous shrinkage of alkali activated slag mortars: Basic mechanisms and mitigation methods. *Cement and Concrete Research*. 2018;109:1–9. https://doi.org/10.1016/j.cemconres.2018.04.004

18. Abate SY, Park S, Kim H-K. Parametric modeling of autogenous shrinkage of sodium silicateactivated slag. *Construction and Building Materials. 2020;*262:120747. https://doi.org/10.1016/j.conbuildmat.2020.120747

19. Gowripalan N. Autogenous Shrinkage of Concrete at Early Ages. In: *ACMSM25. Lecture Notes in Civil Engineering*. Singapore: Springer; 2020. https://doi.org/10.1007/978-981-13-7603-0_27

20. Holt E. *Early age autogenous shrinkage of concrete*. Espoo: VTT Publications; 2001. 184 p. URL: https://publications.vtt.fi/pdf/publications/2001/P446.pdf (accessed: 16.01.2025).

21. Nassif H, Suksawang N, Mohammed M. Effect of curing methods on early-age and drying shrinkage of high-performance concrete. *Transportation research record*. 2003;1834:4858. https://doi.org/10.3141/1834-07

22. Soliman AM, Nehdi ML. Effect of drying conditions on autogenous shrinkage in ultra-high-performance concrete at early-age. *Materials and Structures*. 2011;44:879–899. https://doi.org/10.1617/s11527-010-9670-0

23. Saje D. Reduction of the Early Autogenous Shrinkage of High Strength Concrete. *Advances in Materials Science and Engineering*. 2015;4:310641. https://doi.org/10.1155/2015/310641

24. Soliman AM. *Early-Age Shrinkage of Ultra High-Performance Concrete: Mitigation and Compensating Mechanisms*. Electronic Thesis and Dissertation Repository; 2011. 145 p. URL: https://ir.lib.uwo.ca/etd/145/ (accessed: 17.01.2025).

25. Qin Y, Yi Z, Wang W, Wang D. Time-Dependent Behavior of Shrinkage Strain for Early Age Concrete Affected by Temperature Variation. *Materials Science and Engineering.* 2017;3627251. https://doi.org/10.1155/2017/3627251

26. Kalinovskaya NN, Osos RF, Kuchuk EV. Concreting the Foundation Plate of the Turbine Unit of the Belarusian NPP Using Self-sealingConcrete. *Concrete Technologies.* 2017;3–4(128–129):15–19. (In Russ.) URL: http://tehnobeton.ru/pdf/2017-3-4/15-19.pdf (accessed: 17.01.2025).

27. Murtazaev SAYu, Saidumov MS, Alaskhanov AKh, Murtazaeva TSA. High-strength Concretes of Increased Viability for the Structures of the Foundations of the IFC Akhmat Tower. In: *Collection of Reports of the International Online Congress "Fundamentals of Building Materials Science".* Belgorod: BSTU named after V.G. Shukhov; 2017. Pp. 875–883, (In Russ.) URL: https://elibrary.ru/item.asp?id=36305899 (accessed 18.01.2025).

28. Pickett G. Effect of aggregate on shrinkage of concrete and a hypothesis concerning shrinkage. *ACI Journal*. 1956;52:581–590.

29. Babkov VV, Bazhenov YuM, Bykova AA, Galdina VD, Gridchin AM, Ivantsov VA. and others. *Cements, Concretes, Mortars, and Dry Mixes.* Part I. Komokhov P.G. (ed.). St. Petersburg: Professional; 2007. 804 p. (In Russ.).

30. Lura P, Jensen OM, Van Breugel K. Autogenous shrinkage in high-performance cement paste: an evaluation of basic mechanisms. *Cement and Concrete Research.* 2003;33(2):223–232. https://doi.org/10.1016/S0008-8846(02)00890-6

About the Authors:

Grigory V. Nesvetaev, Dr.Sci. (Eng.) Professor of the Department of Construction Production Technology at the Don State Technical University (1 Gagarin Square, Rostov-on-Don, 344003, Russian Federation), ScopusID, ORCID, nesgrin@yandex.ru

Yulia I. Koryanova, Cand.Sci. (Eng.), Associate Professor of the Department of Construction Production Technology at the Don State Technical University (1 Gagarin Square, Rostov-on-Don, 344003, Russian Federation), ScopusID, ORCID, koryanova.yi@mail.ru

Vladimir V. Shut, Master's student at the Don State Technical University (1 Gagarin Square, Rostov-on-Don, 344003, Russian Federation), ORCID, don-com-ru@mail.ru

Claimed Contributorship:

GV Nesvetaev: formation of the basic concept, goals and objectives of the study, justification of criteria, general planning of the experiment, analysis of the research results, editing the manuscript, correction of the conclusions.

YuI Koryanova: detailed planning, organization and implementation of the research, analysis of the research results, preparing the manuscript, formulation of the conclusions.

VV Shut: operational planning and implementation of the research, processing the research results, analysis of the research results.

Conflict of interest statement: **the authors do not have any conflict of interest.**

All authors have read and approved the final version of manuscript.

Об авторах:

Несветаев Григорий Васильевич, доктор технических наук, профессор кафедры технологии строительного производства Донского государственного технического университета (344003, Российская Федерация, г. Ростов-на-Дону, пл. Гагарина, 1), ScopusID, ORCID, nesgrin@yandex.ru

Корянова Юлия Игоревна, кандидат технических наук, доцент кафедры технологии строительного производства Донского государственного технического университета (344003, Российская Федерация, г. Ростов-на-Дону, пл. Гагарина, 1), ScopusID, ORCID, koryanova.yi@mail.ru

Шуть Владимир Валерьевич, магистрант Донского государственного технического университета (344003, Российская Федерация, г. Ростов-на-Дону, пл. Гагарина, 1), ORCID, don-com-ru@mail.ru

Заявленный вклад авторов:

Г.В. Несветаев: формирование основной концепции, цели и задач исследования, обоснование критериев, общее планирование эксперимента, анализ результатов исследований, редактирование текста, корректировка выводов.

Ю.И. Корянова: детальное планирование, организация и реализация исследований, анализ результатов исследований, подготовка текста, формулировка выводов.

В.В. Шуть: рабочее планирование и реализация исследований, обработка результатов исследований, анализ результатов исследований.

Конфликт интересов: **авторы заявляют об отсутствии конфликта интересов.**

Все авторы прочитали и одобрили окончательный вариант рукописи

Received / Поступила в редакцию 19.02.2025
Reviewed / Поступила после рецензирования 07.03.2025
Accepted / Принята к публикации 12.03.2025

CONSTRUCTION MECHANICS
СТРОИТЕЛЬНАЯ МЕХАНИКА

UDC 624.44:539.376
https://doi.org/10.23947/2949-1835-2025-4-1-54-67

Original Empirical Research

EDN: KDXNZY

Examples of Testing a Program for Modeling Long-Term Deformation of Prestressed Reinforced Concrete Beams

Peter P. Gaydzhurov[1] ✉, **Elvira R. Iskhakova**[2], **Nina A. Savelyeva**[1]
[1] Don State Technical University, Rostov-on-Don, Russian Federation
[2] South Russian State Polytechnic University (NPI) named after M.I. Platov, Novocherkassk, Russian Federation
✉ gpp-161@yandex.ru

Abstract

Introduction. Currently, there is very little information in the Russian literature on the development and practical application of numerical methods for studying the stress-strain state of concrete and reinforced concrete structures, taking into account the creep of concrete. As a rule, when analyzing the long-term deformation of such structures, calculators apply an empirical approach based on the use of the reduced modulus of deformation in combination with the coefficient of creep. The purpose of this study is to verify and validate the developed finite element algorithm and the corresponding software based on the results of experimental studies of the stress-strain state, prestressed reinforced concrete beam structures, taking into account the creep of concrete, available in the literature.

Materials and Methods. As a mathematical tool for modeling the process of long-term deformation of reinforced concrete girder structures, the finite element method was used in combination with a simple procedure for numerical integration along the time coordinate of the operator-matrix resulting equation. The program code is implemented on the basis of the Microsoft Visual Studio computing platform and the Intel Parallel Studio XE compiler with the built-in Intel Visual Fortran Composer XE text editor. The processes of storing and processing working arrays are implemented in terms of sparse matrices. The descriptive graphics of the Matlab computer system were used to visualize the calculation results. All of the computational experiments were performed using the authorized Polygon complex. The objectives of the study include evaluating the accuracy of the proposed methodology for analyzing the long-term deformation of reinforced concrete structures with various methods of external force action, including the effect of prestressing.

Results. A program for calculating reinforced concrete beam structures in a three-dimensional formulation has been developed and debugged using a discrete reinforcement scheme, according to which the reinforcing frame is modeled by rod (beam), and the concrete array by volumetric finite elements. To determine the restoring force caused by the tension of the cable reinforcement on concrete, a two-dimensional finite element model consisting of truss and spring finite elements is used. The simulation of long-term deformation was performed within the framework of the theory of linear viscoelasticity in combination with the principle of superimposition of influences.

Discussion and Conclusion. A comparative analysis of the results of field and computational experiments on the stress-strain state of reinforced concrete beams of rectangular cross-section with post- and prestress is performed. The proposed method makes it possible to calculate prestressed reinforced concrete girder structures with variable quasi-static loading, taking into account the linear creep of concrete.

Keywords: finite element method, creep of concrete, pre-tensile stress, reinforced concrete girder structures

For citation. Gaydzhurov PP, Iskhakova ER, Savelyeva NA. Examples of Testing a Program for Modeling Long-Term Deformation of Prestressed Reinforced Concrete Beams. *Modern Trends in Construction, Urban Planning and Territorial Planning.* 2025;4(1):54–67. https://doi.org/10.23947/2949-1835-2025-4-1-54-67

Оригинальное эмпирическое исследование

Примеры тестирования программы моделирования длительного деформирования предварительно напряженных железобетонных балок

П.П. Гайджуров[1] ✉ , Э.Р. Исхакова[2], Н.А. Савельева[1]
[1] Донской государственный технический университет, г. Ростов-на-Дону, Российская Федерация
[2] Южно-Российский государственный политехнический университет (НПИ) имени М.И. Платова, г. Новочеркасск, Российская Федерация
✉ gpp-161@yandex.ru

Аннотация
Введение. В настоящее время в отечественной литературе приведено крайне мало сведений о разработке и применении на практике численных методов исследования напряженно-деформированного состояния бетонных и железобетонных конструкций с учетом ползучести бетона. Как правило, при анализе длительного деформирования подобных конструкций расчетчики применяют эмпирический подход, основанный на использовании коэффициента ползучести. Цель настоящего исследования заключается в верификации и валидации разработанного конечно-элементного алгоритма и соответствующего программного обеспечения на базе имеющихся в литературе результатов экспериментальных исследований напряженно-деформированного состояния предварительно напряженных железобетонных балочных конструкций с учетом ползучести бетона.
Материалы и методы. В качестве математического аппарата для моделирования процесса длительного деформирования железобетонных балочных конструкций применен метод конечных элементов в сочетании с шаговой процедурой численного интегрирования по временной координате результирующего операторно-матричного уравнения. Программный код реализован на базе вычислительной платформы Microsoft Visual Studio и компилятора Intel Parallel Studio XE со встроенным текстовым редактором Intel Visual Fortran Composer XE. Процессы хранения и обработки рабочих массивов реализованы в терминах разреженных матриц. Для визуализации результатов расчетов использована дескрипторная графика компьютерной системы Matlab. Все вычислительные эксперименты выполнены с помощью авторизированного комплекса Polygon. В задачи исследования входит оценка точности предлагаемой методики анализа длительного деформирования железобетонных конструкций при различных способах внешнего силового воздействия, включая эффект предварительного напряжения.
Результаты исследования. Разработана и отлажена программа расчета железобетонных балочных конструкций в трехмерной постановке с использованием дискретной схемы армирования, согласно которой армирующий каркас моделируется стержневыми (балочными) конечными элементами, а массив бетона — объемными. Для определения восстанавливающего усилия, обусловленного натяжением тросовой арматуры на бетон, применена двухмерная конечно-элементная модель, состоящая из ферменных и пружинных конечных элементов. Моделирование длительного деформирования выполнено в рамках теории линейной вязкоупругости в сочетании с принципом наложения воздействий.
Обсуждение и заключение. Выполнен сравнительный анализ результатов натурных и вычислительных экспериментов исследования напряженно-деформированного состояния железобетонных балок прямоугольного поперечного сечения с пост- и преднапряжением. Предлагаемая методика позволяет выполнить расчет предварительно напряженных железобетонных балочных конструкций при переменном характере квазистатического нагружения с учетом линейной ползучести бетона.

Ключевые слова: метод конечных элементов, ползучесть бетона, предварительное напряжение, железобетонные балочные конструкции

Для цитирования. Гайджуров П.П, Исхакова Э.Р., Савельева Н.А. Примеры тестирования программы моделирования длительного деформирования предварительно напряженных железобетонных балок. *Современные тенденции в строительстве, градостроительстве и планировке территорий*. 2025;4(1):54–67. https://doi.org/10.23947/2949-1835-2025-4-1-54-67

Introduction. It is widely known that concrete has been the most common building material over the last two centuries. There have been hundreds of unique high-rise buildings all over the world constructed using high-strength concrete structurally reinforced with a steel frame, offshore platforms for hydrocarbon production as well as protective shells of nuclear reactors have also been manufactured. It is difficult to imagine hydropower, large-span bridges, subways, large-scale motorway interchanges and transport tunnels without concrete. However, unlike steel, which is no less common in construction, concrete is much more susceptible to creep deformation that largely depends on the "age" of the binder, the size of the structure, the nature and sequence of application or removal of external loads, as well as the temperature and humidity conditions of the environment. It has been experimentally found that creep has a considerable impact on the redistribution of internal forces in concrete and reinforced concrete structures. Moreover, the displacements caused by creep deformation can be several times higher than those caused by the application of the load at the initial moment of time. There is now a significant amount of experimental and theoretical material available on concrete creep. At the same time, the well-known approaches to calculating concrete and reinforced concrete structures taking into account creep are mostly focused on solving problems with a relatively simple product geometry and they fail to take into account the technological background associated with the formation of the initial stress state and the effect of inheritance of the stress-strain due to the history of loading the structure. Therefore, we are being faced with a pressing problem of developing a more general finite element algorithm implementing a model of an elastic creeping body allowing one to consider the effect of rapidly increasing creep at the time of application of an operational load, the partial reversibility of creep deformation while removing a long-acting load (elastic after-impact), various methods and schemes of reinforcement prestressing.

The objective of the study is to test an authorized finite element software package by means of comparing the results obtained with other authors' data.

Materials and Methods. In compliance with G.N. Maslov — N.H. Harutyunyan's assumption, the total relative longitudinal deformation $\delta(t,\tau)$ of a prismatic concrete sample during compression is commonly represented as the following sum [1–4]:

$$\delta(t,\tau) = \frac{1}{E(t)} + C(t,\tau),$$

where τ is the parameter corresponding to the "age" of the concrete; $\frac{1}{E(t)}$ is the elastic instantaneous deformation of the sample; $E(t)$ is the the current value of the modulus of deformation; $C(t,\tau)$ is the creep deformation at the time of observation t ($\tau \le t < \infty$).

The function $C(t,\tau)$ is commonly referred to as the creep measure. Depending on the type of the function $C(t,\tau)$, creep deformation following unloading can be completely or partially reversible [5]. As noted in [1, 3, 4], it is convenient to approximate the function $E(t)$ using the following dependence:

$$E(t) = E_0\left(1 - \xi e^{-\beta t}\right),$$

where $E_0$is the limiting value of the modulus of elasticity of "mature age" concrete.

The parameters ξ, βincluded in the expression $E(t)$ are determined experimentally and depend on the composition and conditions of concrete hardening.

These are the expressions for the creep measure function:

by N.H. Harutyunyan [1]:

$$C(t,\tau) = \varphi(\tau)\left[1 - e^{-\gamma(t-\tau)}\right]; \tag{1}$$

by S.V. Aleksandrovskiy [3]:

$$C(t,\tau) = \psi(\tau) - \psi(t)\left(\frac{1-A_2e^{-\gamma\tau}}{1-A_2e^{-\gamma t}}\right)e^{-\gamma(t-\tau)} + \Delta(\tau)\left[1 - e^{-\alpha(t-\tau)}\right]. \tag{2}$$

The rapidly decreasing functions here are the following:

$$\varphi(\tau) = C_1 + \frac{A_1}{\tau},\ \psi(\tau) = C_3 + \frac{A_3}{\tau},\ \Delta(\tau) = C_1 - C_3 + \frac{A_1 - A_3}{\tau}.$$

It should be noted that the function $\varphi(\tau)$ was first set forth by N.H. Harutyunyan [1]. The graph of the function $\varphi(\tau)$ for various parameter values $C_1$and A_1 is shown in Fig. 1. In this figure, the curves $\varphi(\tau)$ tend to the limiting value C_1/A_1. The constants in expressions (1) and (2) in units of measurement adopted in [3] are

$$\alpha = 6\ \text{day}^{-1};\ \gamma = 0.03\ \text{day}^{-1}; A_1 = 4.62\cdot10^{-5}\,\frac{day}{kgsec/cm^2}\ \left(4.7095\cdot10^{-10}\,\frac{day}{N/m^2}\right);$$

$$A_2 = 1;\ A_3 = 3.416\cdot10^{-5}\,\frac{day}{kgsec/cm^2}\ \left(3.48226\cdot10^{-10}\,\frac{day}{N/m^2}\right);\ C_1 = 0.975\cdot10^{-5}\ \text{cm}^2/\text{kgsec}\ (9.9388\cdot10^{-10}\ \text{m}^2/\text{N});$$

$$C_3 = 0.756\cdot10^{-5,5}\ \text{cm}^2/\text{kgsec}\ (7.7064\cdot10^{-11}\ \text{m}^2/\text{N}).$$

The values of the constants converted into the SI system are shown in the parentheses. The graph of the function $C(t,\tau)$ for various values in the range t from 0 to 100 days while using the values of the constants in the SI system is shown in Fig. 2.

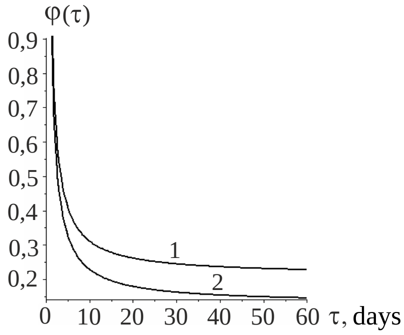

Fig. 1. Graph $\varphi(\tau) = \frac{1}{A_1}\left(C_1 + \frac{1}{\tau}\right)$:
1 — $C_1 = 0.975 \cdot 10^{-5}$ cm²/kgsec; $A_1 = 4.62\ 10^{-5}$ days·(kgsec/cm²)⁻¹;
2 — $C_1 = 0.238 \cdot 10^{-5}$ cm²/kgsec; $A_1 = 1.85\ 10^{-5}$ days·(kgsec/cm²)⁻¹

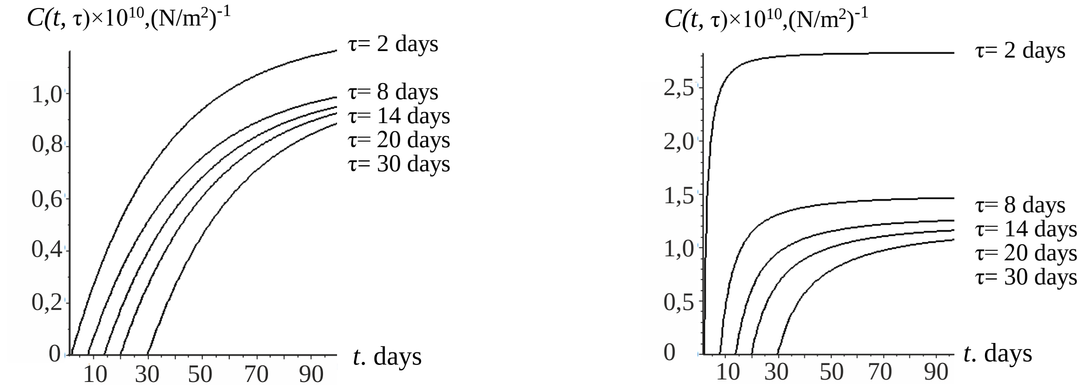

a) *b)*

Fig. 2. Graphs of the functions $C(t,\tau)$: (N/m²)⁻¹
a – by N.H. Harutunyan [1]; *b* – by S.V. Aleksandrovskiy [3]

Comparing the graphs in Fig. 2, *a* and 2, *b* at τ = 2 days and *t* = 100 days, we find that the values calculated using formula (2) are almost 2.5 times higher than the data based on formula (1). At τequalling 8, 14, 20, 30 days and *t* = 100 days of the value of $C(t,\tau)$ calculated using formulas (1) and (2) are not much different. It should also be noted that the initial steepness of the curves $C(t,\tau)$ in Fig. 2, b is sharper than in Fig. 2, *a*.

For the finite element analysis of monolithic reinforced concrete structures taking into account the creep of concrete, the relationship between stresses and deformations is presented in the matrix operator form:

$$\{\sigma(t)\} = [E(t)](1 - R)\{\varepsilon(t)\},$$

where $\{\sigma(t)\}$, $\{\varepsilon(t)\}$are the vectors-columns of the stresses and deformations corresponding to the moment of time *t*; $[E(t)]$is the elasticity matrix (with the dimensionality 6×6$6 \times 6$in the general case); $R\varepsilon_{ij} = \int_{\tau_1}^{t} R(t,\tau)\varepsilon_{ij}(\tau)d\tau,\ i,j = 1{,}3$is the linear integral operator establishing a correspondence between the current deformations $\varepsilon_{ij}$and the "history" of long-term deformation $\varepsilon_{ij}(\tau)$.

The so-called hereditary function $R(t,\tau)$ is introduced in the expression under the integral sign . The type of hereditary function is known to determine how real modeling of a creep process is, particularly taking into account the system response when the load is partially or completely removed. In relation to the theory of creep of hereditary concrete, three major directions are identified [3, 4]: the theory of elastic heredity; the theory of aging; the theory of elastic-creeping body. Let us take a closer look at the main features of hereditary functions that are at the core of each of the above theories.

In *the theory of elastic heredity*, it is assumed that complete reversibility (zeroing) of deformations occurs during unloading. The hereditary function in this case takes the form [3]:

$$R(t - \tau) = E_0 C_1 \gamma e^{-\gamma(1+E_0C_1)(t-\tau)}, \qquad (3)$$

where E_0 is the initial elasticity modulus; C_1, $\gamma$are the constants identified experimentally using the creep curves.

The graph $R(t,\tau)$ based on expression (3) for various values of the parameter τ is shown in Fig. 3. Hereafter, the constants included in (3) are assumed to be the same as in expressions (1) and (2). The value of the initial modulus of elasticity of concreteE_0 = 2.55·1010 N/m^2. The computer mathematics environment of the Maple system was used to design the graph [6].

τ, days

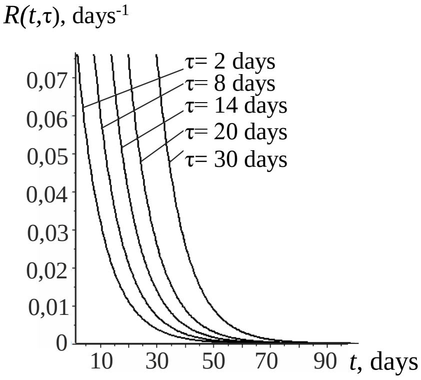

Fig. 3. Graph $R(t,\tau)$ according to the theory of elastic heredity

As can be seen, the curves in Fig. 3 for various values of τmimic one another with a displacement. This is due to the fact that in expression (3) the modulus of elasticity is assumed to be constant, i.e. the effect of "aging" of the material is not considered in this theory. The theory of elastic heredity is only applicable to "old" concrete. In this case, it is assumed that the creep deformation depends only on the duration of the operating load.

The theory of aging relies on the assumption that the reversibility of creep deformations during partial or complete unloading is completely denied. The expression for the function $R(t,\tau)$ taking into account the change in the deformation properties of the material over time provided in the biography of S.V. Alexandrovsky [3] takes the following form:

$$R(t,\tau) = \frac{1}{E(t)} \cdot \frac{\partial}{\partial \tau}\left[E(\tau) e^{-\int_{\tau}^{t} E(\tau)\frac{\partial}{\partial \tau}C(\tau,\tau_1)d\tau}\right], \qquad (4)$$

where $E(t) = E_0\left(1 - e^{-\beta t}\right)$ is an approximation of the modulus of elastic deformations (parameter = 0.206 days^{-1}); τ_1 is "age" of concrete at the time of loading, days.

Visualization of the function $R(t,\tau)$ in the form of a graph based on expression (4) in the Maple environment is shown in Fig. 4.

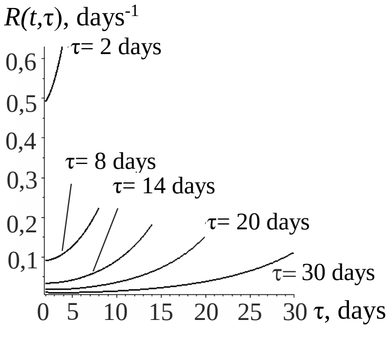

«Age» of concrete $\tau \equiv \tau_1$ in days by the moment deformations occur

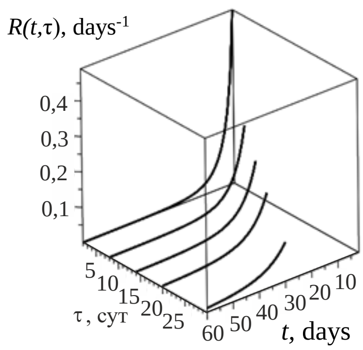

Fig. 4. Graph $R(t,\tau)$ according to the theory of aging

As noted in [3], the theory of aging is applicable for calculations of concrete and reinforced concrete structures under a short-term load. Furthermore, in the case of unloading, this theory causes a considerable overestimation of the aftereffect deformations for “young” concrete and an underestimation of those for “old” concrete.

The theory of elastic-creeping body takes into consideration the partial reversibility of creep deformations during unloading. In the monograph by S.V. Aleksandrovsky [3] within the framework of the theory of elastic-creeping body the following expression for the hereditary function of concrete is set forth:

$$R(t,\tau) \approx -\frac{1}{E(t)}K^2(\tau)F^{'}(\tau)(e^{\gamma\tau} - A_2) - K^{'}(\tau) - \left[K(\tau)(e^{\gamma\tau} - A_2)e^{-\eta(\tau)}\right]^{'}\int_{\tau}^{t} K(\tau)F^{'}(\tau)e^{\eta(\tau)}\,d\tau + +B_3(t)e^{-\mu(t)(t-\tau)}\}, \quad (5)$$

where $(\ldots)^{'} = \partial\ldots/\partial\tau$; $B_3(t) = F^{'}(t)(e^{\gamma t} - A_2)[E^2(t) - K^2(t)] - \alpha E^2(t)\Delta(t) + K^{'}(t) - E^{'}(t)$;

$$\mu(t) = \frac{1}{B_3(t)}\{B_3^{'}(t) + \gamma e^{\gamma t}F^{'}(t)[E^2(t) - K^2(t)] -$$
$$-F^{'2}(t)(e^{\gamma t} - A_2)^2[E^3(t) - K^3(t)] - \alpha E(t)[E(t)\Delta(t)]^{'} -$$
$$-\alpha^2 E^3(t)\frac{\Delta(t)}{K(t)} + \frac{1}{2}F^{'}(t)(e^{\gamma t} - A_2)[E^2(t) - K^2(t)]^{'} +$$
$$+2\alpha E^3(t)\Delta(t)F^{'}(t)(e^{\gamma t} - A_2)\};$$
$$K(t) = \frac{E(t)}{1+\Delta(t)E(t)};\ .$$

For a rapidly decreasing function $\Delta(t)$, the following dependencies are set forth in the monograph [3]:

$$1)\ \Delta(t) = (0.25 + 0.99^{-\alpha t}) \cdot 10^{-5};$$
$$2)\ \Delta(t) = C_1 - C_3 + \frac{A_1 - A_3}{t};$$
$$3)\ \Delta(t) = \left(\frac{80}{t} + 2.714\right) \cdot 10^{-7};$$
$$4)\ \Delta(t) = (11.2 + 34 \cdot e^{-0.125\cdot t}) \cdot 10^{-7}.$$

The graph of the function $\Delta(t)$ designed using the above expressions for $\Delta(t)$ is shown in Fig. 5. The numbers indicate the curves corresponding to the dependency numbers $\Delta(t)$.

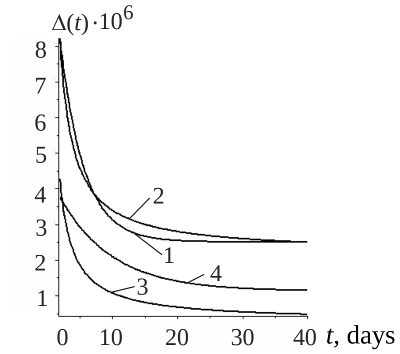

Fig. 5. Graph of the function $\Delta(t)$ for dependencies 1, 2, 3, 4

Given the qualitative coincidence of the curves $\Delta(t)$ in Fig. 5, in the future a more universal dependence (2) will be used.

In order to make formula (5) look convenient for programming, the symbolic processor of the Maple system [6] will be used. The curves of the function $R(t,\tau)$for different "ages" of concrete obtained by means of computational technology [7] are shown in Fig. 6. Figure 7 shows a similar graph $R(t,\tau)$from the monograph [3]. The range of variation of the parameter in Fig. 6 and 7 is almost identical.

Comparing the graphs $R(t,\tau)$in Fig. 6 and 7, it is found that that the curves of the hereditary function are identical within the visualization for the same parameter values. It is critical to note that the curves $R(t,\tau)$ shown in Fig. 6 are clearly indicative of the consideration of the so-called rapidly increasing creep observed in practice at a moment in time $t = \tau + \delta t$ where δt ≤1 day [3].

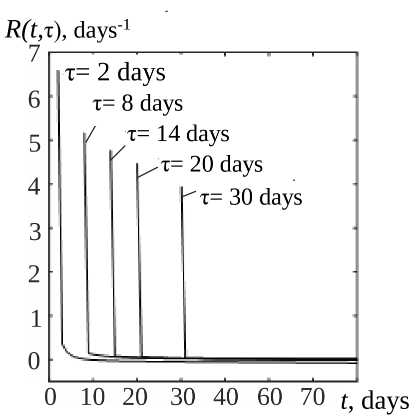

Fig. 6. Graph $R(t,\tau)$ [7]

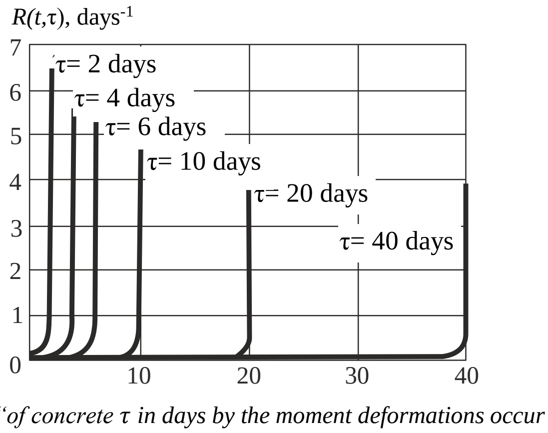

Fig. 7. Graph $R(t,\tau)$ [3]

For "old" concrete, the following expression for the hereditary function is recommended in the monograph [3]:

$$R(t-\tau) = A_1 e^{-\rho_1 (t-\tau)} + A_2 e^{-\rho_2 (t-\tau)}, \tag{6}$$

where

$$A_1 = \frac{E_0}{\rho_1 - \rho_2}\{(\gamma\psi_0 + \alpha\Delta_0)[E_0(\gamma\psi_0 + \alpha\Delta_0) - \rho_2] + \alpha^2\Delta_0 + \gamma^2\psi_0\};$$

$$A_2 = E_0(\gamma\psi_0 + \alpha\Delta_0) - A_1;$$

$$\rho_{1,2} = \frac{1}{2}\{\alpha + \gamma + E_0(\gamma\psi_0 + \alpha\Delta_0) \pm$$

$$\pm\sqrt{{E_0}^2(\gamma\psi_0 + \alpha\Delta_0)^2 + (\alpha-\gamma)^2 - 2E_0(\gamma\psi_0 - \alpha\Delta_0)(\alpha-\gamma)}\}.$$

When calculating $R(t-\tau)$in expression (6), we assume $\Delta(t) = \Delta_0 = const, \psi(t) = \psi_0 = const.$

Research Results. As the first test example, let us look into the problem of prolonged deformation of a cylindrical prismatic concrete sample while compressed axially. The results of similar physical experiments are provided in [8]. The diameter and height of the prismatic sample as in [8] were assumed to be 12 cm and 30 cm, respectively. A pressure of 15 MPa was applied to the free end of the sample. Taking into consideration the axial symmetry of geometry and loading during finite element modeling, ¼ of the prismatic sample was considered. The grid step was assumed to be uniform and equal to 1 cm. While boundary conditions were set, connections were introduced at the ends of the prism in order to prevent radial movements. Therefore the nodes of the free end have only one degree of freedom in the form of axial displacement.

For calculations the authorized Polygon complex [9, 10] is used. The obtained graphs $u_z \sim t$for two concrete models and two loading schemes are shown in Fig. 8. The initial modulus of elasticity of concrete is E = 2.8 · 10^4 MPa. The observation time is 200 days. The right-hand side of Fig. 8 shows a graph $u_z \sim t$for the loading and full unloading mode at t = 60 days.

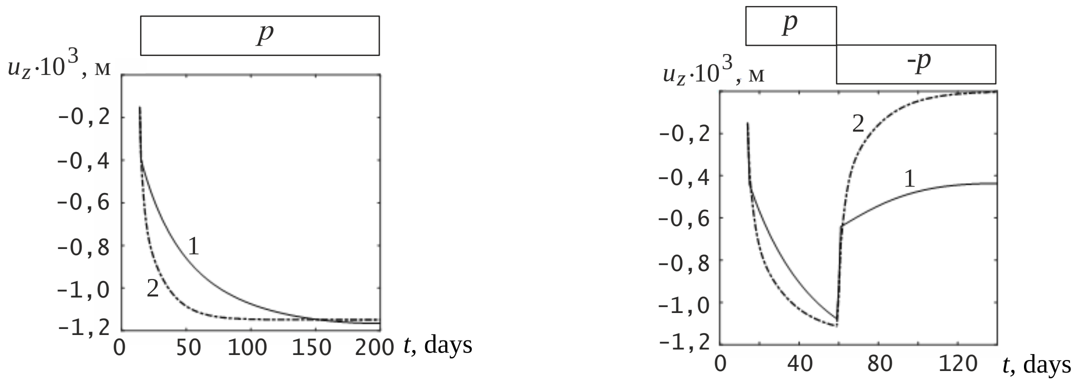

Fig. 8. Graphs of the movement of the prismatic sample: 1 — model of an elastic-creeping body (5); 2 — model of "old" concrete (6)

As can be seen, for the "old" concrete model (6), complete reversibility of creep deformation occurs during unloading.

Visualization of the distribution of axial displacement fields and stress intensity for the elastic-creeping body model (5) and time = 60 days is shown in Fig. 9 and 10.

Fig. 9. Distribution pattern in 1/4 of the prismatic sample at t = 60 days

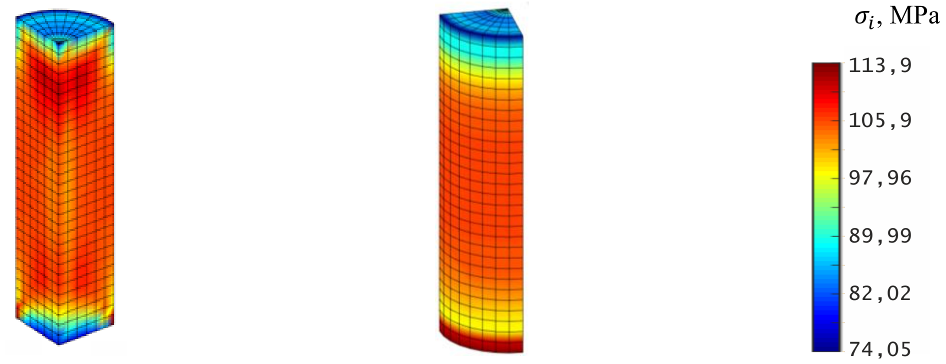

Fig. 10. Distribution pattern $\sigma_i$in 1/4 of the prismatic sample at t = 60 days

Fig. 10 is clearly indicative of the impact of the accepted boundary conditions on the stress distribution over the height of the prism. The highest concentration σ_i= 113.9 MPa is observed at the lower end of the sample.

In order to study the accuracy of the developed mathematical and software, the results of field experiments on the long-term creep of double-support beams under two-point loading provided in [11] were used. In these experiments, prestressed reinforced concrete beams were subjected to prolonged (over 4.5 years) force exposure. The constant load F = $const$ $F = const$ was maintained by hydraulic jacks.

The loading scheme and cross-section options of the beams are shown in Fig. 11 and 12, respectively (the dimensions are in millimeters).

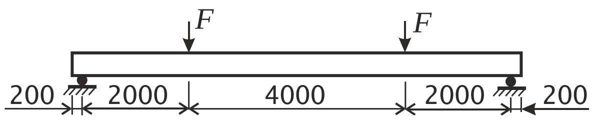

Fig. 11. Loading scheme of the beam

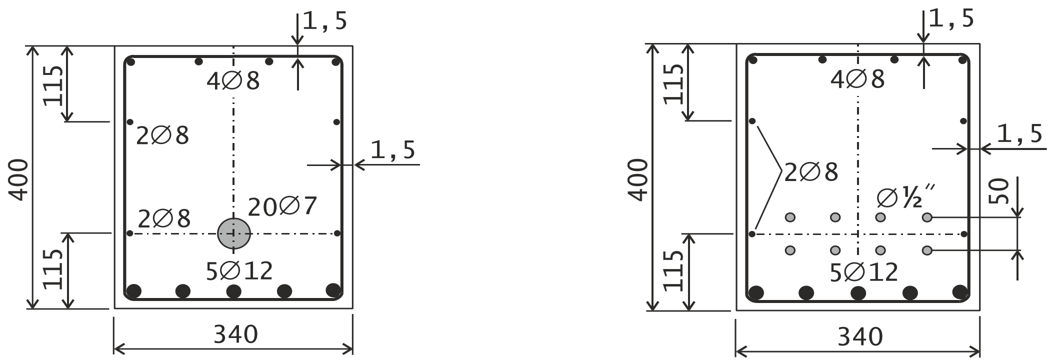

R-C *R-S*

Fig. 12. Cross sections of RC and R-S series beams in the middle of the span [11]

These figures show the placement schemes of the "background" longitudinal and "active" prestressed fittings. According to the data [11], the initial stress state was generated in the beams of the R-C series by compressing concrete at the "age" of 28 days along the ends with cable reinforcement. These are the so-called post-stress beams. The cable was made up of twenty strands with a nominal diameter of 7.2 mm (the cross-sectional area of one strand was 38.70 mm^2). The diagram of the trajectory of the "active" reinforcement of the R-C series beam is shown in Fig. 13. During testing, a beam variant with the following parameters was considered: a = 0.115 m; b = 0.227 m. The tensile strength for a single strand strand is 1770 MPa.

The prestressing in the R-S series beam was created according to the scheme of tension of the reinforcement on the stops. 28 days after the concrete had been laid in the appropriate form, the "active" reinforcement had been "removed" from the stops, and the initial stress state occurred in the beam. The voltage in the "active" reinforcement for the R-C and R-S series beams was assigned based on the following condition:

$$\sigma = 0.7 f_{ptk}.$$

Then for the R-C series beam we have:

$$F_{pr} = \sigma n A_{R-C} = 0.7 \cdot 1770 \cdot 10^{6} \cdot 20 \cdot 38.7 \cdot 10^{-6} = 959 \text{ kN},$$

where n is the number of cable strands (n = 20); $A_{R\text{-}C}$ is the cross—sectional area of the cable strand.

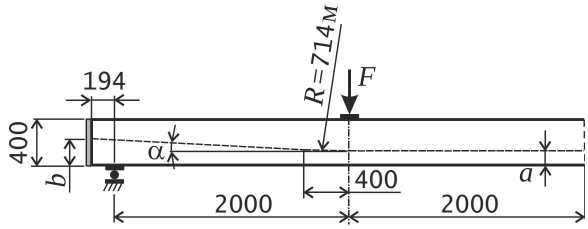

Fig. 13. Diagram of the trajectory of the "active" reinforcement of the 1/2 part of the R-C series beam

For a qualitative and quantitative assessment of the restoring effect caused by the tension of the rope in the beam of the R-C series, we use an auxiliary two-dimensional finite element model. This model is formed from truss and spring finite elements (Fig. 14). In this case, the vertical reactions in the spring elements r_i are equivalent to discrete values of the restoring forces.

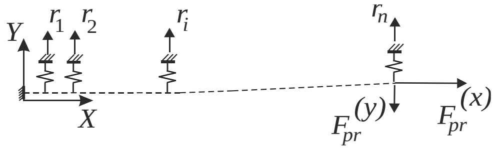

Fig. 14. Diagram for identifying the restoring force

As a result of the modelling, we get: $F_{pr}^{(x)}$= 958 kN; $F_{pr}^{(y)}$= 51.1 kN. A plot of the distribution of the restorative efforts of Frest is shown in Fig. 15.

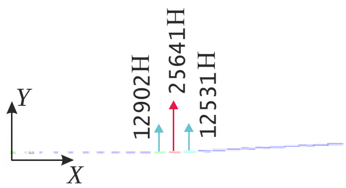

Fig. 15. A timeline of restorative efforts F_{rest}

The prestress in the R-S series beam is created by eight cables ∅ $1/2'$. The nominal diameter of each cable is 10.9 mm (cross-sectional area 93.3 mm^2). For this series, the tension force is given by the formula:

$$F_{pr} = 0.7 \cdot 1860 \cdot 10^{-6} \cdot 93.3 \cdot 10^{-6} = 121.4 \text{ kN}.$$

We assume that the effort $q_{пр}$ from the prestretched cable in the R-S series beam acts on a section with a length of $l_р$ = 15·d where d is the diameter of the reinforcement (Fig. 16). The value $q_{пр}$ is defined as the ratio F_{pr}/l_p.

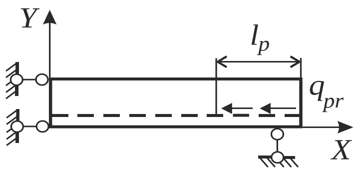

Fig. 16. Prestressing scheme in the R-S series beam

The design scheme for the 1/2 part of the R-C series beam and the corresponding finite element model with the allocation of an array of concrete and a reinforcing frame are shown in Fig. 17 and 18, respectively. The force applied to 1/2 part of the beam, Fsust = 63.75 kN. In order to reduce the stress concentration in the force application zones and the support, pads with a thickness of 10 cm have been introduced. The material of the platforms is steel.

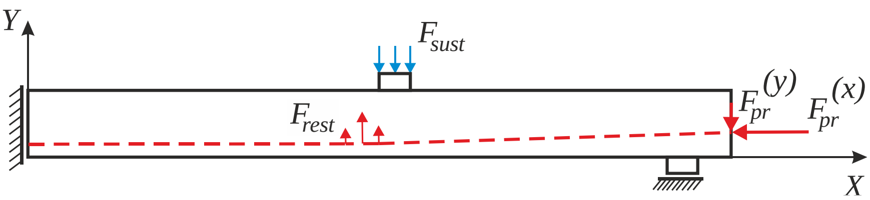

Fig. 17. Calculation scheme of 1/2 part of the R-C series beam

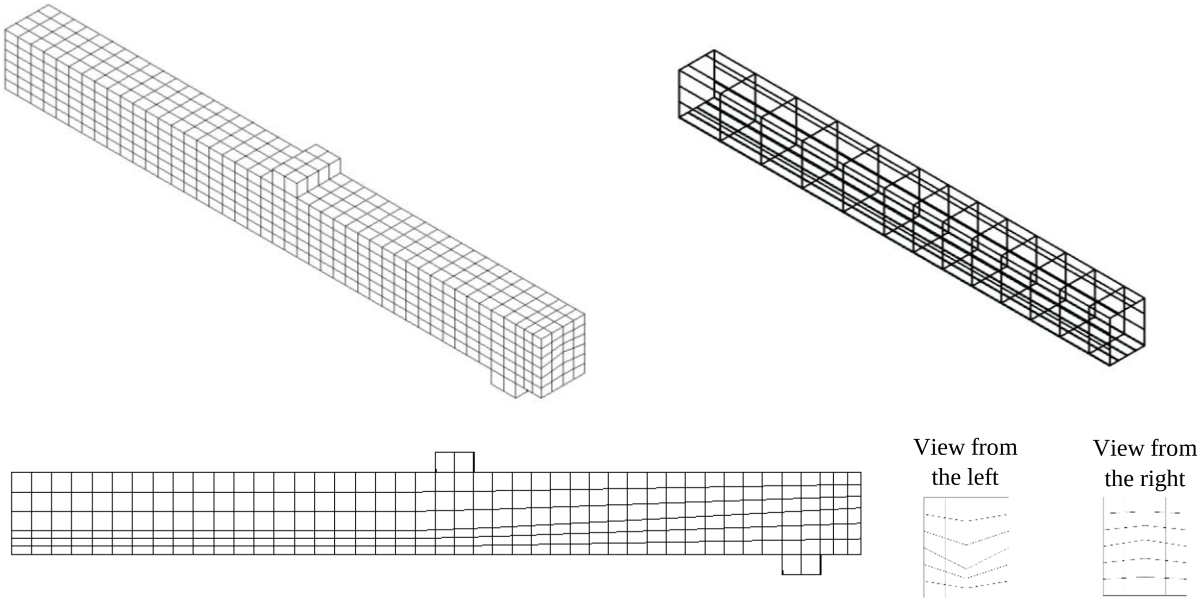

Fig. 18. Finite element model 1/2 part of the R-C series beam

The design scheme for the 1/2 part of the R-S series beam and the corresponding finite element model with the allocation of an array and a reinforcing frame are shown in Fig. 19 and 20, respectively.

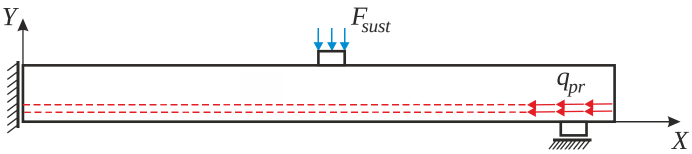

Fig. 19. Calculation scheme of 1/2 part of the R-S series beam

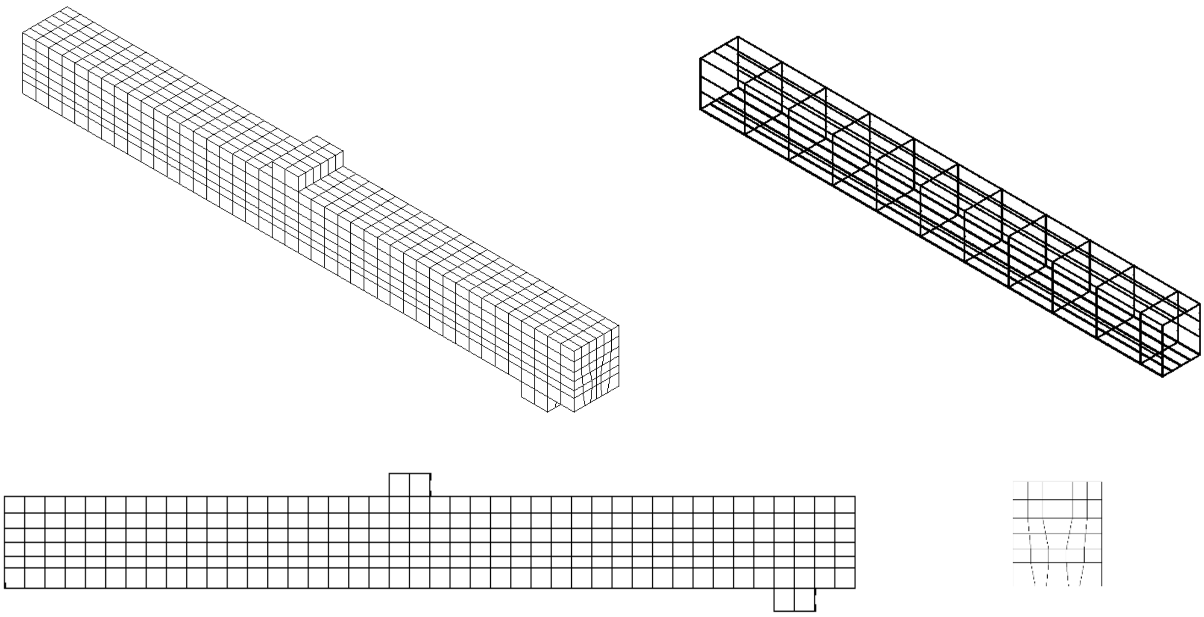

Fig. 20. Finite element model 1/2 part of the R-S series beam

The results of finite element modeling of deflection changes u_y in the center of the beam span of the R-C and R-S series at the stages of prestressing at the "age" of concrete for 14 days and loading with F_{sust} force at the time of 28 days are shown in Fig. 21, *a*. The estimated observation time was 100 days. Fig. 21, *b* shows the graphs $u_y \sim t$ obtained experimentally [11].

As can be seen from Fig. 21, *a* and 21, *b*, the deflection values obtained numerically and experimentally at time points 28 days and 100 days almost coincide.

Visualization of longitudinal fields σ_{xx} and tangential σ_{xy} The stresses for the R-C series beam (time point 100 days) are shown in Fig. 22 and 23. Similar stress distribution patterns σ_{xx} and σ_{xy} The R-S series beams are shown in Fig. 24 and 25. Fig. 22-25 shows the beam fragments corresponding to the section $0 \le x \le 3{,}71$m, i.e., without a support area.

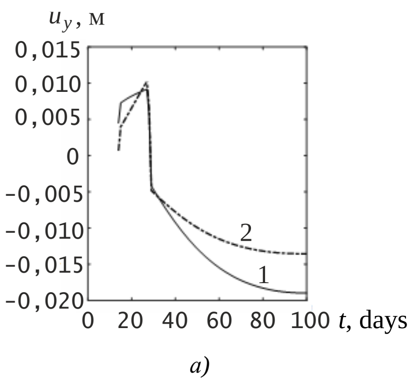

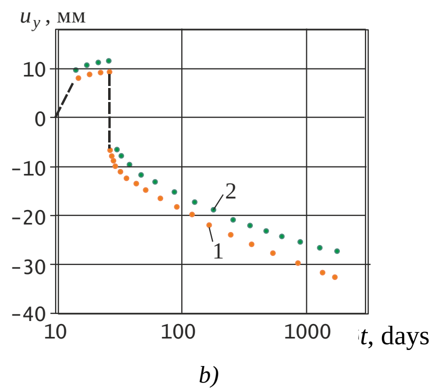

Fig. 21. Graphs $u_y \sim t$: 1 — R-C series beam; 2 — R-S series beam

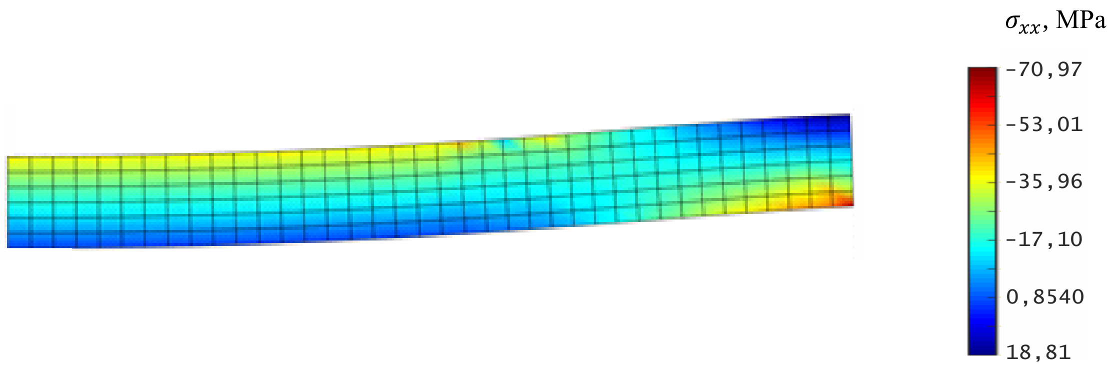

Fig. 22. Visualization of the distribution σ_{xx} for the R-C series beam, *t* = 100 days

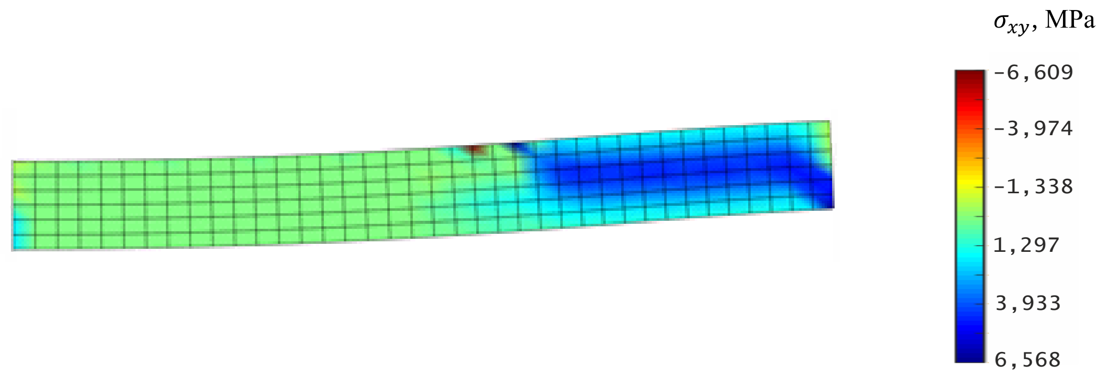

Fig. 23. Visualization of the distribution σ_{xy} for the R-C series beam, *t* = 100 days

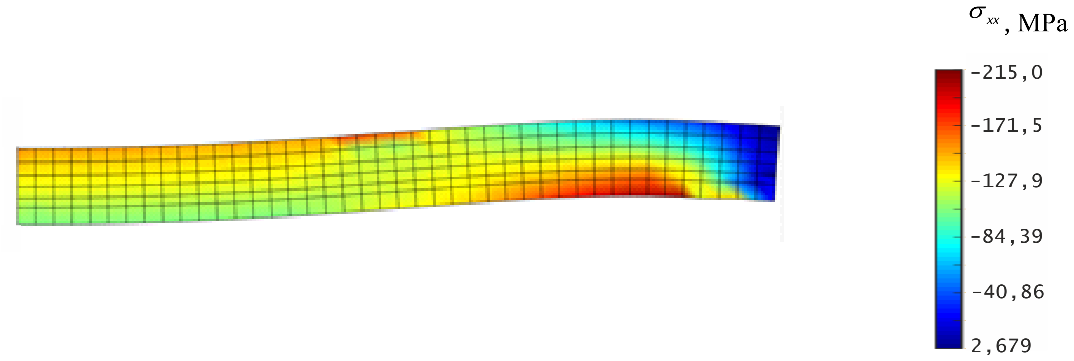

Fig. 24. Visualization of the distribution σ_{xx} for the R-C series beam, *t* = 100 days

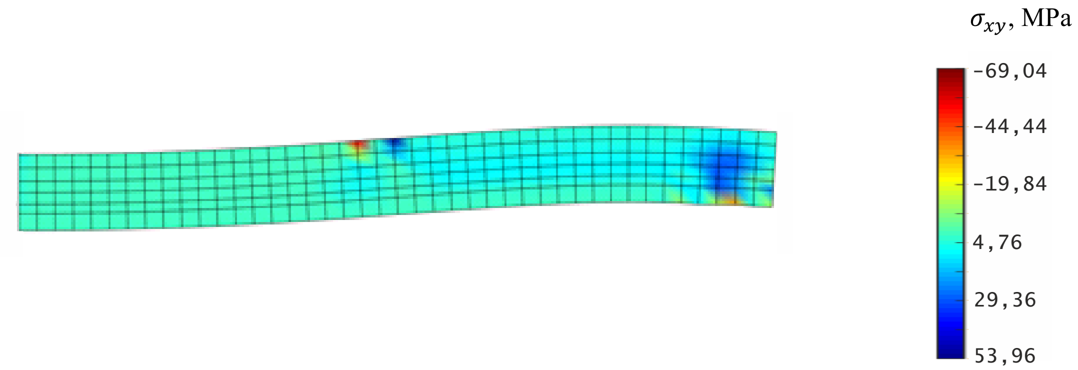

Fig. 25. Visualization of the distribution σ_{xy} for the R-C series beam, *t* = 100 days

Based on the above results, the effect of prestressing on the RS series beam is more pronounced than on the R-C series beam. Hence in the case of the R-C series beam, tensile stresses are formed in the lower layer when loaded with a given F_{sust} force. σ_{xx} = 18.8 MPa, while in the R-S series beam, compressive stresses of the order of 100 MPa are observed in the area under the same load.

The stress distribution pattern σ_{xy} is of particular interest for the investigated beam schemes (Fig. 23 and 25). Comparing the data in Fig. 23 and 25, we find that the voltage field is more uniform. σ_{xy} corresponds to the R-S series beam. Minor disturbances in the distribution σ_{xy} for this beam, it is observed at the place of application of the load and the area adjacent to the support. It should be noted that the background reinforcement for the beams of both series was assigned to be almost identical.

Discussion and Conclusion. The analysis of the distribution of displacements and stresses in the considered reinforced concrete beams considering the creep of concrete and the pre-stress generated by the cable reinforcement thus enables the following conclusions to be made.

1. The distributed scheme of "background" reinforcement from a physical point of view allows the most realistic modelling of the joint work of the reinforcing frame and the concrete array.

2. The suggested concept for identifying the restoring force caused by the tension of the "active" reinforcement can be implemented in the software complexes ANSYS, Lira CAD and SCAD Office certified by the Russian Academy of Architecture and Building Sciences.

3. It was found that the deflection values of the beams obtained numerically and experimentally for time points 28 days and 100 days almost coincide.

4. The analysis of the longitudinal and tangential stress fields in the beams of the R-C and R-S series for a time of 100 days revealed a considerable effect of the "active" reinforcement scheme on the load-bearing capacity of the structures in terms of the appearance of tensile stresses in concrete. The developed mathematical and software allows the accuracy and reliability of strength calculations of monolithic prestressed girder structures made of reinforced concrete to be improved.

References

1. Harutyunyan NH. *Some Issues of the Theory of Creep*. Moscow: Gostekhteoretizdat; 1952. 323 p. (In Russ.).
2. Harutyunyan NH, Zevin AA. *Calculation of Building Structures Considering Creep*. Moscow: Stroyizdat; 1988. 256 p. (In Russ.).
3. Aleksandrovsky SV. *Calculation of Concrete and Reinforced Concrete Structures for Temperature and Humidity Changes Considering Creep*. Moscow: Stroyizdat; 1973. 432 p. (In Russ.).
4. Prokopovich IE, Zedgenidze VA. *Applied Theory of Creep*. Moscow: Stroyizdat; 1980. 240 p. (In Russ.).
5. Kharlab VD. *Fundamental Issues of the Linear Theory of Creep (in Relation to Concrete)*. St. Petersburg: SPbGASU; 2014. 207 p. (In Russ.).
6. Dikonov VP. *The MAPLE Mathematical System in R3/R4/R5*. Moscow: SOLON; 1998. 399 p. (In Russ.).
7. Gaydzhurov PP, Iskhakova ER. *Models of Concrete Creep Theory and their Finite Element Implementation*. Bulletin of DSTU. 2012;7:99-107. (In Russ.) URL: https://www.vestnik-donstu.ru/jour/article/view/654/653 (accessed: 05.01.2025)
8. Ross AD. Creep of Concrete under Variable Stress. *Journal of the American concrete institute*. 1958;54(3):739–758. https://doi.org/10.14359/11466
9. Gaydzhurov PP, Iskhakova ER. *Finite Element Solution of the Planar Issue of the Theory of Hereditary Aging of Concrete Considering the Principle of Superposition of Impacts and Fast-Moving Creep of the Material (Polygon)*. Certificate of State Registration of the Computer Program No. 201462079. 2014. (In Russ.).
10. Gaydzhurov PP, Iskhakova ER, Savelyeva NA. Numerical Modeling of the Volumetric Stress-Strain of Prestressed Reinforced Concrete Structures Considering the Creep of Concrete. News of higher educational institutions. *The North Caucasus region*. Technical Sciences. 2023;2:17-24. (In Russ.) http://dx.doi.org/10.17213/1560-3644-2023-2-17-24
11. Reybrouck N, Van Mullem T, Taerwe L, Caspeele R. Influence of long-term creep on prestressed concrete beams in relation to deformations and structural resistance: Experiments and modeling. *Structural Concrete*. 2020;21(4):1458–1474. https://doi.org/10.1002/suco.201900418

About the Authors:

Peter P. Gaydzhurov, Dr.Sci. (Eng.), Professor of the Department of Structural Mechanics and Theory of Structures, Don State Technical University (1 Gagarin Square, Rostov-on-Don, 344003, Russian Federation), ORCID, gpp-161@yandex.ru

Elvira R. Iskhakova, Cand.Sci. (Eng.), Associate Professor of the Department of Urban Planning, Design of Buildings and Structures, Platov South Russian State Polytechnic University (NPI) (132 Prosveshcheniya St., Novocherkassk, 346428, Russian Federation), ORCID, elvira.ishakova@yandex.ru

Nina A. Savelyeva, Cand.Sci. (Eng.), Senior Lecturer of the Department of Structural Mechanics and Theory of Structures, Don State Technical University (1 Gagarin Square, Rostov-on-Don, 1344003, Russian Federation), ORCID, ninasav86@mail.ru

Claimed contributorship:

PP Gaydzhurov: basic concept formulation, selecting the solution method, analysis and generalization of the research results.

ER Iskhakova: writing and fixing the software code, preparing the original data for numerical modelling.

NA Savelyeva: developing the mathematical model of concrete creep, working with the text of the manuscript, analysis and generalization of the research results.

Conflict of interest statement: **the authors do not have any conflict of interest.**

All authors have read and approved the final version of manuscript.

Об авторах:

Гайджуров Петр Павлович, доктор технических наук, профессор кафедры строительной механики и теории сооружений Донского государственного технического университета (344003, Российская Федерация, г. Ростов-на-Дону, пл. Гагарина, 1), ORCID, gpp-161@yandex.ru

Исхакова Эльвира Рашидовна, кандидат технических наук, ассистент кафедры градостроительства, проектирования зданий и сооружений Южно-Российского государственного политехнического университета им. М.И.Платова (НПИ) (346428, Российская Федерация, г. Новочеркасск, ул. Просвещения, 132), ORCID, elvira.ishakova@yandex.ru

Савельева Нина Александровна, кандидат технических наук, старший преподаватель кафедры строительной механики и теории сооружений Донского государственного технического университета (344003, Российская Федерация, г. Ростов-на-Дону, пл. Гагарина, 1), ORCID, ninasav86@mail.ru

Заявленный вклад авторов:

П.П. Гайджуров: постановка задачи, выбор метода решения, обсуждение результатов.

Э.Р. Исхакова: написание кода и отладка программного обеспечения, подготовка исходных данных для численного моделирования.

Н.А. Савельева: разработка математической модели ползучести бетона, подготовка текста, формулирование выводов.

Конфликт интересов: **авторы заявляют об отсутствии конфликта интересов.**

Все авторы прочитали и одобрили окончательный вариант рукописи.

Received / Поступила в редакцию 14.01.2025
Reviewed / Поступила после рецензирования 30.01.2025
Accepted Принята к публикации 08.02.2025

LIFE CYCLE MANAGEMENT OF CONSTRUCTION FACILITIES
УПРАВЛЕНИЕ ЖИЗНЕННЫМ ЦИКЛОМ ОБЪЕКТОВ СТРОИТЕЛЬСТВА

Original Empirical Research

UDC 697.1, 697.3
https://doi.org/10.23947/2949-1835-2025-4-1-68-75

EDN: ZJATYD

Development of the Structure of the Life Cycle of the Heating System of a Construction Facility

Ekaterina P. Lysova ✉, **Oksana N. Paramonova**
Don State Technical University, 1 Gagarin Square, Rostov-on-Don, Russian Federation
✉ katerina.lysova0803@gmail.com

Abstract

Introduction. The heating system is an integral part of the construction site. In the article, the author explores the life cycle of a heating system, a complex system of engineering and technical support for buildings and structures, the elements of which must function stably, efficiently and fully throughout the heating period during the entire service life. The productive operation of the heating system is laid at the stage of its design, installation, adjusted and maintained at the stages of operation and modernization. Therefore, studying the life cycle of a heating system is an important scientific and practical task, and managing the stages of the life cycle becomes important, as it allows for efficiency, adaptability, cost-effectiveness and reliability.

Materials and methods. The authors have developed the structure of the life cycle of a building heating system using methods of analogy, comparative analysis and synthesis based on scientific and practical research results. The study focuses on the water heating system of residential and public buildings. The purpose of the work is to create a model of the life cycle for effective management of its stages and stages.

Results. The study of the heating system helped to identify five stages of its operation (pre-design, design, operation, modernization and disposal) and to create a life cycle structure. In the future, this will make it possible to create an energy-efficient, reliable and economical system that meets modern operational requirements, improve the quality of its maintenance, and simplify the management process.

Discussion and conclusion. The life cycle of a heating system includes all stages from design to modernization. Proper management of these stages ensures efficient operation of the system, increasing comfort and reducing costs. An integrated management approach makes it possible to maximize the heating potential. A systematic study of each stage helps to choose the optimal system that meets the criteria of efficiency, safety and cost-effectiveness. The structure of the life cycle allows one to create a single digital model for intelligent management of an object at all stages.

Keywords: life cycle, heating system, life cycle management, construction site

For citation. Lysova EP, Paramonova ON. Development of the Structure of the Life Cycle of the Heating System of a Construction Facility. *Modern Trends in Construction, Urban Planning and Territorial Planning.* 2025;4(1):68–75. https://doi.org/10.23947/2949-1835-2025-4-1-68-75

Оригинальное эмпирическое исследование

Разработка структуры жизненного цикла системы отопления строительного объекта

Е.П. Лысова ✉, **О.Н. Парамонова**

Донской государственный технический университет, Ростов-на-Дону, Российская Федерация

✉ katerina.lysova0803@gmail.com

Аннотация

Введение. Система отопления является неотъемлемой частью строительного объекта. В статье авторы исследуют жизненный цикл системы отопления — сложной системы инженерно-технического обеспечения зданий и сооружений, элементы которой должны стабильно, эффективно и полноценно функционировать на протяжении отопительного периода в течение всего срока эксплуатации. Продуктивная работа системы отопления закладывается на этапе ее проектирования, монтажа, корректируется и поддерживается на этапах эксплуатации и модернизации. Следовательно, изучение жизненного цикла системы отопления представляет собой важную научную и практическую задачу, а управление этапами жизненного цикла становится важным, т.к. позволяет обеспечить эффективность, технологичность, экономичность и надежность. Цель работы — создать модель жизненного цикла для эффективного управления его этапами и стадиями.

Материалы и методы. Авторы разработали структуру жизненного цикла системы отопления зданий, используя методы аналогии, сравнительного анализа и синтеза на основе научных и практических результатов исследований. Исследование сфокусировано на системе водяного отопления жилых и общественных зданий.

Результаты исследования. Исследование системы отопления помогло выделить пять этапов ее функционирования (предпроектная подготовка, проектирование, эксплуатация, модернизация и утилизация) и создать структуру жизненного цикла. В дальнейшем это дает возможность создать энергоэффективную, надежную и экономичную систему, отвечающую современным требованиям эксплуатации, повысить качество ее обслуживания, а также упростить процесс управления ею.

Обсуждение и заключение. Жизненный цикл системы отопления включает все этапы от проектирования до модернизации. Грамотное управление этими этапами обеспечивает эффективную работу системы, повышая комфорт и снижая расходы. Комплексный подход к управлению позволяет максимально использовать потенциал отопления. Системное исследование каждого этапа помогает выбрать оптимальную систему, соответствующую критериям эффективности, безопасности и экономичности. Структура жизненного цикла позволяет создать единую цифровую модель для интеллектуального управления объектом на всех стадиях.

Ключевые слова: жизненный цикл, система отопления, управление жизненным циклом, строительный объект

Для цитирования. Лысова Е.П., Парамонова О.Н. Разработка структуры жизненного цикла системы отопления строительного объекта. *Современные тенденции в строительстве, градостроительстве и планировке территорий*. 2025;4(1):68–75. https://doi.org/10.23947/2949-1835-2025-4-1-68-75

Introduction. The concept of system management of the stages of the life cycle is commonly used in lots of areas of human economic activity in order to increase the efficiency, manufacturability, cost-effectiveness and reliability of an object (project, system, item or product) [1–3]. In the construction industry, this concept is also ubiquitous and is oftentimes applied mostly to buildings and structures, i.e. capital construction facilities [4, 5].

In compliance with the basic provisions [6], the life cycle of a building or a structure is thus conceptualized as the period when engineering surveys, architectural and construction design, construction (including conservation), operation (including ongoing repairs), reconstruction, major repairs, and demolition of a building or a structure take place. The authors of the study [7] call the life cycle of a building the time from the moment of justification of the need for construction to the onset of the economic inexpediency of its operation and identify eight of its stages, beginning with the feasibility study of the construction of the facility and finishing with that of its reconstruction.

Regarding construction sites, engineering systems are the foundation of their infrastructure and are designed to provide comfortable and safe living conditions. However, the issues of modeling the life cycle of engineering systems are not paid due attention to in scientific studies. For instance, based on the "circle of quality", the life cycle of heat supply systems is set forth using the example of a cogeneration plant for a thermal power plant [8], and a methodology for developing a digital information model of heat supply system elements at all stages of its life cycle is shown [9, 10]. The study [11] describes an algorithm for increasing the life cycle of air conditioning systems and [12] develops a model for managing the life cycle of the ventilation system of a construction facility.

As an integral part of buildings or structures, heating systems ensure the required values of microclimate parameters during the cold season are complied with. However, the conducted analytical studies indicate a considerable lack of scientific research dedicated to comprehensive studies of the life cycle of heating systems. Hence investigating the stages of the heating system life cycle model to optimize costs, improve quality and efficiency, as well as ultimately manage it is an crucial scientific and practical task. The productive operation of the heating system is laid at the stage of its design and installation, adjusted and maintained at the stages of operation and modernization, while each stage involves implementing a series of works to achieve certain outcomes.

The lack of a holistic approach to studying the life cycle causes a significant decrease in the quality of decisions made and an increase in operating costs, which is yet again indicative of the need for a comprehensive study of all stages of the heating system as a single technological process.

Based on a detailed study of these stages, the structure of the life cycle of a heating system is set forth as a complex system of engineering and technical support for buildings and structures whose elements must function stably, efficiently and fully throughout the heating period during the entire service life. Knowledge of specific features of each stage of the life cycle makes it possible to manage them and ensure maximum efficiency, adaptability, cost-effectiveness as well as reliability of the system.

Materials and Methods. The use of methods of analogy, comparative analysis and synthesis based on the generalization of scientific and practical research results enabled the authors to design a model of the life cycle of the heating system of buildings and structures as an integral part of a construction site. At the same time, the object of the study was a water heating system, while the objective of the study was to develop a model of the life cycle of a water heating system for residential and public buildings. To this end, the main stages of the life cycle and their stages are identified and analyzed in order to be able to manage them.

Research Results. Conceptualizing the heating system as one of the engineering and technical support systems for buildings and structures, the authors assume that the life cycle of a heating system is a series of interrelated, interdependent and consistent processes of design, installation, operation, modernization and recycling of a system supplying heat to rooms and maintaining the required temperatures during the cold season.

Choosing a schematic diagram of a heating system depends on a whole host of factors: the purpose of the room, the type of a coolant, the mode of operation of a heating system, the method of movement of the coolant, the relative location of the main elements, etc. If a residential or public building is assumed to be as a construction object, a water heating system is the most preferable option according to the set of requirements for heating systems. Water heating systems are extremely diverse (Fig. 1) with each having its own advantages and disadvantages. Accounting for all of its features and customer requirements, choice of the optimal system option for a specific facility is determined by the operating conditions, technical and economic requirements.

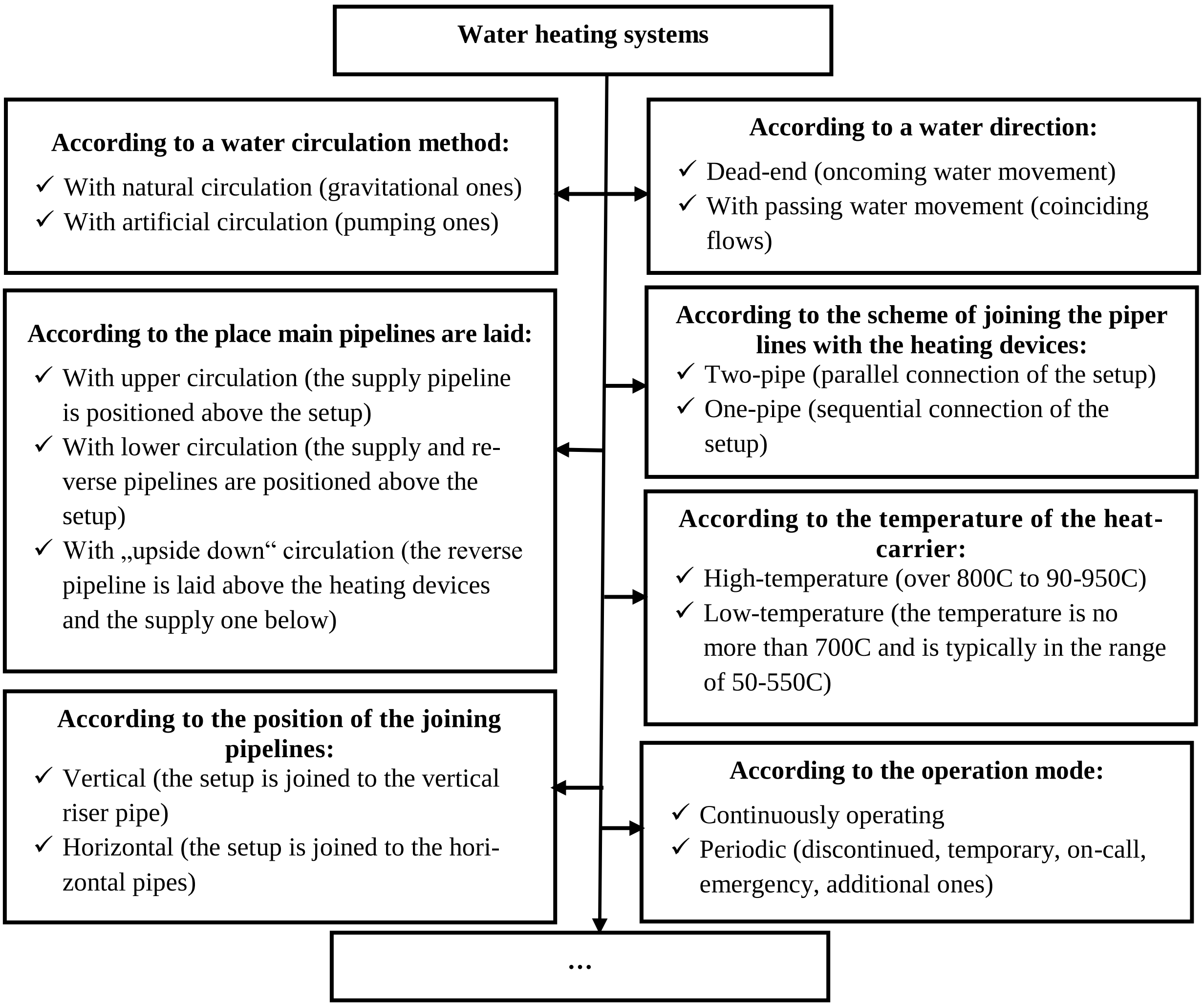

Fig. 1. Classification of water heating systems

Each of the system options assumes the presence of basic and additional equipment (Fig. 2) [13–15] whose composi-tion and configuration features are dependent on the selected water heating system option.

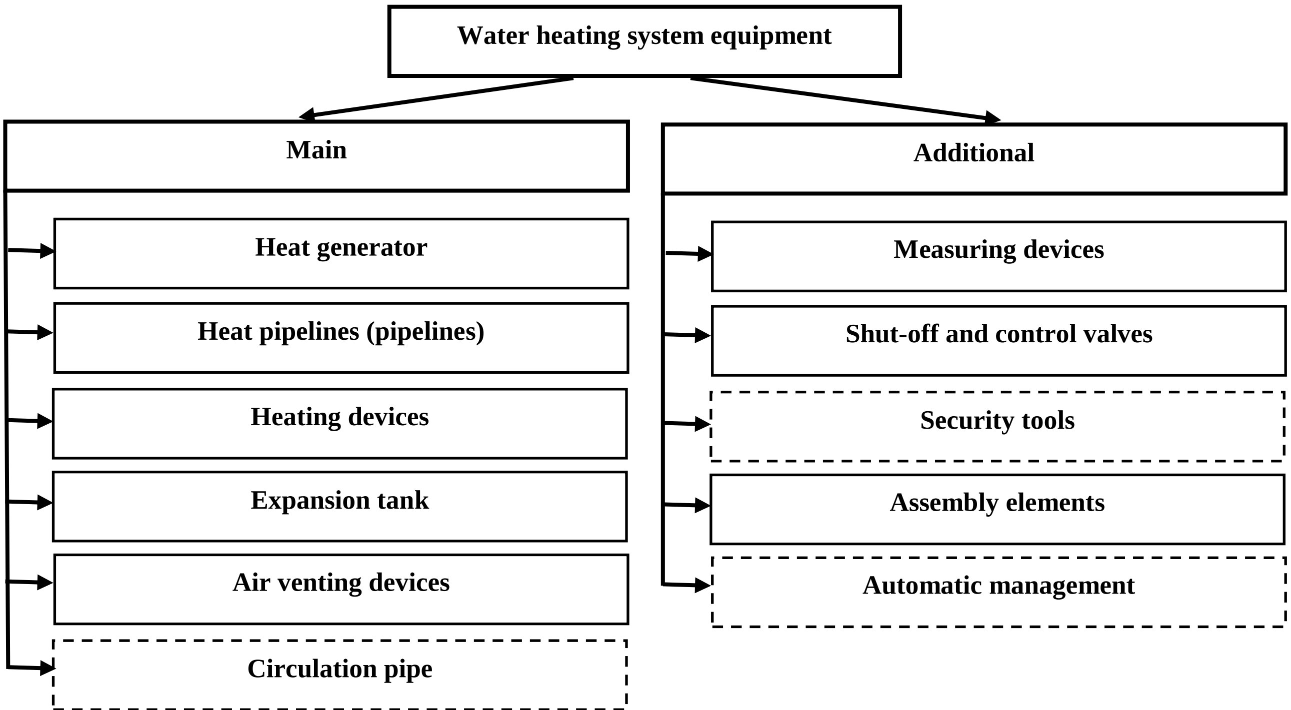

Fig. 2. Water heating system equipment

A range of possible design and technical solutions for water heating systems, a continiously growing variety of basic and additional equipment poses some difficulties in the design, installation and operation, as it requires accounting for numerous parameters and characteristics of each element of the system. The problem of choosing the optimal water heating system, which must comply with the comprehensive criteria of efficiency, safety and economic feasibility, is increasingly relevant.

Therefore the study of the stages of the life cycle of heating systems appears to be methodologically justified and necessary in practical terms to ensure efficient and reliable operation in the long term.

The study of the heating system involves identifying five stages of its operation: pre-design preparation, design, operation, modernization and recycling. Each of them is characterized by implementation stages that are critical to the current state of the heating system, a series of of necessary works and their expected outcomes.

The pre-design preparation stage is when the feasibility of designing a heating system and collecting initial information is identified. This stage includes two consecutive steps:

Step 1 — Request and collection of initial data for design (information on the climatic and meteorological conditions of the construction area, calculated parameters of outdoor and indoor air, information on heat supply sources, parameters of heat carriers, etc.), including initial data from related sections of the design documentation (general plan of a building or a structure, plans, sections, etc.).

Step 2 — development of technical specifications for the design (accounting for the category and functional purpose of the building or a structure).

The design stage of the heating system is critical in designing the engineering infrastructure of a construction facility. It is at this stage that the main parameters of the future system - efficiency, safety and economic feasibility - are specified. The design stage of the heating system life cycle involves the following steps:

Step 1 (3) — analysis of the initial data, followed by the thermal engineering calculation of enclosing structures, calculation of heat losses and identifying the thermal capacity of the heating system as well as of the schematic diagram of the heating system by hydraulic and its thermal calculation as well as the composition, and selection of the basic and additional equipment.

This step is key for the formation of a technically sound and cost-effective solution providing the required indoor climate parameters with optimal energy consumption.

Step 2 (4) — preparation of an explanatory note and development of the graphical part of the project based on the results of calculations.

The result of this stage of the life cycle of the heating system is the design of a future heating system for a construction site.

The stage of technical operation starts with installing the heating system, involves routine maintenance, monitoring the condition of the equipment and timely troubleshooting through the course of the actual system operation. The third stage includes four steps.

Step 1 (5) — assembly, i.e. installation of a heating system by an assembly company involving that of heating devices, pipes as well as connecting the system to a heat source, etc.

Step 2 (6) — pre-launching and launching aimed at checking, configuring and testing the heating system (checking whether it is in compliance with design parameters, performing hydraulic tests, adjusting and fixing the pumping and boiler equipment, etc.).

Step 3 (7) — actual operation of the heating system in an optimal operating mode (efficient heating is combined with cost minimization) that entails coordinated and balanced operation of all its elements during the heating period throughout the entire service life.

Step 4 (8) — scheduled maintenance and preventive maintenance aimed at keeping the heating system in working condition during the heating period throughout its entire service life (prevention, detection and elimination of technical malfunctions and errors to ensure long-term trouble-free use).

Physical wear and outdated heating system elements, a decrease in its heating capacity, changes in the consumers' thermal energy needs, as well as the need to reduce energy consumption and increase the energy efficiency of buildings or structures over time call for the next stage of the life cycle — *modernization* of the heating system. Modernization entails updating the heating system by replacing „physically and morally" outdated components with modern and more energy efficient ones by means of introducing automation and control systems. The modernization stage includes several ones.

Step 1 (9) — formation of technical specifications for modernization, study of modernization options of the heating system and a detailed study of suggested technical solutions (replacement of heating appliances, installation of individual thermostats with an air temperature sensor, etc.).

Step 2 (10) — choosing and implementing a modernization option.

The final stage of the life cycle of the heating system is *the stage of recycling* when the maximum condition of the operational characteristics of the equiment is achieved. In this case, the life cycle of the heating system is completed, the outdated equipment is dismantled and recycled.

Under optimal operating conditions, regular as well as scheduled preventive maintenance, the life cycle of a water heating system is 40–50 years, in actual fact it reaches 25–30 years [16, 17], which corresponds to the minimum service life. These are average figures accounting for the average duration of operation of the main elements of the heating system (for heat generators — 15–25 years, for heating appliances — 20–40 years, heat pipelines — 20–40 years, shut — off valves — 15–20 years, expansion tanks – 20 years, circulation pumps — 10-15 years, heat exchangers — about 20 years).

A detailed study of the stages and stages of the life cycle of a heating system allows one to tackle a few important tasks:

1) forming a comprehensive view of the heating system, which is conducive to making informed management decisions and improving the quality of its operation;

2) capacity to evaluate the efficiency of the system at all of the stages of its existence (analysis, correction and selection of design solutions, assessment of the quality of the installation and subsequent operation);

3) capacity to identify potential problems in a timely manner and prevent them from escalating;

4) cost optimization not only at the stage of system design and installation, but also at the operational stage due to competent maintenance and repair planning based on the actual data on the current condition of the system;

5) extending the service life of the equipment;

6) reducing possible associated emergencies;

7) the capacity to predict operation and modernization (if needed).

Ultimately, a systematic study of the heating life cycle enables an energy-efficient, reliable and economical system to be designed in compliance with the modern operational requirements, improves the quality of its maintenance and makes it considerably easier to manage.

Discussion and Conclusion. The life cycle of a heating system covers all of the stages of its existence, from design and installation to operation and modernization. Understanding and managing these stages appropriately makes it possible to ensure efficient and cost-effective operation of the heating system of buildings and structures, increasing comfort and reducing operating costs.

Life cycle management of a heating system is key to ensuring its efficient and cost-effective operation throughout its entire service life. An integrated approach, including design, installation, operation, modernization and management, maximizes the potential of the heating system, providing comfort and reducing operating costs.

A comprehensive study of each stage of the life cycle of a heating system provides the opportunity to choose the optimal water heating system in compliance with the comprehensive criteria of efficiency, safety and economic feasibility as well as the capacity to predict its technical condition, plan repairs and modernization contributing to increased reliability and economic efficiency in the long run.

Apart from all of the above, the life cycle model provides the opportunity to create a single information (digital) model and allows for intelligent dynamic control at all of the operation stages — from engineering surveys to reconstruction and modernization.

References

1. Zhdanov VYu. A New Look at the Stages of the Organization's Life Cycle. *Moscow Economic Journal*. 2021(6): 378–388. (In Russ.) URL: https://doi.org/10.24411/2413-046X-2021-10347 .

2. Agibalova VG, Basha IV, Subbota AV, Wassuf FS. Features of Organization Management Taking into Account the Stages of the Life Cycle. *Natural Sciences and Humanities Research*. 2023;5(49):367–370. (In Russ.) URL: https://esj.today/PDF/50ECVN122.pdf (accessed: 19.01.2025).

3. Beglaryan KE. Theoretical Aspects of the Enterprise Life Cycle Analysis. *Scientific Palette*. 2020;2(28):14. (In Russ.) URL: https://s.esrae.ru/culture/pdf/2020/2(28)/891.pdf (accessed: 19.01.2025).

4. Fedosov SV, Fedoseev VN, Zaytseva IA, Voronov VA. Life Cycle Management of a Steady state of a Construction Object. *Expert: Theory and Practice*. 2023;3(22);131–137. (In Russ.) https://doi.org/10.51608/26867818_2023_3_131.

5. Topchiy DV. Organizational and Technical Solutions to Ensure the Quality of Construction and Installation Works at Various Stages of the Life Cycle of a Construction Project. *Bulletin of MSAU*. 2023;18(2):283–292. (In Russ.) https://doi.org/10.22227/1997-0935.2023.2.283-292.

6. Belyaev AV, Antipov SS. Life Cycle of Construction Projects in Information Modeling of Buildings and Structures. *Industrial and Civil Engineering*. 2019(1):65–72. (In Russ.) URL: https://elibrary.ru/item.asp?id=36973984 (accessed: 22.01.2025).

8. Bespalov VI, Gurova OS, Lysova EP, Grishin GS. Analysis of the Life Cycle of Combined-cycle Gas Turbine TECs. Modern Trends in Construction, Urban and Territorial Planning. 2022;1(4):32–43. (In Russ.) URL: https://doi.org/10.23947/2949-1835-2022-1-4-32-43

9. Tikhomirov AL, Pirozhnikova AP. Formation of Principles of Quantitative Rregulation of Parameters of the Heat Supply System Based on the Analysis of its Life Cycle. *Modern Trends in construction, Urban and Territorial Planning*. 2023;2(2):29–35. URL: https://doi.org/10.23947/2949-1835-2023-2-2-29-35.

10. Tikhomirov A. L., Pirozhnikova A. P. Development of an Information Model of the Heat Supply System at Various Stages of its Life Cycle. *Modern Trends in Construction, Urban and Territorial Planning*. 2022;1(3):35–42. https://doi.org/10.23947/2949-1835-2022-1-3-35-42.

11. Bespalov VI, Tkacheva YuYu, Nikolaev AI. Development of an Algorithm for Increasing the Llife Cycle of Air Conditioning Systems (ACSs). *Modern Trends in Construction, Urban and Territorial Planning*. 2023;2(4):127–136. https://doi.org/10.23947/2949-1835-2023-2-4-127-136.

12. Samarskaya NS. Life Cycle Management of the Ventilation System of a Construction Site. *Modern Trends in Construction, Urban and Territorial Planning*. 2023;2(4):137–143. https://doi.org/10.23947/2949-1835-2023-2-4-137-143.

13. Usikov SM, Aksenova AA. Quality Management of the Water Heating System. *Innovations and Investments*. 2021;2:179–182. (In Russ.) URL: https://cyberleninka.ru/article/n/upravlenie-kachestvom-raboty-sistemy-vodyanogo-otopleniya (accessed: 22.01.2025).

14. Navaseltsau U., Navaseltsava D. Study of the Effectiveness of Various Methods of Balancing Systems Water Heating. *Bulletin of Polotsk State University*. *Series F. Construction. Applied Sciences.* 2021(16):94–98. (In Russ.) URL: file:///C:/Users/sstudennikova/Downloads/1163-%D0%A2%D0%B5%D0%BA%D1%81%D1%82%20%D1%81%D1%82%D0%B0%D1%82%D1%8C%D0%B8-2245-2-10-20220408.pdf (accessed: 22.01.2025).

15. Navaseltsau U., Navaseltsava D. Assessment of the Operability of the Water Heating System, Not Relevant to the Project. *Bulletin of Polotsk State University. Series F. Construction. Applied Sciences*. 2022(14):58–63. https://doi.org/10.52928/2070-1683-2022-32-14-58-63.

16. Yamleeva EU. On the Reliability and Ddurability of Heating Systems of Buildings. *Bulletin of the Ulyanovsk State Technical University.* 2018;1(81):53–57 (In Russ.) URL: https://lib.ulstu.ru/venec/disk/2017/252.pdf (accessed: 22.01.2025).

17. Loginova AA, Pankova TA. Comparative Analysis of Heating Systems. *Proceedings of the 11th National Conference with International Participation Modern Problems and Pprospects for the Development of Construction, Heat and Gas Supply and Energy Supply*. Saratov: SSAU named after N.I. Vavilov; 2021. P. 31–33. (In Russ.) URL: https://www.elibrary.ru/item.asp?id=46541348 (accessed: 22.01.2025).

About the Authors:

Ekaterina P. Lysova, Cand.Sci. (Eng.), Associate Professor of the Department of Heat and Gas Supply, Climate Engineering and Alternative Energy Installations at the Don State Technical University (1 Gagarin Square, Rostov-on-Don, 344003, Russian Federation), ScopusID, ORCID, katerina.lysova0803@gmail.com

Oksana N. Paramonova, Cand.Sci. (Eng.), Associate Professor of the Department of Heat and Gas Supply, Climate Engineering and Alternative Energy Installations at the Don State Technical University (1 Gagarin Square, Rostov-on-Don, 344003, Russian Federation), ScopusID, ORCID, paramonova_oh@mail.ru

Claimed Contributorship:

EP Lysov: formation of the basic concept, analysis of the research results, correction of the conclusions, graphic design, revision of the manuscript.

ON Paramonova: goals and objectives of the research, analysis of the research results, correction of the conclusions.

Conflict of Interest Statement: **the authors declare no conflict of interest.**

All authors have read and approved the final manuscript.

Об авторах:

Лысова Екатерина Петровна, кандидат технических наук, доцент кафедры теплогазоснабжения, климатехники и альтернативных энергоустановок Донского государственного технического университета (344003, Российская Федерация, г. Ростов-на-Дону, пл. Гагарина, 1), ScopusID, ORCID, katerina.lysova0803@gmail.com

Парамонова Оксана Николаевна, кандидат технических наук, доцент кафедры теплогазоснабжения, климатехники и альтернативных энергоустановок Донского государственного технического университета (344003, Российская Федерация, г. Ростов-на-Дону, пл. Гагарина, 1), ScopusID, ORCID, paramonova_oh@mail.ru

Заявленный вклад соавторов:

Е.П. Лысова: формирование основной концепции, анализ результатов исследований, корректировка выводов, графическое оформление, доработка текста.

О.Н. Парамонова: цели и задачи исследования, анализ результатов исследований, корректировка выводов.

Конфликт интересов: **авторы заявляют об отсутствии конфликта интересов.**

Все авторы прочитали и одобрили окончательный вариант рукописи.

Received / Поступила в редакцию 28.01.2025

Reviewed / Поступила после рецензирования 12.02.2025

Accepted / Принята к публикации 26.02.2025

Modern Trends in Construction, Urban and Territorial Planning. 2025;4(1):76–85. eISSN 2949–1835

LIFE CYCLE MANAGEMENT OF CONSTRUCTION FACILITIES

УПРАВЛЕНИЕ ЖИЗНЕННЫМ ЦИКЛОМ ОБЪЕКТОВ СТРОИТЕЛЬСТВА

UDC 005.41
https://doi.org/10.23947/2949-1835-2025-4-1-76-85

Original Empirical Research

Life Cycle Analysis of Construction Facilities Using the Eexample of Wind Power Facilities

Natalia S. Samarskaya ✉
Don State Technical University, Rostov-on-Don, Russian Federation
✉ nat-samars@yandex.ru

EDN: FNVSUB

Abstract

Introduction. Construction plays a major role in the economy of the Russian Federation contributing to sustainable development and improving the living conditions of the population. Modern construction facilities include residential and commercial buildings, municipal and infrastructural structures such as roads and bridges, as well as industrial and energy facilities, including wind power facilities. Wind energy is becoming an important part of the construction industry, contributing to innovation and technological progress. As objects of the construction industry, wind power facilities go through their life cycle which includes the main stages: design, construction, operation and disposal (renovation). Each stage requires effective management to ensure reliable operation and safety of the facility. Thus, in order to ensure the future generation of environmentally safe energy by a wind power plant, it becomes necessary to analyze the planned construction site and, as a result, manage solutions at the design and construction stages. During such an analysis, it becomes possible to identify potential problems during the operation phase of a wind power facility. These include, first of all, wear, corrosion of structural elements and frostbite of the blades. These problems are the reason for the decrease in performance and service life of the object. The aim of the work was thus to search for the possibility of extending the service life in the life cycle of wind power facilities by solving the problem of blade icing at the design and construction stages.

Materials and methods. The research is based on the method of analyzing the life cycle of construction facilities, including the systematization and optimization of their management processes. The model of the life cycle of wind power facilities, developed by the author earlier, helped to identify the problems of the facility's operation phase. The most significant problem that significantly affects the duration of the operation phase is the problem of blade icing. An analysis of the life cycle of a wind power facility has shown that it is advisable to ensure a successful solution to this problem at the design and construction stages of the facility. The data of the conducted analysis of the problem are based on the research results of domestic and foreign authors.

As a result, a generalization and systematization of existing anti-icing methods was carried out, on the basis of which a new method of implementation was set forth and an appropriate work methodology was developed. Such a solution, envisaged at the design stage of the construction facility, will enable one to successfully manage its life cycle, and, in particular, the operation stage.

Results. Throughout the course of the research, the author has been able to increase the duration of the operation stage in the life cycle of wind power facilities. To this end, an analysis of the life cycle of construction facilities was carried out, during which the causes affecting the life of the facility were identified. The most significant reason leading to a sharp reduction in the service life of the construction site is the problem of icing of the blades during the cold season.

Based on the analysis of operating conditions, the causes of icing of the blades of wind power structures have been determined, the basic principles of anti-icing protection have been established, and a new method for solving this problem using UAVs (unmanned aerial vehicles) has been set forth, as well as a technique for applying hydrophobic coatings to prevent the icing process. The implementation of the research results will ensure the required performance, which, in turn, will increase the service life of the wind power plant.

Discussion and conclusion. Successful lifecycle management of such construction facilities as wind power plants requires attention not only at the stage of operation of the facility, but also at the stages of design and construction. The key task of

the operation stage of a wind power facility is to ensure the necessary productivity and increase the service life of the facility. This can be solved by carefully analyzing the life cycle and preventing future operational problems at the design and construction stages. The method set forth in the study to combat blade icing can be implemented not only for existing wind power plants that do not have special anti-icing systems, but also for projected facilities. Moreover, the suggested solutions for combating icing of the blades can be included in the design documentation as mandatory types of work carried out during the construction phase, as well as subsequently during the operation phase with a certain frequency.
Solving the problem at the design stage of the facility will ensure an increase in productivity and an increase in the service life of a wind power plant operating in cold and humid climates. Thus, the results of the study provide a theoretical basis for managing the life cycle of wind power facilities, as one of the promising construction projects.

Keywords: life cycle, construction sites, wind power facilities, anti-icing of blades, hydrophobic coatings.

For citation. Samarskaya NS. Life Cycle Analysis of Construction Facilities Using the Example of Wind Power Facilities. *Modern Trends in Construction, Urban Planning and Territorial Planning*. 2025;4(1):76–85. https://doi.org/10.23947/2949-1835-2025-4-1-76-85

Оригинальное эмпирическое исследование

Анализ жизненного цикла объектов строительства на примере ветроэнергетических сооружений

Н.С. Самарская ✉

Донской государственный технический университет, г. Ростов-на-Дону, Российская Федерация

✉ nat-samars@yandex.ru

Аннотация

Введение. Строительство играет ключевую роль в экономике Российской Федерации, способствуя устойчивому развитию и улучшению условий жизни населения. Современные строительные объекты представляют собой жилые и коммерческие здания, коммунальные и инфраструктурные сооружения, такие как дороги и мосты, а также промышленные и энергетические объекты, включая ветроэнергетические сооружения. Ветроэнергетика становится важной частью строительной отрасли, способствуя инновациям и технологическому прогрессу.
Как объекты строительной отрасли ветроэнергетические сооружения (ВЭС) проходят свой жизненный цикл, включающий основные этапы: проектирование, строительство, эксплуатацию и утилизацию (реновацию). Каждый этап требует эффективного управления для обеспечения надежного функционирования и безопасности объекта. Так, для обеспечения в будущем генерации экологически безопасной энергии ветроэнергетическим сооружением возникает необходимость анализа планируемого объекта строительства и, как следствие, управление решениями еще на этапах проектирования и строительства. В ходе такого анализа появляется возможность выявить потенциальные проблемы этапа эксплуатации ветроэнергетического сооружения. К ним прежде всего можно отнести износ, коррозию конструктивных элементов и обморожение лопастей.
Данные проблемы являются причиной снижения производительности и срока службы объекта. В связи с этим целью работы являлся поиск возможности увеличения срока эксплуатации в жизненном цикле ветроэнергетических сооружений за счет решения проблемы обледенения лопастей на этапах проектирования и строительства.
Материалы и методы. Исследования базируются на методе анализа жизненного цикла строительных объектов, включающем систематизацию и оптимизацию процессов управления ими. Модель жизненного цикла ветроэнергетических сооружений, разработанная автором ранее, помогла выявить проблемы этапа эксплуатации объекта. Наиболее значимой проблемой, существенно влияющей на продолжительность этапа эксплуатации, является проблема обледенения лопастей. Анализ жизненного цикла ветроэнергетического сооружения показал, что обеспечить успешное решение этой проблемы целесообразно на этапах проектирования и строительства объекта. Данные проведенного анализа проблемы базируются на результатах исследований отечественных и зарубежных авторов.
В результате произведено обобщение и систематизация существующих методов борьбы с обледенением, на основе чего предложен новый способ реализации и разработана соответствующая методика выполнения работ. Такое решение, предусмотренное еще на этапе проектирования строительного объекта, позволит успешно управлять его жизненным циклом и, в частности, этапом эксплуатации.
Результаты исследования. В ходе проведенных исследований автором достигнута цель — увеличение продолжительности этапа эксплуатации в жизненном цикле ветроэнергетических сооружений. Для достижения поставленной цели проведен анализ жизненного цикла объектов строительства, в ходе которого выявлены причины, оказывающие влияние на срок эксплуатации объекта. Наиболее значимой причиной, приводящей к резкому сокращению срока службы объекта строительства, является проблема обледенения лопастей в холодный период года.

На основе анализа условий эксплуатации определены причины обледенения лопастей ветроэнергетических сооружений, установлены основные принципы защиты от обледенения и предложен новый способ решения этой проблемы с применением беспилотного летательного аппарата (далее — БПЛА), а также разработана методика нанесения гидрофобных покрытий для предотвращения процесса обледенения. Внедрение результатов исследования позволит обеспечить требуемую производительность, что, в свою очередь, увеличит срок службы ветроэнергетического сооружения.

Обсуждение и заключение. Успешное управление жизненным циклом таких объектов строительства как ветроэнергетические сооружения требует внимания не только на этапе эксплуатации объекта, но и на этапах проектирования и строительства. Ключевая задача этапа эксплуатации ветроэнергетического сооружения — обеспечение необходимой производительности и увеличение срока службы объекта — может быть решена путем тщательного анализа жизненного цикла и предотвращением будущих проблем эксплуатации еще на этапах проектирования и строительства. Предложенный в исследовании способ борьбы с обледенением лопастей может быть внедрен не только для существующих ветроэнергетических сооружений, не имеющих специальных систем против обледенения, но и для проектируемых объектов. Причем предлагаемые решения для борьбы с обледенением лопастей могут быть включены в проектную документацию как обязательные виды работ, осуществляемые на этапе строительства, а также впоследствии — на этапе эксплуатации с определенной периодичностью.

Решение проблемы на этапе проектирования объекта позволит обеспечить повышение производительности и увеличение срока службы ветроэнергетического сооружения, функционирующего в условиях холодного и влажного климата. Таким образом, результаты исследования представляют собой теоретическую базу для управления жизненным циклом ветроэнергетических сооружений как одних из перспективных объектов строительства.

Ключевые слова: жизненный цикл, объекты строительства, ветроэнергетические сооружения, борьба с обледенением лопастей, гидрофобные покрытия

Для цитирования. Самарская Н.С. Анализ жизненного цикла объектов строительства на примере ветроэнергетических сооружений. *Современные тенденции в строительстве, градостроительстве и планировке территорий*. 2025;4(1):76–85. https://doi.org/10.23947/2949-1835-2025-4-1-76-85

Introduction. Construction is one of the major sectors of the country's economy playing a key role in its sustainable social and economic development and improving the living conditions of the population. Modern construction industry facilities are made up of a diverse range of structures with each having its unique role in the infrastructural development of society. These include residential and commercial buildings, infrastructure facilities such as roads, bridges, and tunnels, as well as industrial structures. Recent years have seen special attention paid to wind power facilities becoming increasingly crucial in sustainable development and the search for alternative energy sources. Wind power facilities not only help reduce dependence on fossil fuels, but also minimize the environmental footprint by providing clean and renewable energy. Their integration into the construction industry opens up new avenues for innovation and technological progress making wind energy a key element of modern construction practice. Like any other construction projects, wind power facilities go through a specific life cycle including a few key stages: design, construction, operation and liquidation or renovation. Each calls for thorough management and control for ensuring efficiency, safety and durability of structures. At the design stage it is thus important to account for climatic conditions, topography, and potential wind resources to maximize productivity of structures to be built in the future. The construction phase of wind power facilities calls for the use of high-quality materials and advanced technologies to guarantee reliability and stability of structures. The operation of wind power plants is a crucial stage, since their economic feasibility and environmental efficiency are dependent on it. Regular maintenance and monitoring of equipment condition can serve to prevent breakdowns and extend the service life of structures. The liquidation or renovation stage involves either dismantling outdated structures or upgrading them to improve efficiency. This is similar to the life cycle of other construction projects where it is also critical to account for aspects of sustainable development and minimize environmental impact. The tasks of managing the life cycle of wind power facilities at each stage are thus unique and call for a variety of approaches and solutions. At the same time, it is to be noted that to maximize the efficiency of generating environmentally friendly energy by wind power facilities in the long term, it is necessary to perform a comprehensive analysis of a facility being planned at the initial stages of its life cycle. This entails implementing a comprehensive approach to managing design and construction solutions as early as at the stage of designing and constructing a structure. Performing such a multifactorial analysis enables potential problem areas to be encountered during the operation of the construction site to be pinpointed.

The most major factors include:

– mechanical wear of structural elements;

– corrosion impacting metal components;

– icing of the rotor blades, particularly at low temperatures;

– degradation of electronic components under the influence of aggressive external factors.

The impact of these negative factors causes a considerable decrease in the operational characteristics of a facility, including a decline in power output and a reduction in maintenance intervals. In the long term, this involves a decrease in the overall efficiency of a wind power plant and calls for extra costs for maintenance and restoration.

Timely identification and consideration of potential problems at the early stages of the life cycle of a facility enable it to develop preventive measures to improve the reliability and durability of a structure, which in the long run optimizes the operational characteristics of a facility throughout its entire period of operation.

One of the major problems having a considerable impact on the life of a wind power plant is the icing of the blades. This problem seems to be crucial for facilities situated in regions with a cold and humid climate (Fig. 1). This curbs the efficient energy production (with ice thickness up to 30 cm power generation is reduced by 80 %) resulting in an imbalance due to the uneven distribution of ice on the blades, heavier structure and reducing the efficiency of rotation [3]. As a result, there is accelerated wear of the equipment: a shift in the center of gravity, increased load on the rotation mechanisms and mechanical damage to the surface of the blades. Icing might thus lead to malfunctions and need for premature maintenance [4].

Icing, which is the deposition of ice on the streamlined parts of a wind power plant commonly takes place during fogs, rains or sleets. At the same time, sufficient conditions to induce icing are high humidity, negative air temperature and low temperature of the working surfaces [5].

Fig. 1. Example of icing on a wind turbine blade

An essential parameter inherent to blade icing is the icing intensity, i.e., the thickness of the ice forming per unit surface area in contact with precipitation [6]. There are three degrees of icing intensity:

– mild icing, which is an accumulation of ice caling for no considerable effort to be eliminated. It does not pose a severe threat to wind power plants;

– moderate icing when the rate of ice accumulation is still not sufficient to seriously impact the safety and stability of wind power plants;

– severe icing, which is a large-scale accumulation of ice likely to cause a noticeable loss of wind turbine rotation speed. This degree of icing intensity will be crucial in terms of safety and involve serious economic repercussions (reduced productivity, increased maintenance costs and shorter service life of equipment).

Given the significance of the issue of icing on the blades of wind power structures, the scholarly community sets forth a few of strategies to reduce the negative impact of ice formations [7, 8]. Modern anti-icing methods comprise:

– the use of heating systems in the turbine design or heating elements at the ends of the blades. By means of maintaining temperatures above zero, the aerodynamic properties of the blades are retained and the stable operation of the wind power plant is ensured in icing conditions;

– the use of hydrophobic plastic in the design of the blades reduces the adhesion of water and mineral particles to the surface. Moisture retention on the blade surface is thus curbed and icing is less likely;

– applying special coatings to the blades of a wind power plant to create a protective layer. Such coatings have properties preventing ice structures from forming;

– mechanical de-icing using climbing equipment or a lift, as well as ice removal from a helicopter using hot liquids. However, this method enables one to address the problem of icing in the short term and calls for considerable organizational costs.

Based on the analysis of modern anti-icing methods, applying special coatings to the blades of a wind power plant can be regarded as the most efficient solution. This method of anti-icing is fairly simple to use, has lower energy consumption compared to heating systems, provides relatively long-term protection, retains aerodynamic characteristics of an object and causes almost no changes to the mass of the blades.

However, accounting for the size of wind power facilities and the need for repeated and routine application of special coatings, choosing the way of implementing this method is still a considerable problem.

Materials and Methods. The ongoing study relies on a methodology for analyzing the life cycle of construction facilities including a comprehensive systematization and optimization of managing all stages of a life cycle of a structure [9].

The model of the life cycle of wind power facilities previously developed by the author enabled a detailed analysis of potential problems that might occur during the operation of a facility [2]. Among the factors identified, special attention was given to blade icing, which has a considerable effect on the duration and efficiency of the operational stage.

The analysis of the life cycle of a wind power facility has indicated that the most appropriate solution is to address the problem of icing at the initial stages of the design and construction of a facility. The empirical foundation of the research relies on the analysis of the results of the studies by domestic and foreign researchers in the field. Through the course of the research, the existing anti-icing methods were classified making it possible to come up with an innovative approach to solving this problem and design an appropriate methodology for implementing anti-icing measures.

Implementing the suggested solution in the design concept of a construction facility will be conducive to effective management of a life cycle of a wind power facility prioritizing its operation efficiency.

Research Results. The problem of anti-icing of wind turbine blades can be successfully addressed by means of applying hydrophobic coatings to create a protective layer and prevent ice formation. These coatings are typically designed using materials with micro- or nanostructures lending the surface extremely high water-repellent properties [10]. Microstructures on the coating surface contribute to water droplets not being able to be evenly distributed over the surface, but instead forming into balls and roll off, carrying moisture with them and preventing ice formation.

In order to address the problem of icing of wind turbine blades, two compositions (Silokor-Anti-Ice and graphene) were chosen, which, owing to their physical and chemical characteristics and the capacity to sustain hydrophobic properties for a long time, are best suited for appropriate climatic operating conditions of wind turbines. The major components and chemicals comprising Silokor-Antiled are siloxane polymer (the major component providing the hydrophobic properties of the coating), solvents for polymer dilution, technological additives improving the performance of a coating and fillers enhancing the mechanical properties of a coating [11].

Unlike Silokor-Antiled, graphene is a two-dimensional allotropic modification of carbon comprised of carbon atoms arranged in a hexagonal crystal lattice [12]. Graphene consists exclusively of carbon atoms. Each has 6 electrons: 2 in the inner shell and 4 in the outer one. Graphene is thus chemically identical to diamond and graphite, since it is made up of the same carbon atoms. However, the difference in physical properties is owing to their special spatial arrangement. It is thanks to this feature that the material *posseses* unique properties such as hydrophobicity, high strength and electrical conductivity. Hence it can also be employed to combat icing of wind turbine blades.

For the preferred choice of the composition, a comparative analysis was performed shown in Table 1.

Table 1

Comparative analysis of hydrophobic compositions for combating anti-icing of wind turbine blades

Index	Hydrophobic composition	
	«Silokor-Anti-Ice»	Graphene
Durability	Long service life provided there is appropriate surface preparation and application	High durability owing to its strength and resistance to external influences, suitable for extreme conditions
Economic effectiveness	A more cost-effective solution, particularly for large facilities	High cost of production and application
Environmental friendliness	It contains solvents, which might call for additional disposal and safety measures to be taken	An environmentally friendly material provided that safe production and application methods are utilized
Compatibility with surfaces	Suitable for metal, concrete, painted and other surfaces	Diverse, can be applied to a variety of materials, including complex and delicate surfaces
Light transmission	High light transmission coefficient, which might be critical for some types of applications	Does not affect light transmission, can be used in transparent coatings
Application and treatment	Easy to apply owing to a two-component system. Calls for thorough surface preparation prior to application	A more complex application procedure commonly calling for the use of specialized methods

Analyzing the data in Table 1, it can be concluded that Silokor-Antiled composition might be the preferred choice for most applications due to its accessibility and effectiveness. Graphene may actually be an optimal solution for specialized and high-load operating conditions, where its unique properties can be enhanced. Both compositions are successfully utilized to protect pitched roofs, gutters, mast structures from icing, for processing ceramic and polymer tiles, slate [11]. Given such a wide range of applications, these compositions can be considered for protecting the blades of a wind turbine in constantly recurring cycles of freezing and thawing. On top of that, the results of the analytical studies have confirmed that coatings using graphene are extremely promising. For example, Rice University scientists have proposed graphene nanoribbons should be employed as an effective de-icer for various surfaces including airplane wings, power lines, and helicopter blades [13, 14]. Graphene nanoribbons make up a bond in a composite by conducting an electric current through the material with a minimum load. The resulting electrothermal heat results in heating of an object surface. Meltwater forms between the surface and the ice in the course of melting allowing the ice to be removed without having to wait for the process to come to an end. Graphene coating is thus a promising material that can be applied to the surface of wind turbine blades or alternatively, graphene nanoribbons can be used reducing the likelihood of icing on the work surfaces and thus prolonging the service life of a facility.

As the application of hydrophobic coatings in this work is considered on an already erected and functioning wind turbine, there is a task of arranging this process. Instead of human labor or the use of bulky aircraft, coatings can be provided using an unmanned aerial vehicle (UAV). The integration of UAVs in the field of high-altitude work would enhance the efficiency of maintenance of wind turbines, since this field is poorly developed these days. Despite the time limitations of the use of UAVs for peaceful purposes, this tool remains extremely promising for tackling a whole host of tasks.

The suggested method of applying hydrophobic coatings to the surface of the blades of a wind turbine entails the selection of an appropriate UAV, as well as the development of a procedure for performing operations.

In order to implement spraying of hydrophobic compositions, the aircraft must be designed for suspended equipment to be set up on its body. The most suitable option is thus an agrotron which can be equipped with a suspension system for both sowing and spraying fields. In terms of of anti-icing, suspended spraying equipment will be employed to apply hydrophobic compositions to the surface of a wind turbine.

In order to apply hydrophobic compositions to the blades of a wind turbine, the following fly-around scheme can be employed (Fig. 2).

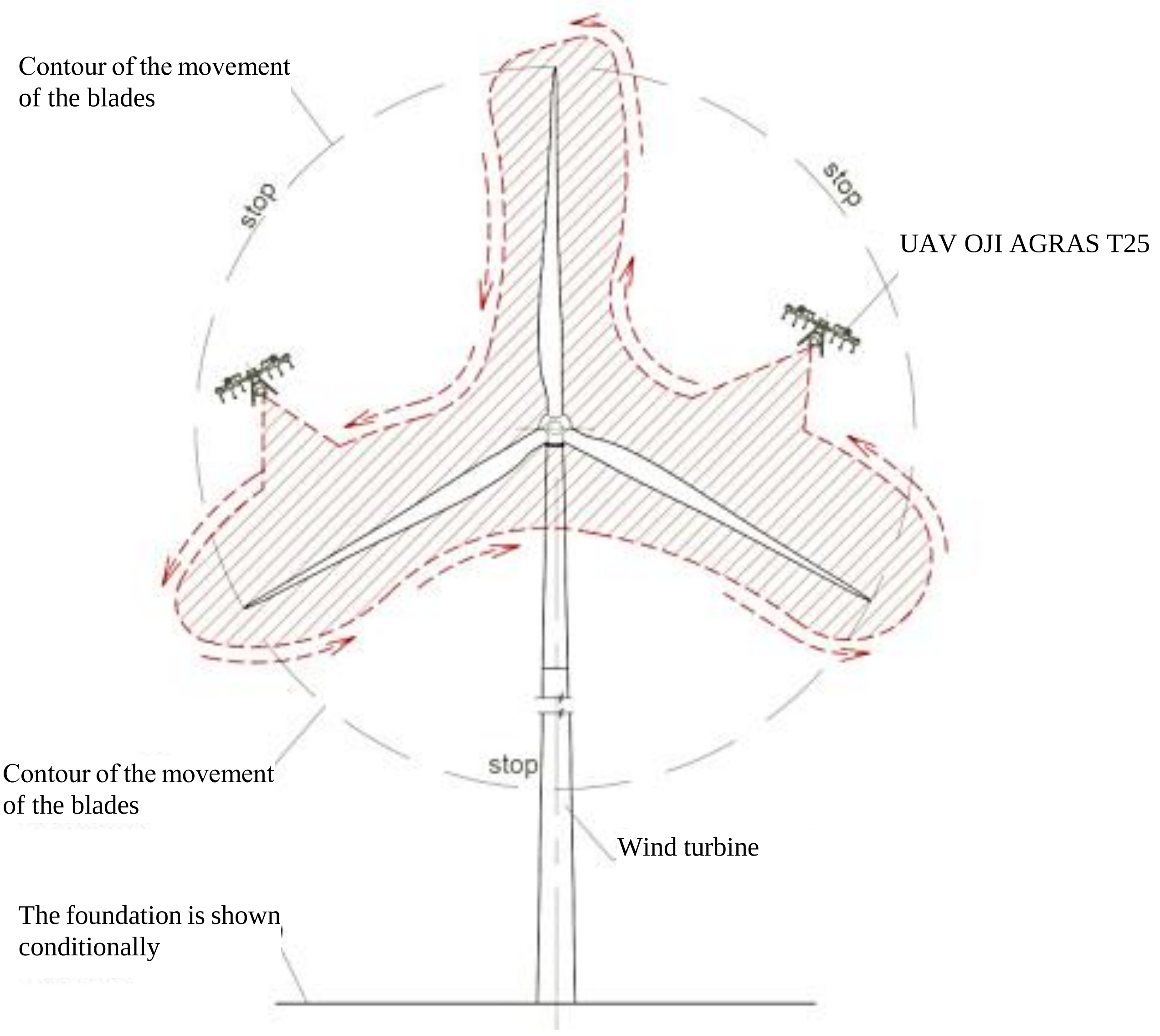

Fig. 2. Fly-around scheme for the treatment of blades with hydrophobic coatings using UAVs

The OJI EAGLES T25 UAV designed for agricultural needs was considered as an example. The device is capable of carrying up to 25 kg of useful load allowing it to be used for spraying large volumes of material. The time spent in the air is 15 minutes, and the control range is about 5 km enabling the operator to freely move and control the device at a long distance. A special feature of this UAV model is a high-precision spray system that ensures uniform distribution of the substance.

The device is also equipped with modern sensors and navigation systems, including GPS allowing it to closely follow set itineraries and avoid obstacles on the way. Agrotron can be equipped with multispectral cameras and sensors to collect data on the state of a coating assisting in making more informed technical decisions.

Based on the analysis of existing anti-icing methods and accounting for the flaws of current approaches in the context of the above problems, a technique for applying hydrophobic compositions to the surface of wind turbines using UAVs has been developed. The suggested methodology includes the following steps:

Preparing and collecting weather data. Prior to applying a hydrophobic composition to the blades of a wind turbine, up-to-date weather data, including wind speed, air temperature and humidity must be collected. These parameters are key to ensure the safety of UAV operation and the quality of surface treatment.

Preliminary fly-around of the wind turbine with photofixation. Possible places of ice formation as well as damage and problem areas must be identified. At this stage, hard-to-reach areas can also be evaluated and the flight time can be recorded.

Selecting and preparing a hydrophobic composition. Based on the characteristics of a wind-generating facility, climatic data and criteria in Table 1, an informed choice of hydrophobic materials should be made. Next, the solution is prepared and the ingredients are mixed in a prepared container.

Assembling and preparing the UAV. If necessary, an unmanned aerial vehicle equipped with a spray system should be assembled and refueled. All the elements must be in good order and set up properly.

Flying around the wind turbine and applying a hydrophobic coating. The hydrophobic anti-icing coating is applied in a few stages until a layer thickness of 50-70 mkm is achieved.

Stage 1. Controling the UAV with a complete fly-around of the wind turbine according to the scheme (Fig. 2) and applying the first layer of coating by means of a pneumatic method. An important task is to ensure the composition is distributed evenly over the surface of the blades.

Stage 2. Drying of the first layer within 15 minutes and applying the second layer of the hydrophobic composition in a similar manner ensuring the material is distributed evenly over the surface.

Stage 3. After complete drying, there is a fly-around of the wind turbine and the third coating layer is applied.

Controling the coating quality. To control of the coating quality visually for defects, it is necessary to fly around the wind generator with photo (video) fixation. If defects are detected, adjustments must be made by applying another layer of a hydrophobic coating.

Documentation and reporting. Work progress must be reported including the time and date of the work, weather conditions, the selected composition of a hydrophobic coating and all the stages of applying the composition to the working surfaces of the wind turbine.

Discussion and Conclusion. Effective management of the life cycle of wind power plants as capital construction objects entails the use of an integrated approach combining management decisions at all the stages: from the design concept to operational monitoring.

The primary objective of the operational period of a wind power facility is to enhance productivity while increasing its operational life. This is achieved by means of a preventive analysis of potential operational risks and their mitigation at the initial stages of the life cycle of a facility. The developed methodology for combating icing of blade elements is indicative of the diversity of its application both in existing wind power structures that are not equipped with specialized de-icing systems and for promising projects. At the same time, the complex of de-icing measures can be assigned in the design documentation as imperatives both at the construction stage and as part of routine operation maintenance.

Introducing preventive measures at the design preparation stage ensures a considerable increase in the service life of wind power facilities operated under adverse climatic conditions with high humidity and low temperature conditions. The results obtained throughout the study are thus a theoretical and methodological foundation for implementing multidimensional lifecycle management of wind power facilities positioned as an essential segment of the modern construction sector.

References

1. Bezhan AV. Role of Wind Energy in the Socio-economic Development of the Arctic Regions of the Russian Federation (Using the Example of the Murmansk Region). Arctic: Ecology and Economy. 2021;11(3):449–457. https://doi.org/10.25283/2223-4594-2021-3-449-457

2. Samarskaya NS, Paramonova ON, Lysova EP, Chistyakova VD. Development of a Life Cycle Model for a Wind Power Plant. Modern Trends in Construction, Urban and Territorial Planning. 2022;1(4):25–31. https://doi.org/10.23947/2949-1835-2022-1-4-25-31

3. Umurzakov AK. Ways to Combat Icing of Wind Turbine Blades. *Modern World Natural Science Research. Technological Progress.* 2023; 229-230. (In Russ.).

4. Okulov V, Kabardin I, Mukhin D, Stepanov K, Okulova N. Physical Deicing Techniques for Wind Turbine Blades. *Energies*. 2021;14(20):6750. https://doi.org/10.3390/en14206750

5. Martini F, Contreras Montoya LT, Ilinca A. Review of Wind Turbine Icing Modelling Approaches. *Energies*. 2021;14(16):5207. https://doi.org/10.3390/en14165207

6. Wang Q, Yi X, Liu Y, Ren J. Numerical Investigation of Dynamic Icing of Wind Turbine Blades under Wind Shear Conditions. *Renewable Energy*. 2024;227:120495. https://doi.org/10.1016/j.renene.2024.120495

7. Contreras Montoya LT, Lain S, Ilinca A. A Review on the Estimation of Power Loss Due to Icing in Wind Turbines. *Energies*. 2022;15(3):1083. https://doi.org/10.3390/en15031083

8. Meledin VG, Kabardin I, Dvoinishnikov SV, Zuev VO. Experimental Research on Combined Methods against Icing of Wind Turbine Blades. *Journal of Engineering Thermophysics*. 2024; 33(4):779–791. https://doi.org/10.1134/S181023282404009X

9. Belyaev AV, Antipov SS. Life Cycle of Construction Objects in Information Modeling of Buildings and Structures. *Industrial and Civil Engineering*. 2019;1:65–72. (In Russ.) URL: https://www.elibrary.ru/item.asp?id=36973984 (accessed: 10.02.2025).

10. Shustikov SA, Ulyanova NV. Review of Constructive Solutions for Aircraft Deicing. *Proceedings of All-Russian Scientific Practical Conference Modern Technologies in Shipbuilding and Aviation Education, Science and Manufacturing*. 2021. P. 337–344 (In Russ.). URL: https://www.elibrary.ru/item.asp?id=48286208 (accessed: 10.02.2025).

11. Akhremenko SA, Viktorov DA, Protchenko MV. Analysis of Prospects for the Development of Modern Deicing Systems. *Innovations in Construction*. 2019. P. 136–142. (In Russ.) URL: https://www.elibrary.ru/item.asp?id=43811094. (accessed: 10.02.2025).

12. Kurkina II. Investigation of the Structural, Electrical and Optical Properties of Fluorinated Graphene and Graphene/fluorinated Graphene/silicon Structures. *New materials and technologies in the Arctic*. 2022. P. 43–44. (In Russ.) URL: https://www.elibrary.ru/item.asp?id=49580222 (accessed: 10.02.2025).

13. Lebedeva OS, Lebedev NG. Piezo Conductivity of Graphene Nanoribbons. Elastoplastic Deformations. Solid State Physics. 2024;66(4):608-614. https://doi.org/10.61011/FTT.2024.04.57799.25

14. Wang H, Wang HS, Ma C, Chen L, Jiang C, Xie X. et al. Graphene Nanoribbons for Quantum Electronics. *Nature Reviews Physics*. 2021;3(12):791–802. https://doi.org/10.1038/s42254-021-00370-x

About the Author:

Natalia S. Samarskaya, Cand.Sci.(Eng.), Associate Professor of the Department of Heat and Gas Supply, Climate Engineering and Alternative Energy Installations at the Don State Technical University (1 Gagarin Square, Rostov-on-Don, 344003, Russian Federation), ScopusID, ORCID, nat-samars@yandex.ru

***Conflict of Interest Statement*: the author declares no conflict of interest.**

The author has read and approved the final manuscript.

Об авторе:

Самарская Наталья Сергеевна, кандидат технических наук, доцент кафедры теплогазоснабжения, климатехники и альтернативных энергоустановок Донского государственного технического университета (344003, Российская Федерация, г. Ростов-на-Дону, пл. Гагарина, 1), ScopusID, ORCID, nat-samars@yandex.ru

Конфликт интересов: **автор заявляет об отсутствии конфликта интересов.**

Автор прочитал и одобрил окончательный вариант рукописи.

Received / Поступила в редакцию 22.02.2025
Reviewed / Поступила после рецензирования 04.03.2025
Accepted / Принята к публикации 13.03.2025